GABRIELLY NAYARA TAVARES SILVA RODRIGUES

POTASSIUM RECYCLING FROM ORGANIC WASTE AND URINE FOR THE PRODUCTION OF ENGINEERED BIOCHARS TO USE AS FERTILIZERS

LAVRAS – MG
2025

GABRIELLY NAYARA TAVARES SILVA RODRIGUES

POTASSIUM RECYCLING FROM ORGANIC WASTE AND URINE FOR THE PRODUCTION OF ENGINEERED BIOCHARS TO USE AS FERTILIZERS

Thesis presented to the Federal University of Lavras, as part of the requirements of the Graduate Program in Soil Science, area of concentration in Soil Fertility and Plant Mineral Nutrition, to obtain the title of Doctor.

Carlos Alberto Silva, PhD
Advisor

LAVRAS-MG
2025

Ficha Catalográfica elaborada pelo Sistema de Geração de Ficha Catalográfica da Biblioteca Universitária da UFLA, com dados informados pelo(a) próprio(a) autor(a).

Rodrigues, Gabrielly.
Potassium recycling from organic waste and urine for the production of engineered biochars to use as fertilizers / Gabrielly Rodrigues. - 2025.
104 p. : il.

Orientador: Carlos Silva

Tese (Doutorado) - Universidade Federal de Lavras, 2025.
Bibliografia.

1. Composites. 2. Slow-release potassium fertilizers. 3. K in soil solution. 4. K struvite. 5. Waste K recycling. I. Silva, Carlos. II. Universidade Federal de Lavras. III. Título.

GABRIELLY NAYARA TAVARES SILVA RODRIGUES

RECICLAGEM DE POTÁSSIO DE RESÍDUOS ORGÂNICOS E URINA PARA A PRODUÇÃO DE BIOCARVÕES PROJETADOS PARA USO COMO FERTILIZANTES

POTASSIUM RECYCLING FROM ORGANIC WASTE AND URINE FOR THE PRODUCTION OF ENGINEERED BIOCHARS TO USE AS FERTILIZERS

Thesis presented to the Federal University of Lavras, as part of the requirements of the Graduate Program in Soil Science, area of concentration in Soil Fertility and Plant Mineral Nutrition, to obtain the title of Doctor.

APPROVED on April 29, 2025.

Dr. Leônidas Carrijo Azevedo Melo	UFLA
Dr. Guilherme Lopes	UFLA
Dr. Ronaldo Fia	UFLA
Dr. José Ferreira Lustosa Filho	UnB

Carlos Alberto Silva, PhD
Advisor

LAVRAS-MG
2025

To God, my source of strength and inspiration.

ACKNOWLEDGMENTS

First and foremost, I thank God, my greatest source of inspiration. To Him, I owe all the countless blessings I have received throughout my life.

To my husband Leandro, the love of my life. Thank you for your unconditional support throughout my academic journey, for being my safe harbor during moments of great challenge, and for your infinite love, which was fundamental to achieving this milestone.

To my mother, who taught me never to give up on my dreams, who shaped my values, and who loved me unconditionally. To my brother Marcos, my sister-in-law Mônica, and my goddaughter Catarina, for their support, love, and affection. To my father, for all his admiration. To my grandparents, Dona Lia (in memoriam) and Seu Vicente (in memoriam), for all their wisdom and teachings. To my parents-in-law, Adma and Domício, and to my brother-in-law Igor, for their constant kindness. To all my family.

To my friends, longstanding and new, who were always present throughout my journey. In particular, I thank the friends I made during my doctoral studies: my lab mates Everton and Loren, who significantly contributed to the development of this thesis; my classmates; and the members of NECS (Study Group in Soil Science). I also thank my friends during my time in the United States, especially my roommates Mari, Antônio, Renato, Martha, Paulo, and Muniz, and my lab friends Lucinda, Maria, and Candace. Thank you for your support and for making my experience in the U.S. even more magical. And to so many others who crossed my path during this important chapter of my life.

To my advisor, Professor Carlos, for all his patience and guidance, and especially for his support during the development of my sandwich PhD program. Thank you for the philosophical conversations and for helping me develop the critical and questioning mindset that is essential in a researcher's life. To Professor Johannes Lehmann, who welcomed me at Cornell and guided me throughout the development of my research. To all the laboratory technicians who assisted me during the execution of the experiments. To the professors of the Department of Soil Science for all their teachings. To the Federal University of Lavras, the Department of Soil Science, and the Graduate Program in Soil Science for the structure and resources provided. To CAPES for funding my doctoral scholarship in Brazil and the sandwich PhD scholarship (CAPES-PROEX/AUXPE 593/2018 and grant #CAPES PRINT: 88887.839592/2023-00). And to CNPq and FAPEMIG for additional funding. This study was financed in part by the Coordenação de Aperfeiçoamento de Pessoal de Nível Superior – Brasil (CAPES) – Finance Code 001. **Thank you!**

“Look deep into nature, and then you will understand everything better”

Albert Einstein

RESUMO PORTUGUÊS

O potássio (K) é um dos nutrientes mais exigidos pelas plantas, participando de processos como ativação enzimática, regulação estomática e transporte de carboidratos. Em solos altamente intemperizados, como os brasileiros, a baixa disponibilidade natural de K exige aplicações elevadas de fertilizantes potássicos, especialmente o KCl, que apresenta alta solubilidade, elevado índice salino e teor de cloro. Essas características podem prejudicar o desenvolvimento das culturas, exigindo alternativas mais sustentáveis. Resíduos orgânicos surgem como fontes potenciais de potássio, desde que seu uso seja tecnicamente avaliado para evitar riscos ambientais. Dentre as alternativas, o biocarvão (BC) tem ganhado destaque nas últimas décadas por seu potencial como fonte de nutrientes. Esta tese teve como objetivo investigar estratégias para a recuperação e uso de potássio a partir de diferentes resíduos, utilizando tecnologias baseadas em biocarvão e precipitação química. Foram avaliadas questões como: (i) Qual o potencial de diferentes biomassas ricas em K (casca de banana, palha de café e esterco de galinha), processadas em duas temperaturas de pirólise (300 e 650 °C), e sua co-pirólise com KCl, na produção de fertilizantes potássicos com alto valor agronômico?; (ii) Qual a cinética de liberação de K desses fertilizantes em condições controladas e reais de cultivo de milho?; (iii) Esses materiais são agronomicamente eficazes na substituição parcial ou total do KCl no crescimento do milho em solos com diferentes texturas e teores de matéria orgânica?; (iv) Quais os principais fatores químicos e físicos que afetam a recuperação do potássio da urina sintética na forma de K-estruvita?; (v) Modelos termodinâmicos como o PHREEQC e o Visual MINTEQ são eficazes na previsão da precipitação da K-estruvita em diferentes condições químicas?; (vi) O biocarvão pode ser utilizado como material de nucleação eficaz na recuperação do K na forma de K-estruvita?; (vii) A adição do biocarvão altera os fatores que influenciam a precipitação da K-estruvita pura?; (viii) O tipo de biocarvão influencia a formação da K-estruvita?; (ix) Os tempos de agitação e repouso influenciam na formação da K-estruvita? Os resultados indicaram que tipo de biomassa, temperatura de pirólise e co-pirólise com KCl influenciam a eficiência agronômica dos fertilizantes. A casca de banana pirolisada a 650 °C foi o material mais promissor, permitindo reduzir em 82% a necessidade de KCl. Em solos arenosos, indicou-se o parcelamento da aplicação ou granulação dos compósitos para reduzir perdas por lixiviação. No contexto da urina humana sintética, a precipitação como K-estruvita foi maximizada em pH 10 e na razão molar Mg:K:P de 2:1:2, alcançando eficiência superior a 78%. O modelo PHREEQC foi mais preciso na previsão da K-estruvita que o Visual MINTEQ. Biocarvões de madeira pirolisados a 500 °C melhoraram a nucleação e recuperação da K-estruvita, enquanto os de esterco liberaram K na solução, prejudicando a precipitação. Testes de cinética mostraram que compósitos biocarvão + K-estruvita atuam como fontes de liberação lenta de potássio, com potencial uso agrícola. Assim, esta tese propõe abordagens sustentáveis e integradas para a reciclagem de K a partir de resíduos, com aplicação na agricultura circular e no saneamento descentralizado.

Palavras-chave: Compósitos; Fertilizantes Potássicos de Liberação Lenta; Potássio Na Solução Do Solo; K-Estruvita; Modelagem Termodinâmica; Reciclagem De Potássio De Resíduos.

ABSTRACT

Potassium (K) is one of the most essential nutrients required by plants, playing a key role in processes such as enzyme activation, stomatal regulation, and carbohydrate transport. In highly weathered soils, such as those found in Brazil, the naturally low availability of K demands high applications of potassium fertilizers, especially KCl, which presents high solubility, a high salt index, and elevated chloride content. These characteristics can negatively affect crop development, highlighting the need for more sustainable alternatives. Organic residues have emerged as potential sources of potassium, provided their use is technically evaluated to prevent environmental risks. Among these alternatives, biochar (BC) has gained prominence over the past decades for its potential as a nutrient source in agricultural systems. This thesis aimed to investigate strategies for potassium recovery and utilization from different waste materials, using biochar-based technologies and chemical precipitation. The following research questions were evaluated: (i) What is the potential of different K-rich biomasses (banana peel, coffee husk, and chicken manure), processed at two pyrolysis temperatures (300 and 650 °C), and their co-pyrolysis with KCl, in producing potassium fertilizers with high agronomic value? (ii) What is the potassium release kinetics from these fertilizers under controlled conditions and real corn cultivation scenarios? (iii) Are these materials agronomically effective in partially or fully replacing KCl for corn cultivation in soils with different textures and organic matter contents? (iv) What are the main chemical and physical factors affecting potassium recovery from synthetic urine in the form of K-struvite? (v) Are thermodynamic models such as PHREEQC and Visual MINTEQ effective in predicting K-struvite precipitation under different chemical conditions? (vi) Can biochar be used as an effective seeding material to enhance K recovery as K-struvite? (vii) Does the addition of biochar alter the factors influencing the precipitation of pure K-struvite? (viii) Does the type of biochar affect K-struvite formation? (ix) Do mixing and resting times influence the crystallization of K-struvite? The results indicated that biomass type, pyrolysis temperature, and co-pyrolysis with KCl significantly affect the agronomic efficiency of biochar-based fertilizers. Banana peel pyrolyzed at 650 °C was the most promising material, allowing for an 82% reduction in KCl use. In sandy soils, split application or granulation of the composites was recommended to reduce potassium leaching. In the context of synthetic human urine, potassium recovery as K-struvite was maximized at pH 10 and a Mg:K:P molar ratio of 2:1:2, with efficiency exceeding 78%. PHREEQC proved more accurate than Visual MINTEQ in predicting K-struvite formation. Biochars derived from wood pyrolyzed at 500 °C enhanced nucleation and K-struvite recovery, while manure-derived biochars released K into the solution, hindering precipitation. Kinetic tests showed that biochar + K-struvite composites act as slow-release potassium carriers, with strong potential as agricultural fertilizers. Thus, this thesis proposes sustainable and integrated approaches for potassium recycling from waste materials, with applications in circular agriculture and decentralized sanitation systems.

Keywords: Composites; Slow-release potassium fertilizers; K in soil solution; K-struvite; thermodynamic modeling; Waste K recycling.

INDICADORES DE IMPACTO

Esta pesquisa foi desenvolvida com foco em estratégias sustentáveis para a recuperação de potássio a partir de resíduos sólidos e líquidos, utilizando tecnologias baseadas em biocarvão e precipitação química (K-estruvita). Embora os resultados ainda não tenham sido aplicados em contextos produtivos, os experimentos laboratoriais e os ensaios controlados representam um avanço científico significativo, com forte potencial de aplicação futura em sistemas agrícolas sustentáveis. O trabalho foi realizado em dois contextos institucionais. O primeiro capítulo foi conduzido na Universidade Federal de Lavras (UFLA), no Departamento de Ciência do Solo (DCS), envolvendo experimentos em laboratório e na casa de vegetação. O segundo capítulo foi desenvolvido na Universidade de Cornell (Estados Unidos), sob a supervisão do professor Johannes Lehmann, um dos principais especialistas mundiais em biocarvão. Essa etapa internacional foi viabilizada por meio do Programa CAPES PRINT, promovendo a internacionalização da pós-graduação brasileira e fortalecendo a cooperação científica entre instituições. O projeto contou com a participação direta da autora, do orientador professor Carlos Alberto Silva, do professor Johannes Lehmann em Cornell e de dois pesquisadores de pós-doutorado. Embora o trabalho não tenha caráter extensionista direto, os resultados obtidos oferecem uma base científica sólida para futuras iniciativas em agricultura circular e recuperação de nutrientes em sistemas de saneamento descentralizado. O território potencialmente impactado inclui regiões agrícolas com solos altamente intemperizados e baixa disponibilidade natural de potássio, como o bioma Cerrado brasileiro. Além disso, os achados contribuem para o desenvolvimento de alternativas ao uso intensivo de fertilizantes minerais importados, fortalecendo a segurança alimentar nacional e a independência tecnológica do setor agropecuário. Esta pesquisa se insere principalmente nas áreas temáticas da Política Nacional de Extensão em Meio Ambiente e Tecnologia e Produção, ao propor soluções sustentáveis para o reaproveitamento de resíduos e a redução da dependência de insumos químicos convencionais. Também está alinhada a diversos Objetivos de Desenvolvimento Sustentável (ODS) das Nações Unidas, incluindo o ODS 2, ao propor fertilizantes alternativos que aumentam a eficiência do uso de nutrientes; o ODS 6, por meio da recuperação de nutrientes da urina humana; o ODS 12, ao promover o reaproveitamento de resíduos orgânicos; e o ODS 13, ao explorar o potencial do biocarvão para o sequestro de carbono e a redução dos impactos ambientais associados à fertilização convencional.

IMPACT INDICATORS

This research was developed with a focus on sustainable strategies for potassium recovery from solid and liquid waste, using biochar-based technologies and chemical precipitation (K-struvite). Although the results have not yet been applied in productive contexts, the laboratory experiments and controlled trials represent a significant scientific advancement, with strong potential for future application in sustainable agricultural systems. The work was carried out in two institutional contexts. The first chapter was conducted at the Federal University of Lavras (UFLA), in the Department of Soil Science (DCS), involving laboratory experiments and greenhouse trials. The second chapter was developed at Cornell University (USA), under the supervision of Professor Johannes Lehmann, a leading global expert in biochar. This international stage was made possible through the CAPES PRINT Program, promoting the internationalization of Brazilian graduate education and strengthening scientific cooperation between institutions. The project involved the direct participation of the author, the advisor Professor Carlos Alberto Silva, Professor Johannes Lehmann at Cornell, and two postdoctoral researchers. Although the work did not have a direct extensionist nature, the results provide a solid scientific basis for future initiatives in circular agriculture and nutrient recovery in decentralized sanitation systems. The potentially impacted territory includes agricultural regions with highly weathered soils and low natural potassium availability, such as Brazil's Cerrado biome. Furthermore, the findings contribute to the development of alternatives to the intensive use of imported mineral fertilizers, supporting national food security and technological independence in the agricultural sector. This research primarily aligns with the thematic areas of the National Extension Policy in Environment and Technology and Production, as it proposes sustainable solutions for waste reuse and reduction in dependency on conventional chemical inputs. It is also aligned with several United Nations Sustainable Development Goals, including SDG 2, by proposing alternative fertilizers that improve nutrient use efficiency; SDG 6, through the recovery of nutrients from human urine; SDG 12, by promoting the reuse of organic waste; and SDG 13, through the potential of biochar to sequester carbon and reduce environmental impacts associated with conventional fertilization.

SUMMARY

1 FIRST PART

1.1 GENERAL INTRODUCTION

Potassium is a macronutrient for plants, ranking as the second most abundant element in plant tissue and required in large quantities (CLARKSON; HANSON, 1980; PARAMISPARAM *et al.*, 2021). Absorbed as K^+, the dominant cation in living plant cells, it plays key physiological roles in enzyme activation, membrane transport, stomatal regulation, and photosynthesis (BRITTO; COSKUN; KRONZUCKER, 2021; CLARKSON; HANSON, 1980). Since soil is the main K source, its availability is influenced by environmental and management factors, making the understanding of soil K dynamics critical for plant nutrition and overall food system sustainability (MALAVOLTA, 1980).

Soil potassium exists in four forms: solution, exchangeable, fixed, and structural, with about 98% in fixed or structural forms, which are not readily available to plants (SPARKS, 2000). Maintaining adequate levels of exchangeable K, the main source for plant uptake, requires managing the balance among forms, which is governed by soil properties and reaction dynamics (BAO *et al.*, 2024; BILIAS *et al.*, 2023).

Tropical soils, like those in Brazil, are highly weathered, with low potassium availability and poor cation exchange capacity (CEC), which enhances K leaching. In the Brazilian Cerrado, for example, around 85% of soils are classified as K-deficient, with average available K values near 31 mg dm^{-3} (LOPES; GUIMARÃES GUILHERME, 2016). These limitations, combined with the demands of high-yielding cultivars and the high solubility of fertilizers like KCl, require split applications to improve nutrient use efficiency (SHARMA; SINDHU; GLICK, 2024).

Potassium chloride (KCl) is the most used K fertilizer in Brazil, yet national reserves are scarce and demand exceeds 6.7 million tons, making the country heavily reliant on imports (SCHUELER *et al.*, 2021). In 2022, over 7.5 million tons were imported, mainly from Canada, Belarus, Germany, Israel, and Russia (FAO, 2021). Beyond high import costs, the use of KCl increases production expenses due to its high solubility, which requires split applications (CASTRO-SUAREZ; COLPAS-CASTILLO; TARON-DUNOYER, 2023). Additionally, the Cl^- ion has a high salt index that can impair germination, hinder crop development, and inhibit the growth of Cl sensitive species (BEGUM *et al.*, 1992; GEILFUS, 2018; VAN LOON; VAN DEN BERG, 2003). These limitations highlight the need for alternative potassium sources and synthetic routes that reduce both agronomic risks and Brazil's dependence on imported inputs.

Soil Organic Matter (SOM) is essential for maintaining soil quality, improving nutrient supply, CEC, water dynamics, and erosion control (GREGORICH *et al.*, 1994; HOFFLAND *et*

al., 2020). In tropical soils, SOM plays a fundamental role in the sustainability of agricultural ecosystems. Therefore, maintaining adequate SOM levels and ensuring the biological cycling of nutrients are crucial for the success of any soil management strategy in tropical regions (LEHMANN; RONDON, 2006). Practices such as no-till farming, crop rotation, and organic residue application are effective strategies to increase SOM content and functionality (MORI ALVEZ *et al.*, 2024; NORTJÉ; LAKER, 2021).

Although widely used to improve nutrient cycling and fertilizer efficiency, organic residues in tropical soils decompose rapidly, limiting their long-term effectiveness (ATKINSON; FITZGERALD; HIPPS, 2010; LEHMANN; RONDON, 2006). Issues like short persistence, contamination risks, and irregular availability have led to increasing interest in biochar, a more stable alternative that also addresses growing potassium demands and improves organic waste utilization (BRICHI *et al.*, 2023).

Biochar (BC) is a solid material obtained through the pyrolysis of organic residues, such as agricultural waste, animal manure, sewage sludge, and other organic materials (JIA *et al.*, 2021), under partial or complete exclusion of oxygen, using various types of reactor configurations. The process results in the production of a solid material (biochar), along with gases and bio-oil, which can be used for energy generation (JOHANNES LEHMANN, 2007).

The production and application of biochar in agricultural soils offer multiple benefits. One of its most notable effects is climate change mitigation through the sequestration of carbon in a more stable form than raw feedstock, while simultaneously increasing soil organic carbon content (ATKINSON; FITZGERALD; HIPPS, 2010; MELO *et al.*, 2022; WOOLF *et al.*, 2021). It also improves CEC, nutrient availability, microbial activity, macrofauna abundance, plant productivity, and the stabilization of toxic elements (DOMINGUES *et al.*, 2020; JIN *et al.*, 2017; KAMAU *et al.*, 2019; LEHMANN; RONDON, 2006). Additionally, its high water adsorption capacity supports its use as a slow-release potassium fertilizer (CHEN, Guanyi *et al.*, 2023; CHENG *et al.*, 2023; XIU *et al.*, 2023).

The composition and the physical and chemical characteristics of biochar (BC) are directly influenced by the properties of the feedstock used and the pyrolysis conditions applied during production (JI *et al.*, 2022). Therefore, both the feedstock and the pyrolysis parameters can be intentionally selected and adjusted to achieve specific properties in the resulting biochar (WEBER; QUICKER, 2018) . In terms of feedstock, animal-based residues generally yield more biochar and nutrients due to higher ash content (DOMINGUES *et al.*, 2017). Regarding pyrolysis temperature, lower ranges (300 °C to 400 °C) tend to preserve more volatile organic compounds and functional groups, which enhance the cation exchange capacity (CEC) and

nutrient retention. In contrast, higher temperatures (above 500 °C) yield biochars with greater fixed carbon content, increased surface area and porosity and a more alkaline pH (LIN *et al.*, 2023; TAO *et al.*, 2024). Feedstock and pyrolysis conditions also influence how biochar interacts with potassium. Temperature affects both the total K content and its speciation, altering the presence of compounds like K_2SO_4, KNO_3, KCl, and K–graphite layers, which determine biochar's potential as a direct K fertilizer (TAN *et al.*, 2017).

Pristine biochars may not always exhibit the desired characteristics for specific applications. To enhance their performance, certain modifications can be applied before, during, or after the pyrolysis process. One such strategy is co-pyrolysis, in which two or more feedstocks, such as different feedstocks or the one feedstock combined with mineral fertilizers, are thermochemically treated under the same conditions as conventional pyrolysis (DAI *et al.*, 2022). Synergistic interactions can enhance pore structure, reduce ash content, and improve nutrient retention or contaminant stabilization (AHMED; HAMEED, 2020; FAN *et al.*, 2018; JIN *et al.*, 2017). However, studies on K- enriched biochars via co-pyrolysis with KCl remain scarce.

While biochar engineering provides a solid-phase route for enhancing K availability, liquid waste streams also offer promising opportunities for potassium recovery (ARSLANOĞLU; TÜMEN, 2021). Among them, effluents such as vinasse and domestic wastewater also represent valuable sources of potassium (SUDARSAN; ROY; NITHIYANANTHAM, 2021; TÜRK; ARSLANOĞLU, 2024; VAN NGUYEN *et al.*, 2025). Recovering K from these waste streams aligns with circular economy principles and supports sustainable nutrient management. Although human urine accounts for less than 1% of domestic wastewater by volume, it contributes approximately 80% of the nitrogen (N), 56% of the phosphorus (P), and 63% of the potassium (K) found in household effluents (RANDALL; NAIDOO, 2018; SALIU; OLADOJA; SAUVÉ, 2023). In human urine ammonium concentrations range from 0.32 to 0.5 g L^{-1}, phosphate from 0.3 to 1.07 g L^{-1}, and potassium from 0.16 to 4 g L^{-1}, making urine a valuable resource for K recycling and the sustainable synthesis of fertilizers (PATHY; RAY; PARAMASIVAN, 2021; RANDALL; NAIDOO, 2018).

The recovery of nitrogen and phosphorus from urine is extensively documented in the literature, with struvite precipitation being one of the most studied approaches (GUNNARSSON; LALANDER; MCCONVILLE, 2023). Struvite is a mineral composed of magnesium, ammonium, and phosphate ($MgNH_4PO_4 \cdot 6H_2O$) and has a solubility product (pKsp) of approximately 13.26. It precipitates readily under alkaline conditions and is widely

studied as a slow-release fertilizer (MARTIN *et al.*, 2022). A structural analogue of struvite, K-struvite ($MgKPO_4 \cdot 6H_2O$, MPP) in which potassium replaces ammonium in the crystal lattice, can also be recovered via precipitation, with a pKsp of approximately 12.2 (KABDAŞLI; SICILIANO; *et al.*, 2022). A third compound, Na-struvite ($MgNaPO_4 \cdot 6H_2O$, MSP), where sodium replaces ammonium, has an estimated pKsp of approximately 11.6 and forms under even more alkaline conditions (KABDAŞLI; SICILIANO; *et al.*, 2022). The solubility product governs the precipitation sequence of these minerals: MAP forms first under favorable conditions. If ammonium is limited but magnesium and phosphate ions remain available, K-struvite may then precipitate, followed by Na-struvite at higher pH (XU *et al.*, 2015).

Prioritizing MPP over MAP precipitation can represent a more sustainable and cost-effective strategy for potassium recovery, especially when NH_4^+ is removed beforehand via techniques such as stripping or adsorption (CHEN, Tse Lun *et al.*, 2021; HE *et al.*, 2024). MPP formation depends on specific chemical conditions, particularly the concentrations of Mg^{2+} and PO_4^{3-} and the pH. Studies have shown that a Mg:K:P molar ratio greater than 1:1:1 is required to optimize precipitation, with the 2:1:2 ratio yielding the best results in synthetic urine (LIU *et al.*, 2024). A pH between 9 and 11 is also recommended for improved MPP formation (KABDAŞLI; KUŞÇUOĞLU; *et al.*, 2022). However, elevated concentrations of Na^+ and Ca^{2+} may hinder MPP crystallization by competing for phosphate and favoring the formation of other minerals, such as MSP and hydroxyapatite (HUANG *et al.*, 2019).

The addition of seed crystals can enhance K-struvite precipitation by reducing induction time and promoting nucleation, increasing recovery when seeds are used (GAO *et al.*, 2018; SHAN *et al.*, 2022). This opens opportunities to explore sustainable, low-cost seed materials that not only facilitate crystallization but also serve as carriers, such as biochar (WU *et al.*, 2023). Due to its chemical properties and origin from recycled organic waste, biochar is a promising carrier for K-struvite recovered from urine. Its dual role supports circular economy goals while improving nutrient delivery when applied to soil.

Thermodynamic modeling is a valuable tool for predicting chemical equilibrium in complex solutions like synthetic urine (DANESHGAR *et al.*, 2018). It allows for preliminary simulations that reduce laboratory workload, reagent use, and analysis time, while also guiding experimental design. These models can simulate conditions impractical to replicate in the lab, making them useful in both pre and post-experimental phases (DAVAND *et al.*, 2022). However, their use must be approached with caution, as the choice of database can significantly influence the results. If the chemical system of interest is not properly represented, the simulations may fail to accurately reflect the actual behavior of the solution (NATIVIDAD-

MARIN; WILLIAM BURNS; SCHNEIDER, 2023; SOLTANI; NATIVIDAD-MARIN; SCHNEIDER, 2023).

Accordingly, this thesis aimed to develop sustainable strategies for recovering potassium from solid and liquid residues, particularly synthetic human urine, by combining biochar production and chemical precipitation as alternative K sources for agriculture. The work was structured into two main chapters. The first focused on evaluating the potential of different K-rich biomasses (banana peel, coffee husk, and chicken manure), processed at two pyrolysis temperatures (300 and 650 °C), and their co-pyrolysis with KCl, to produce biochars with high agronomic value. It also assessed the kinetics of K release and the effectiveness of these materials in replacing KCl, partially or fully, in corn cultivation under contrasting tropical soil conditions. The second chapter investigated the recovery of potassium as K-struvite from synthetic urine, evaluating the influence of chemical parameters (pH and Mg:K:P ratio), the use of biochar as a seeding material, and the predictive capacity of thermodynamic models (PHREEQC and Visual MINTEQ) under varying conditions.

This research contributes to filling key knowledge gaps by exploring the co-pyrolysis of biochar with KCl to produce materials with potassium content comparable to mineral fertilizers; by integrating biochar engineering with the recovery of K-struvite from urine; and by evaluating the predictive accuracy of thermodynamic modeling tools, an approach not yet fully explored in the literature. Collectively, the findings offer promising alternatives for circular nutrient management and decentralized sanitation systems.

REFERENCES

AHMED, M. J.; HAMEED, B. H. Insight into the co-pyrolysis of different blended feedstocks to biochar for the adsorption of organic and inorganic pollutants: A review. **Journal of Cleaner Production**, vol. 265, p. 121762, 2020. DOI 10.1016/j.jclepro.2020.121762. Available at: https://doi.org/10.1016/j.jclepro.2020.121762.

ARSLANOĞLU, Hasan; TÜMEN, Fikret. Potassium struvite (slow release fertilizer) and activated carbon production: Resource recovery from vinasse and grape marc organic waste using thermal processing. **Process Safety and Environmental Protection**, vol. 147, p. 1077–1087, 2021. https://doi.org/10.1016/j.psep.2021.01.025.

ATKINSON, Christopher J.; FITZGERALD, Jean D.; HIPPS, Neil A. Potential mechanisms for achieving agricultural benefits from biochar application to temperate soils: A review. **Plant and Soil**, vol. 337, no. 1, p. 1–18, 2010. https://doi.org/10.1007/s11104-010-0464-5.

BAO, Zhengrong; DAI, Wanning; SU, Xu; LIU, Zunqi; AN, Zhengfeng; SUN, Qiang; JING, Hang; LIN, Li; CHEN, Yixuan; MENG, Jun. Long-term biochar application promoted soil aggregate-associated potassium availability and maize potassium uptake. **GCB Bioenergy**, vol. 16, no. 4, p. 1–13, 2024. https://doi.org/10.1111/gcbb.13134.

BEGUM, Farida; KARMOKER, J. L.; FATTAH, Q. A.; MANIRUZZAMAN, A. F.M. The effect of salinity on germination and its correlation with K+, Na+, Cl- accumulation in germinating seeds of Triticum aestivum L. cv. akbar. **Plant and Cell Physiology**, vol. 33, no. 7, p. 1009–1014, 1992. .

BILIAS, Fotis; KALDERIS, Dimitrios; RICHARDSON, Clive; BARBAYIANNIS, Nikolaos; GASPARATOS, Dionisios. Biochar application as a soil potassium management strategy: A review. **Science of the Total Environment**, vol. 858, no. August 2022, p. 159782, 2023. DOI 10.1016/j.scitotenv.2022.159782. Available at: https://doi.org/10.1016/j.scitotenv.2022.159782.

BRICHI, Lisiane; FERNANDES, João V.M.; SILVA, Beatriz M.; VIZÚ, Juliana de F.; JUNIOR, Jorge N.G.; CHERUBIN, Maurício Roberto. Organic residues and their impact on soil health, crop production and sustainable agriculture: A review including bibliographic analysis. **Soil Use and Management**, vol. 39, no. 2, p. 686–706, 2023. https://doi.org/10.1111/sum.12892.

BRITTO, Dev T.; COSKUN, Devrim; KRONZUCKER, Herbert J. Potassium physiology from Archean to Holocene: A higher-plant perspective. **Journal of Plant Physiology**, vol. 262, no. March, p. 153432, 2021. DOI 10.1016/j.jplph.2021.153432. Available at: https://doi.org/10.1016/j.jplph.2021.153432.

CASTRO-SUAREZ, John R.; COLPAS-CASTILLO, Fredy; TARON-DUNOYER, Arnulfo. Chemical and Morphologic Characterization of Sylvite (KCl) Mineral from Different Deposits Used in the Production of Fertilizers. **Agronomy**, vol. 13, no. 1, 2023. https://doi.org/10.3390/agronomy13010052.

CHEN, Guanyi; WANG, Yuting; WANG, Jiangtao; WANG, Junxia; YU, Fan; MA, Qingxu; CHENG, Zhanjun; YAN, Beibei; SONG, Yuchao; CUI, Xiaoqiang. Production of potassium-enriched biochar from Canna indica: Transformation and release of potassium. **Waste**

Management, vol. 164, no. March, p. 119–126, 2023. DOI 10.1016/j.wasman.2023.03.044. Available at: https://doi.org/10.1016/j.wasman.2023.03.044.

CHEN, Tse Lun; CHEN, Li Heng; LIN, Yupo J.; YU, Chang Ping; MA, Hwong wen; CHIANG, Pen Chi. Advanced ammonia nitrogen removal and recovery technology using electrokinetic and stripping process towards a sustainable nitrogen cycle: A review. **Journal of Cleaner Production**, vol. 309, no. April, p. 127369, 2021. DOI 10.1016/j.jclepro.2021.127369. Available at: https://doi.org/10.1016/j.jclepro.2021.127369.

CHENG, Jiali; ZHANG, Jiaming; XIAO, Xiao; YUAN, Yue; LIAO, Xuepin; SHI, Bi; ZHANG, Suyi. Potassium assisted pyrolysis of Chinese Baijiu distillers' grains to prepare biochar as controlled-release K fertilizer. **Science of the Total Environment**, vol. 884, no. April, p. 163814, 2023. DOI 10.1016/j.scitotenv.2023.163814. Available at: https://doi.org/10.1016/j.scitotenv.2023.163814.

CLARKSON, David; HANSON, John B. The mineral nutrition of higher plants. **Annual review of plant physiology**, vol. 31, p. 239–298, 1980. .

DAI, Qianjin; XIANG, Wei; LIU, Qiang; WANG, Min; ZHANG, Xueyang; ZHANG, Xueyang. Co-pyrolysis biochar derived from sewage sludge and lignin: Synergetic effect and adsorption properties. **Journal of Environmental Chemical Engineering**, vol. 10, no. 3, p. 107898, 2022. DOI 10.1016/j.jece.2022.107898. Available at: https://doi.org/10.1016/j.jece.2022.107898.

DANESHGAR, Saba; BUTTAFAVA, Armando; CALLEGARI, Arianna; CAPODAGLIO, Andrea G. Simulations and laboratory tests for assessing phosphorus recovery efficiency from sewage sludge. **Resources**, vol. 7, no. 3, p. 1–14, 2018. https://doi.org/10.3390/resources7030054.

DAVAND, Hiva; SEPEHR, Ebrahim; MOMTAZ, Hamid Reza; AHMADI, Fatemeh. Wastewater irrigation: An opportunity for improving soil phosphorus availability; PHREEQC modeling and adsorption studies. **Science of the Total Environment**, vol. 851, no. August, p. 158180, 2022. DOI 10.1016/j.scitotenv.2022.158180. Available at: https://doi.org/10.1016/j.scitotenv.2022.158180.

DOMINGUES, Rimena R.; SÁNCHEZ-MONEDERO, Miguel A.; SPOKAS, Kurt A.; MELO, Leônidas C.A.; TRUGILHO, Paulo F.; VALENCIANO, Murilo Nunes; SILVA, Carlos A. Enhancing cation exchange capacity ofweathered soils using biochar: Feedstock, pyrolysis conditions and addition rate. **Agronomy**, vol. 10, no. 6, p. 1–17, 2020. https://doi.org/10.3390/agronomy10060824.

DOMINGUES, Rimena R.; TRUGILHO, Paulo F.; SILVA, Carlos A.; DE MELO, Isabel Cristina N.A.; MELO, Leónidas C.A.; MAGRIOTIS, Zuy M.; SÁNCHEZ-MONEDERO, Miguel A. Properties of biochar derived from wood and high-nutrient biomasses with the aim of agronomic and environmental benefits. **PLoS ONE**, vol. 12, no. 5, p. 1–19, 2017. https://doi.org/10.1371/journal.pone.0176884.

FAN, Shisuo; LI, Hui; WANG, Yi; WANG, Zhen; TANG, Jie; TANG, Jun; LI, Xuede. Cadmium removal from aqueous solution by biochar obtained by co-pyrolysis of sewage sludge with tea waste. **Research on Chemical Intermediates**, vol. 44, no. 1, p. 135–154, 2018.

https://doi.org/10.1007/s11164-017-3094-1.

FAO. FAOSTAT. 2021. Available at: https://www.fao.org/faostat/en/#data/RFN/visualize.
GAO, Yukun; LIANG, Benliang; CHEN, Huaxiang; YIN, Penggang. An experimental study on the recovery of potassium (K) and phosphorous (P) from synthetic urine by crystallization of magnesium potassium phosphate. **Chemical Engineering Journal**, vol. 337, no. December 2017, p. 19–29, 2018. DOI 10.1016/j.cej.2017.12.077. Available at: https://doi.org/10.1016/j.cej.2017.12.077.

GEILFUS, Christoph Martin. Review on the significance of chlorine for crop yield and quality. **Plant Science**, vol. 270, no. December 2017, p. 114–122, 2018. DOI 10.1016/j.plantsci.2018.02.014. Available at: https://doi.org/10.1016/j.plantsci.2018.02.014.

GREGORICH, E. G.; CARTER, M. R.; ANGERS, D. A.; MONREAL, C. M.; ELLERT, B. H. Towards a minimum data set to assess soil organic matter quality in agricultural soils. **Canadian Journal of Soil Science**, vol. 74, no. 4, p. 367–385, 1994. https://doi.org/10.4141/cjss94-051.

GUNNARSSON, Matilda; LALANDER, Cecilia; MCCONVILLE, Jennifer R. Estimating environmental and societal impacts from scaling up urine concentration technologies. **Journal of Cleaner Production**, vol. 382, no. November 2022, p. 135194, 2023. DOI 10.1016/j.jclepro.2022.135194. Available at: https://doi.org/10.1016/j.jclepro.2022.135194.

HE, Jiazhou; ZHOU, Jieqin; YANG, Kui; LUO, Liang; WANG, Pan; WANG, Zhiwei; MA, Jinxing. Pulsed electric field drives chemical-free membrane stripping for high ammonia recovery from urine. **Water Research**, vol. 251, no. January, p. 121129, 2024. DOI 10.1016/j.watres.2024.121129. Available at: https://doi.org/10.1016/j.watres.2024.121129.

HOFFLAND, Ellis; KUYPER, Thomas W.; COMANS, Rob N.J.; CREAMER, Rachel E. Eco-functionality of organic matter in soils. **Plant and Soil**, vol. 455, no. 1–2, p. 1–22, 2020. https://doi.org/10.1007/s11104-020-04651-9.

HUANG, Haiming; ZHANG, Dingding; WANG, Wenjun; LI, Bing; ZHAO, Ning; LI, Jing; DAI, Jiankun. Alleviating Na+ effect on phosphate and potassium recovery from synthetic urine by K-struvite crystallization using different magnesium sources. **Science of the Total Environment**, vol. 655, p. 211–219, 2019. DOI 10.1016/j.scitotenv.2018.11.259. Available at: https://doi.org/10.1016/j.scitotenv.2018.11.259.

JI, Mengyuan; WANG, Xiaoxia; USMAN, Muhammad; LIU, Feihong; DAN, Yitong; ZHOU, Lei; CAMPANARO, Stefano; LUO, Gang; SANG, Wenjing. Effects of different feedstocks-based biochar on soil remediation: A review. **Environmental Pollution**, vol. 294, no. October 2021, p. 118655, 2022. DOI 10.1016/j.envpol.2021.118655. Available at: https://doi.org/10.1016/j.envpol.2021.118655.

JIA, Mingyun; YU, Jinping; LI, Zhu; WU, Longhua; CHRISTIE, Peter. Effects of biochar on the migration and transformation of metal species in a highly acid soil contaminated with multiple metals and leached with solutions of different pH. **Chemosphere**, vol. 278, p. 130344, 2021. DOI 10.1016/j.chemosphere.2021.130344. Available at: https://doi.org/10.1016/j.chemosphere.2021.130344.

JIN, Junwei; WANG, Minyan; CAO, Yucheng; WU, Shengchun; LIANG, Peng; LI, Yanan; ZHANG, Jianyun; ZHANG, Jin; WONG, Ming Hung; SHAN, Shengdao; CHRISTIE, Peter. Cumulative effects of bamboo sawdust addition on pyrolysis of sewage sludge: Biochar properties and environmental risk from metals. **Bioresource Technology**, vol. 228, p. 218–226, 2017. DOI 10.1016/j.biortech.2016.12.103. Available at: http://dx.doi.org/10.1016/j.biortech.2016.12.103.

JOHANNES LEHMANN. Bio-Energy in the Black. **Frontiers in Ecology and the Environment**, vol. 5, no. September, p. 381–387, 2007. Available at: http://www.jstor.org/stable/20440704%0Ahttp://about.jstor.org/terms%0Ahttp://discovery.ucl.ac.uk/1322126/.

KABDAŞLI, Işık; KUŞÇUOĞLU, Sezen; TÜNAY, Olcay; SICILIANO, Alessio. Assessment of K-Struvite Precipitation as a Means of Nutrient Recovery from Source Separated Human Urine. **Sustainability (Switzerland)**, vol. 14, no. 3, 2022. https://doi.org/10.3390/su14031082.

KABDAŞLI, Işık; SICILIANO, Alessio; LIMONTI, Carlo; TÜNAY, Olcay. Is K-Struvite Precipitation a Plausible Nutrient Recovery Method from Potassium-Containing Wastes?—A Review. **Sustainability (Switzerland)**, vol. 14, no. 18, 2022. https://doi.org/10.3390/su141811680.

KAMAU, Solomon; KARANJA, Nancy K.; AYUKE, Fredrick O.; LEHMANN, Johannes. Short-term influence of biochar and fertilizer-biochar blends on soil nutrients, fauna and maize growth. **Biology and Fertility of Soils**, vol. 55, no. 7, p. 661–673, 2019. https://doi.org/10.1007/s00374-019-01381-8.

LEHMANN, Johannes; RONDON, Marco. Bio-Char Soil Management on Highly Weathered Soils in the Humid Tropics. , p. 517–529, 2006. https://doi.org/10.1201/9781420017113.ch36.

LIN, Sheng Lun; ZHANG, Hongjie; CHEN, Wei Hsin; SONG, Mengjie; KWON, Eilhann E. Low-temperature biochar production from torrefaction for wastewater treatment: A review. **Bioresource Technology**, vol. 387, no. June, p. 129588, 2023. DOI 10.1016/j.biortech.2023.129588. Available at: https://doi.org/10.1016/j.biortech.2023.129588.

LIU, Qiting; SUN, Wenhui; ZENG, Qianhao; ZHANG, Haodong; WU, Chengyang; LICHTFOUSE, Eric; LIU, Hongbo. Integrated processes for simultaneous nitrogen, phosphorus, and potassium recovery from urine: A review. **Journal of Water Process Engineering**, vol. 59, no. December 2023, p. 104975, 2024. DOI 10.1016/j.jwpe.2024.104975. Available at: https://doi.org/10.1016/j.jwpe.2024.104975.

LOPES, A. S.; GUIMARÃES GUILHERME, L. R. **A career perspective on soil management in the Cerrado region of Brazil**. [*S. l.*]: Elsevier Inc., 2016. vol. 137, . DOI 10.1016/bs.agron.2015.12.004. Available at: http://dx.doi.org/10.1016/bs.agron.2015.12.004.

MALAVOLTA, E. **Elementos de nutrição mineral de plantas**. São Paulo: Agronômica Ceres, 1980.

MARTIN, Tristan M.P.; ESCULIER, Fabien; LEVAVASSEUR, Florent; HOUOT, Sabine. Human urine-based fertilizers: A review. **Critical Reviews in Environmental Science and Technology**, vol. 52, no. 6, p. 890–936, 2022. DOI 10.1080/10643389.2020.1838214. Available at: https://doi.org/10.1080/10643389.2020.1838214.

MELO, Leônidas Carrijo Azevedo; LEHMANN, Johannes; CARNEIRO, Jefferson Santana da Silva; CAMPS-ARBESTAIN, Marta. Biochar-based fertilizer effects on crop productivity: a meta-analysis. **Plant and Soil**, vol. 472, no. 1–2, p. 45–58, 2022. DOI 10.1007/s11104-021-05276-2. Available at: https://doi.org/10.1007/s11104-021-05276-2.

MORI ALVEZ, Cristina; ERNST BENECH, Oswaldo; GONZÁLEZ BARRIOS, Pablo; PERDOMO VARELA, Carlos. Wheat productivity and nitrogen use efficiency in no-till systems: a comparative analysis of crop-pasture and continuous cropping rotations in Uruguay. **Frontiers in Sustainable Food Systems**, vol. 8, no. December, p. 1–17, 2024. https://doi.org/10.3389/fsufs.2024.1460734.

NATIVIDAD-MARIN, Leynard; WILLIAM BURNS, Max; SCHNEIDER, Phil. A comparison of struvite precipitation thermodynamics and kinetics modelling techniques. **Water Science and Technology**, vol. 87, no. 6, p. 1393–1422, 2023. https://doi.org/10.2166/wst.2023.061.

NORTJÉ, G. P.; LAKER, M. C. Soil fertility trends and management in Conservation Agriculture: a South African perspective. **South African Journal of Plant and Soil**, vol. 38, no. 3, p. 247–257, 2021. https://doi.org/10.1080/02571862.2021.1896039.

PARAMISPARAM, Puvan; AHMED, Osumanu Haruna; OMAR, Latifah; CH'NG, Huck Ywih; JOHAN, Prisca Divra; HAMIDI, Nur Hidayah. Co-application of charcoal and wood ash to improve potassium availability in tropical mineral acid soils. **Agronomy**, vol. 11, no. 10, p. 1–30, 2021. https://doi.org/10.3390/agronomy11102081.

PATHY, Abhijeet; RAY, Jyotiprakash; PARAMASIVAN, Balasubramanian. Challenges and opportunities of nutrient recovery from human urine using biochar for fertilizer applications. **Journal of Cleaner Production**, vol. 304, p. 127019, 2021. DOI 10.1016/j.jclepro.2021.127019. Available at: https://doi.org/10.1016/j.jclepro.2021.127019.

RANDALL, D. G.; NAIDOO, V. Urine: The liquid gold of wastewater. **Journal of Environmental Chemical Engineering**, vol. 6, no. 2, p. 2627–2635, 2018. https://doi.org/10.1016/j.jece.2018.04.012.

SALIU, Toyin Dunsin; OLADOJA, Nurudeen Abiola; SAUVÉ, Sébastien. Eco-friendly and sustainability assessment of technologies for nutrient recovery from human urine—a review. **Frontiers in Sustainability**, vol. 4, no. January, p. 1–20, 2023. https://doi.org/10.3389/frsus.2023.1338380.

SCHUELER, Tamara A.; DOURADO, Marcelo L.; VIDEIRA, Sandy S.; DA CUNHA, Claudia D.; RIZZO, Andréa C.L. Biosolubilization of verdete: An alternative potassium source for agriculture fertilizer. **Biocatalysis and Agricultural Biotechnology**, vol. 34, no. May, 2021. https://doi.org/10.1016/j.bcab.2021.102031.

SHAN, Jinhua; LIU, Hongbo; LONG, Shiping; ZHANG, Haodong; LICHTFOUSE, Eric. Electrochemical crystallization for recovery of phosphorus and potassium from urine as K-struvite with a sacrificial magnesium anode. **Environmental Chemistry Letters**, vol. 20, no. 1, p. 27–33, 2022. DOI 10.1007/s10311-021-01333-5. Available at: https://doi.org/10.1007/s10311-021-01333-5.

SHARMA, Ruchi; SINDHU, Satyavir S.; GLICK, Bernard R. **Potassium Solubilizing Microorganisms as Potential Biofertilizer: A Sustainable Climate-Resilient Approach to Improve Soil Fertility and Crop Production in Agriculture**. [*S. l.*]: Springer US, 2024. vol. 43, . DOI 10.1007/s00344-024-11297-9. Available at: https://doi.org/10.1007/s00344-024-11297-9.

SOLTANI, Saeede; NATIVIDAD-MARIN, Leynard; SCHNEIDER, Philip Andrew. A modelling approach to prepare synthetic urine for struvite precipitation studies. **Water Science and Technology**, vol. 87, no. 11, p. 2622–2633, 2023. https://doi.org/10.2166/wst.2023.157.

SPARKS, D L. Bioavailability of soil potassium. **Handbook of Soil Science**, , p. D38–D53, 2000. .

SUDARSAN, J. S.; ROY, Reenu Lizbeth; NITHIYANANTHAM, S. Mass Balance Study on Domestic Wastewater Treatment Using Constructed Wetlands. **Journal of Water Chemistry and Technology**, vol. 43, no. 6, p. 497–502, 2021. https://doi.org/10.3103/s1063455x21060096.

TAN, Zhongxin; LIU, Liyun; ZHANG, Limei; HUANG, Qiaoyun. Mechanistic study of the influence of pyrolysis conditions on potassium speciation in biochar "preparation-application" process. **Science of the Total Environment**, vol. 599–600, p. 207–216, 2017. DOI 10.1016/j.scitotenv.2017.04.235. Available at: http://dx.doi.org/10.1016/j.scitotenv.2017.04.235.

TAO, Jiaqi; WU, Wenhao; LIN, Daohui; YANG, Kun. Role of biochar pyrolysis temperature on intracellular and extracellular biodegradation of biochar-adsorbed organic compounds. **Environmental Pollution**, vol. 346, no. October 2023, p. 123583, 2024. DOI 10.1016/j.envpol.2024.123583. Available at: https://doi.org/10.1016/j.envpol.2024.123583.

TÜRK, Feride N.; ARSLANOĞLU, Hasan. Recovery of Potassium from Pyrolysis Product of Sugar Fabrication Waste Carbonation Cake and Vinasse Mixture and Production of Adsorbent for Wastewater Treatment. **Sugar Tech**, vol. 26, no. 2, p. 478–488, 2024. DOI 10.1007/s12355-024-01364-6. Available at: https://doi.org/10.1007/s12355-024-01364-6.

VAN LOON, C. D.; VAN DEN BERG, W. The effect of chloride fertilization on blackspot susceptibility and other quality characteristics and on yield of potato. **Potato Research**, vol. 46, no. 3–4, p. 147–154, 2003. https://doi.org/10.1007/BF02736084.

VAN NGUYEN, Quang; NGUYEN, Khai Manh; NGUYEN, Hung The; VAN HOANG, Hung; DUONG, Tuan Dinh; DONG, Mai Thi Ngoc; TRAN, Hang Thi Minh. Transforming Domestic Wastewater into Hydroponic Nutrients Using Corncob-Derived Biochar Adsorption. **Journal of Soil Science and Plant Nutrition**, no. 0123456789, 2025. DOI 10.1007/s42729-025-02362-7. Available at: https://doi.org/10.1007/s42729-025-02362-7.

WEBER, Kathrin; QUICKER, Peter. Properties of biochar. **Fuel**, vol. 217, no. December 2017, p. 240–261, 2018. DOI 10.1016/j.fuel.2017.12.054. Available at: https://doi.org/10.1016/j.fuel.2017.12.054.

WOOLF, Dominic; LEHMANN, Johannes; OGLE, Stephen; KISHIMOTO-MO, Ayaka W.;

MCCONKEY, Brian; BALDOCK, Jeffrey. Greenhouse Gas Inventory Model for Biochar Additions to Soil. **Environmental Science and Technology**, vol. 55, no. 21, p. 14795–14805, 2021. https://doi.org/10.1021/acs.est.1c02425.

WU, Haotian; FOSTER, Xavier; KAZEMIAN, Hossein; VANEECKHAUTE, Céline. N, P, K recovery from hydrolysed urine by Na-chabazite adsorption integrated with ammonia stripping and (K-)struvite precipitation. **Science of the Total Environment**, vol. 857, no. October 2022, 2023. https://doi.org/10.1016/j.scitotenv.2022.159277.

XIU, Liqun; GU, Wenqi; SUN, Yuanyuan; WU, Di; WANG, Yuning; ZHANG, Honggui; ZHANG, Weiming; CHEN, Wenfu. The fate and supply capacity of potassium in biochar used in agriculture. **Science of the Total Environment**, vol. 902, no. March, 2023. https://doi.org/10.1016/j.scitotenv.2023.165969.

XU, Kangning; LI, Jiyun; ZHENG, Min; ZHANG, Chi; XIE, Tao; WANG, Chengwen. The precipitation of magnesium potassium phosphate hexahydrate for P and K recovery from synthetic urine. **Water Research**, vol. 80, p. 71–79, 2015. DOI 10.1016/j.watres.2015.05.026. Available at: http://dx.doi.org/10.1016/j.watres.2015.05.026.

2 SECOND PART

2.1 MANUSCRIPTS

Manuscript 1 - Agronomic Effectiveness of Biochar–KCl Composites for Corn Cultivation in Tropical Soils *(Paper published at Soil Systems Journal DOI: doi.org/10.3390/soilsystems9020045)*

Manuscript 2 - Potassium recovery from urine via struvite precipitation and biochar-enhanced retention *(Preliminary version of manuscript edited following the rules of ABNT)*

Paper published at Soil Systems Journal
DOI: doi.org/10.3390/soilsystems9020045

2.1.1 Agronomic Effectiveness of Biochar–KCl Composites for Corn Cultivation in Tropical Soils

Gabrielly Nayara Tavares Silva Rodrigues[1], Carlos Alberto Silva[1*], Everton Geraldo de Morais[1].

[1] Escola de Ciências Agrárias de Lavras, Universidade Federal de Lavras, Lavras 37200-900, Brazil; ga-briellynts@gmail.com (G.N.T.S.R.); evertonmoraislp@gmail.com (E.G.d.M).

* Correspondence: csilva@ufla.br; Tel.: (C.A.S)

Abstract: Potassium chloride (KCl) is the main source of potassium (K) in Brazilian agriculture, but its high import dependency and the need for split applications increase costs and expose the system to supply and efficiency risks. Understanding the availability and release kinetics of potassium (K) from biochar-based fertilizers (K-BBFs) is crucial for optimizing their use as full or partial substitutes for KCl in Brazilian agriculture. This study evaluated biochars derived from banana peel (BP), coffee husk (CH), and chicken manure (CM), both in their pure form and co-pyrolyzed with KCl (composites) at 300 °C and 650 °C, as K sources for corn grown in two contrasting Oxisols. For pure biochars, feedstock type and pyrolysis temperature significantly influenced K content and release kinetics. Higher pyrolysis temperatures increased K content in BP and CH biochars but not in CM, while also slowing K release in CH and CM. Co-pyrolysis with KCl increased biochar yield, ash content, and K availability. Composites released more K than pure biochar but less than KCl, and at a slower rate. Notably, banana peel biochar co-pyrolyzed with KCl at 650 °C (CBP650) exhibited 36% slower K release and reduced KCl use by 82% while maintaining similar K use efficiency and corn growth. All K-BBFs matched KCl in promoting robust corn growth in clay soil, increasing biomass by 5.3 times and K uptake by 9 times compared to unfertilized (no K addition) plants. In sandy Oxisol, K-BBFs boosted biomass by up to 3.5 times compared to unfertilized plants, though some pure biochars were less effective than KCl in supporting full corn growth. Soil texture strongly influenced K availability, with sandier soils exhibiting higher K levels in solution. These findings suggest that kinetic release studies in abiotic systems, such as lysimeters with sand, are not suitable for evaluating K-BBFs as slow-release fertilizers. Due to lower K retention in sandy soil and solution K levels exceeding 1100 mg L^{-1}, split applications of some K-BBFs are recommended to prevent corn cation uptake imbalances and soil K leaching. Additionally, granulating biochar–KCl composites may enhance K retention and regulate its release in sandy Oxisols.

Keywords: Composites; Co-pyrolysis; Slow-release potassium fertilizers; K in soil solution; waste K recycling.

1. Introduction

Potassium is a nutrient required in large quantities by plants, ranking as the second most abundant element in plant tissue [1,2]. The highly weathered soils in Brazil have naturally low K availability, making crops grown in these soils heavily dependent on K fertilizers imported from foreign countries. In 2022, over 7.5 million tons of KCl were imported, significantly increasing food production costs [3,4]. Potassium chloride is mined in only a few countries and is highly soluble, with a high saline index and elevated Cl content, which can potentially harm seed germination, crop growth, and development [5,6]. As a result, KCl requires splitting and careful application or, in some cases, replacement with alternative K sources that are chloride-free and offer improved agronomic effectiveness [7,8]. In recent years, research on alternative K sources in agriculture, such as biochar used alone or enriched with K fertilizers, has increased [9]. Biochar (BC) is a solid material produced through the pyrolysis of renewable organic wastes in the absence of oxygen [10,11]. Its properties depend on both the type of feedstock and the intensity of the pyrolysis conditions [12–15]. Thus, feedstock selection and pyrolysis temperature can be deliberately adjusted to achieve specific desired properties and K content in the final biochar [16–18]. Due to its diverse characteristics, BC is used to enhance ecosystem functions, including water filtration, greenhouse gas emission reduction, soil organic carbon storage, water retention, soil biota improvement, soil conditioning, and increased crop yields [19–23]. Some biochars also serve as nutrient sources, supplying essential elements such as N, P, and K to crops [24–26]. Consequently, research on the application of biochar for soil fertility improvement and its use as a fertilizer has expanded over the past two decades [27].

Among the alkali metals, K is typically the most abundant element in plant biomass. Its content can vary widely, ranging from 0.5 to 19 g kg^{-1} in common organic residues such as wood and sewage sludge to as high as 40–122 g kg^{-1} in algae and post-harvest food waste [28]. The ability of biochar to supply K to plants depends significantly on the feedstock type and pyrolysis temperature used in its production [29]. Understanding the K content and retention capacity of different feedstocks allows for the optimization of pyrolysis conditions to produce high-value biochar-based K fertilizers (K-BBFs). Pristine biochars often lack sufficient nutrient concentrations to serve effectively as fertilizers, as nutrients may be either inadequately concentrated, lost during pyrolysis, or released too slowly or inconsistently to meet crop demands. To address these challenges, various physical and chemical methods have been developed to enhance the agronomic value of biochars and their use as raw materials for fertilizer synthesis [30,31]. Feedstocks with higher K contents require lower pyrolysis

temperatures for effective K concentration [32], while biomass with lower K contents can be enriched with KCl to produce fertilizers that can be applied at lower rates than raw biochars [28,33]. Identifying K-rich raw materials suitable for direct K-BBF production and integrating biochar with mineral K sources offer an environmentally sustainable and practical strategy for recycling K from waste materials generated in large quantities in Brazil. This approach not only enhances the agronomic effectiveness of mineral K fertilizers but also aligns with circular economy principles while providing the additional benefits of biochar application in agricultural soils [26,30].

Research indicates that potassium fertilizers derived from biochar can achieve equal or even superior efficiency in plant growth compared to mineral fertilizers [34]. Moreover, the potassium release from engineered biochars is slower than that from KCl [35–37]. For the development of these engineered biochars, it is recommended to employ physical and chemical techniques during both the pre- and post-production stages, such as co-pyrolysis, to enhance biochar properties and K content in the final composite. Co-pyrolysis is a process that combines two or more materials to obtain a composite whose technical performance, in a synergistic manner, overcomes its initial inputs. This process is carried out in the same industrial and lab apparatus as simple pyrolysis [16]. Among the benefits of co-pyrolysis, the improvement in the BC pore structure; the increase in heating value, biochar yield, and nutrient enrichment, including K content, in biochars; and the improvement in the control of nutrient release into the soil solution can be mentioned [38,39].

Research on K-rich feedstocks for the production of K-BBFs and the nutrient release dynamics of these fertilizers remains limited in Brazil. Furthermore, no studies have yet investigated the co-pyrolysis of feedstocks with high K content with KCl to produce a fertilizer with a K content comparable to that of mineral K fertilizers (~50% K). Additionally, it remains unclear whether the resulting products, hereafter referred to as composites, can be classified as slow-release K fertilizers. These composites have the potential to combine the benefits of biochar with the readily available K from KCl, ensuring a balanced nutrient supply for plants. To explore this potential, banana peel (BP), coffee husk (CH), and chicken manure (CM) were selected as feedstocks for K-rich BBF production. These feedstocks were chosen based on their relatively high K content compared to those evaluated in previous studies, their widespread availability, and their role in promoting the valorization of Brazilian agricultural and organic wastes [40–44]. Their use contributes to sustainable waste management, enhances the value of agro-industrial byproducts containing K compounds, and allows the production of high agronomic value K fertilizers [45–47]. Corn (Zea mays L.) was selected as the test crop due to

its global agricultural importance and its prominent role in Brazilian farming systems [48]. As one of the most widely cultivated crops in Brazil, corn has high potassium requirements and is highly responsive to K fertilization [49]. Optimizing K fertilization for corn is crucial not only for maximizing yield but also for reducing production costs, especially in regions with sandy soils and low K retention capacity [50].

Therefore, this study aimed to evaluate the potential of different K-rich biomasses (BP, CH, and CM), processed at two pyrolysis temperatures (300 and 650 °C), as well as their co-pyrolysis with KCl, for producing high-value K fertilizers. It also sought to investigate K release kinetics under controlled and soil-based conditions and assess the effectiveness of biochar–KCl composites in supplying K to corn grown in soils with contrasting textures and organic matter content. We hypothesized the following: (i) all K-BBFs would exhibit high agronomic value regardless of feedstock or temperature; (ii) higher pyrolysis temperatures would enhance K content and reduce the need for KCl in composites; (iii) K-BBFs would release K more slowly than KCl; (iv) some K-BBFs would match the agronomic performance of KCl; (v) K release dynamics would depend on soil texture.

2. Materials and Methods

2.1. Biochar Synthesis: Feedstocks and Pyrolysis Conditions

Banana peel (BP), coffee husk (CH), and chicken manure (CM) were collected from different locations in the city of Lavras (Minas Gerais State, Brazil) for biochar production. The collected feedstocks were dried in a forced-air circulation oven at 70 °C until they reached a constant weight, ground, and stored in covered containers for pyrolysis and further analysis of K contents. The K contents found in the feedstocks were as follows: BP 6.2%; CH, 2.6%; and CM 3.0%. For pyrolysis, the feedstocks were placed in stainless steel cylinders with lids, weighed, and then transferred to an electric muffle furnace equipped with a pyrolysis chamber and an automatic temperature sensor for slow pyrolysis. The heating rate was 10 °C min^{-1}, aiming to reach the target temperature (300 °C and 650 °C) which was maintained for 60 min. After pyrolysis, the biochars were cooled to room temperature, weighed to obtain the biochar yield, and then ground using an agate mortar and pestle, following the procedure adapted from Morais et al. (2023) [51]. The ground charred material passed through a 60-mesh sieve for the characterization analyses of the final biochars and synthesized composites. To unveil the capacity of the feedstocks to retain K after pyrolysis, the K retention of the pure biochars was calculated using Equation (1), adapted from Lang et al. [52].

$$Biochar\ K\ Retention\ (\%) = \frac{K\ in\ biochar\ (\%)}{K\ in\ feedstock\ (\%)} * biochar\ yield\ (\%) \quad (1)$$

2.2. Co-pyrolysis

In the co-pyrolysis stage, each feedstock was mixed with KCl to achieve a potential 50% K content in the final composite. The proportions of raw material and KCl were calculated based on the K retention in the composites (Equation (2)), adapted from Carneiro et al. [53]. The composites were also pyrolyzed under the same conditions as described in Section 2.1.

$$K\ retention\ = \frac{K_{Comp} * Yield_{Comp}}{(K_{BC} * Yield_{BC}) + (K_{KCl} * Yield_{KCl})} \quad (2)$$

where K and yield are the K content (%) and yield (%) of the composite, pure biochar, and KCl, respectively. The acronyms, pyrolysis temperatures, and proportions of K from the KCL and feedstocks of the formulated biochars and composites are shown and described in detail in Table 1.

Table 1. The acronyms and descriptions of the main features of the final biochars and produced K-BBFs.

Feedstock	Biochar Type	Pyrolysis temperature (°C)	K from Feedstock (%)	K from KCl (%)	Acronym
Banana peel	Pure	300	100	0	BBP300
	Pure	650	100	0	BBP650
	Composite	300	60	40	CBP300
	Composite	650	82	18	CBP650
Coffee husk	Pure	300	100	0	BCH300
	Pure	650	100	0	BCH650
	Composite	300	65	35	CCH300
	Composite	650	78	22	CCH650
Chicken manure	Pure	300	100	0	BCM300
	Pure	650	100	0	BCM650
	Composite	300	45	55	CCM300
	Composite	650	57	43	CCM650

2.3. Characterization of Feedstocks, Biochars and Composites

Electrical conductivity (EC) and pH were determined in a biochar–water suspension at a ratio of 1:10 (w:v). The suspension was first stirred for 60 min in a shaker table, left at rest for 30 min, and then analyzed using a Hanna HI2221 digital EC and pH meter [54]. Ash content was determined by placing 1 g of each sample in an open porcelain crucible in a muffle furnace at 750 °C for 6 h. The remaining mass after incineration was then weighed on a precision balance. For the total carbon (C) content analysis of the biochars and composites, we used an Elementar Vario TOC Cube automatic analyzer (dry combustion). The spectral signature, bands, and peaks related to functional groups in the biochars and composites were evaluated using Fourier transform infrared–attenuated total reflectance spectroscopy (ATR-FTIR) in an Agilent® Cary 630 spectrometer (Agilent, Santa Clara, CA, USA). This analysis and the ATR-FTIR spectra were generated in the wavelength range of 4000 to 650 cm^{-1} with a resolution of 4 cm^{-1}. The main peaks were identified and interpreted according to infrared libraries and assignments of spectral bands and peaks available in other studies for organic matrices and K fertilizers. The cation exchange capacity of the pure biochars and composites was determined following the methodology proposed by Lago et al. [55], which employs partial least squares regression (PLSR) in combination with Fourier transform infrared spectroscopy (FTIR). For the determination of total K content in BBFs, a total nitric–perchloric digestion was performed with the addition of catalysts (Na_2SO_4, $CuSO_4$, and Se). Potassium concentration in the digested extracts was determined by Inductively Coupled Plasma Optical Emission Spectroscopy (ICP-OES).

2.4. Potassium Release Kinetics

Based on the total K content in the composites and pure biochars, a study of K release kinetics was conducted through sequential extractions of K eluted from sand samples with a 0.01 mol L^{-1} calcium chloride. For this purpose, mini-lysimeters were assembled, each containing a sample of biochar or composite mixed with sand (the sand was successively washed with acid solution and ultra-pure water) in three replicates [51]. A 0.45 μm diameter pore filter was inserted between the top and bottom of the mini-lysimeter; above the filter, 2 cm of glass wool was added, followed by the biochar or composite–sand mixture, and finally, another layer of 2 cm of glass wool was added to reduce the impact of the K eluent solution directly on the fertilizers, as well as to prevent the preferential flow of $CaCl_2$ in the mini-lysimeter. The amount of biochar or composite added through the mixtures corresponded to 2000 mg of K, thus varying the mass of each biochar/composite placed in each mini-lysimeter.

For the experiment, 100 mL of $CaCl_2$ solution was passed through each mini-lysimeter at each extraction time scheduled for the kinetics study, which were as follows: 0, 1, 2, 5, 12, 24, 96, 288, 480, and 672 h after the first extraction. Additionally, KCl was also placed in the mini-lysimeters as a positive control and pure washed sand served as the negative control (no K). Potassium content in the extracts was assessed using a flame photometer. After determining the K content in the extracts, the accumulated K was calculated after each evaluated time, and then the value was converted to the K release rate (%) according to Equation (3).

$$K\ release\ (\%) = \left(\frac{K_t}{K_{t0}}\right) * 100 \quad (3)$$

where Kt is the accumulated K content at each evaluated time (mg Kg^{-1}) and Kt0 is the initial total K content (mg Kg^{-1}) placed in each mini-lysimeter.

2.5. Agronomic Efficiency of Biochars and Composites

To assess the ability of the biochars to supply K to corn (Zea mays L.) plants, a greenhouse study was conducted using 2.7 dm^3 pots. The experiment was conducted in a greenhouse under natural light conditions. The average day-time temperature during the experiment was 35 °C, night-time temperature was 20 °C, and the mean relative humidity was 60%. Corn was cultivated in Red (RO) and Red-Yellow (RYO) Oxisols, which contrast in texture and organic matter (OM) content. Soils were collected from the 0 to 20 cm layer, dried, and sieved (2 mm), to obtain the air-dried fine earth (ADFE) which was used for the chemical analyses (Table 2). Soil acidity correction was performed to raise the base saturation to 70% [56], using $CaCO_3$ and $MgCO_3$ in a 4:1 ratio. Soils were mixed with carbonates and incubated for 30 days, maintaining moisture close to 60% of soil field capacity.

Among the biochars and composites, ten K sources were selected for the study of the agronomic efficiency of K fertilizers, as follows: BBP300, BBP650, CBP300, CBP650, BCH300, BCH650, CCH300, CCH650, BCM300, and CCM650. In addition to treatments with pure biochars and composites, KCl was added as a positive control (KCl), and a negative control ("No KCl") was also tested. All treatments were arranged in a randomized block design in a greenhouse, with three replicates per treatment in each of the two contrasting tropical soils, totaling 72 pots. Potassium was added to soil samples at 400 mg kg^{-1} K, applied once at planting for biochars and composites and split into 4 applications for KCl. For the remaining nutrients,

the corn plants were supplied with 400 mg kg^{-1} N, 50 mg kg^{-1} S, 20 mg kg^{-1} Zn, 5 mg kg^{-1} Mn, 4 mg kg^{-1} Cu, and 1.5 mg kg^{-1} B in both soils. Phosphorus was applied at a rate of 600 mg kg^{-1} for the Red Oxisol and 300 mg kg^{-1} for the Red-Yellow Oxisol. All the nutrients supplied to the corn plants were furnished as pure per analysis as follows: NH_4NO_3, NH_4HPO_4, $CaHPO_4.2H_2O$, $CaSO_4.2H_2O$, $ZnSO_4.7H_2O$, $MnSO_4.H_2O$, $CuSO_4.5H_2O$, and H_3BO_3.

After the initial fertilization, 10 corn seeds were sown, and soil moisture was maintained at approximately 60% of each soil's field capacity. After ten days of planting, thinning was performed, leaving two corn plants per pot. Nitrogen topdressing was performed at 10, 20, and 40 days after planting in all pots, and potassium chloride (KCl) was applied in the positive control. Soil solution samplers [57] were installed in all pots for soil solution collection at 1 (seed), 10 (V3), 20 (V6), and 50 (V12) days after planting to assess the levels of readily available K in the soil liquid phase. Approximately 10 mL of solution was extracted at each sampling time, and Ca, Mg, and K levels were determined using Inductively Coupled Plasma Optical Emission Spectroscopy (ICP-OES). All treatments and controls were tested in triplicate.

After 50 days of cultivation, the plants were harvested, dried in an oven at 60 °C until a constant weight was achieved, ground, and stored for subsequent chemical analyses. The dried biomass was weighed, and the samples were digested in a 4:1 mixture of nitric and perchloric acids. The potassium contents in the digested plant shoot extracts were determined using a flame photometer. Additionally, 30 g soil samples were collected from each experimental unit using a pot soil auger. These samples were then dried, sieved (2 mm), and stored for further analysis. The remaining (after corn cultivation) available K in the soil was extracted based on the Mehlich-1 soil test and quantified by flame spectrophotometry.

Table 2. The characterization and main attributes of the Oxisols used in corn cultivation, under natural conditions (before liming and fertilization practices).

Soil	pH	K^+	Available P	Na^+	Ca^{2+}	Mg^{2+}	Al^{3+}	H+Al
			mg dm^{-3}			$cmol_c$ dm^{-3}		
Red Oxisol	4.5	31	0.1	3.0	0.3	0.2	0.6	7.2
Red-Yellow Oxisol	4.8	226	0.1	2.5	0.9	0.4	0.4	2.8
Soil	SB	ECEC	CEC at pH7	BS	m	Clay	Silt	Sand
		$cmol_c$ dm^{-3}			%		g kg^{-1}	
Red Oxisol	0.6	1.2	7.8	7.7	50.0	620	160	220
Red-Yellow Oxisol	1.9	2.2	4.7	40.0	15.9	470	80	450
Soil	P-Rem	OM.	Zn	Fe	Mn	Cu	B	$S\text{-}SO_4^{2-}$
	mg L^{-1}	dag kg^{-1}			mg dm^{-3}			
Red Oxisol	16.6	3.7	0.3	50.6	3.4	1.1	0.1	2.5

Red-Yellow Oxisol	36.6	1.7	0.2	36.0	3.5	0.0	0.1	1.2

pH in water: 1:2.5 ratio. P, Na, K, Fe, Zn, Mn, Cu: determined with Mehlich-1 soil test. Ca, Mg, Al: extracted with 1 mol L^{-1} KCl. H + Al: extracted with SMP solution. SB: Sum of Bases. ECEC: effective cation exchange capacity at soil current pH. CEC at pH 7: cation exchange capacity at pH 7.0. BS: base saturation. m: Aluminum Saturation. OM, organic matter: determined by oxidation with $Na_2Cr_2O_7$ 4 mol L^{-1} + H_2SO_4 10 mol L^{-1}. P-Rem: remaining Phosphorus content. B: boron, extracted with hot water. S: available S-sulfate extracted with Monocalcium Phosphate mixed with acetic acid.

2.6. Statistical Analysis

For the characterization of K-BFFs, an analysis of variance (ANOVA) was performed for each variable, considering a three-way interaction model (feedstock × pyrolysis temperature × biochar type). When the three-way interaction was not significant, a new ANOVA model was applied, considering only two-way interactions. When the three-way interaction was significant ($p < 0.05$), the treatment means were compared using Duncan's multiple range test ($p < 0.05$), and the results are presented with treatment means, standard deviations, and statistical groupings. When the three-way interaction was not significant, multiple comparisons were performed based on two-way interactions, with the results reported as treatment means and standard deviations.

The data of the K release kinetics were fitted to nonlinear mathematical models to adjust the amount of leached K from the lysimeters over time. The data were fitted to the following mathematical models: a linear model (Equation (4)), exponential model (Equation (5)), power function (Equation (6)), Elovich model (Equation (7)), Toth model (Equation (8)), and Gompertz model (Equation (9)).

$$K_t = a + bt \quad (4)$$

$$K_t = N_0 \exp(-kt) \quad (5)$$

$$K_t = at^b \quad (6)$$

$$K_t = a + b \exp(-ct) \quad (7)$$

$$K_t = \frac{at}{1 + bt^n} \quad (8)$$

$$K_t = \mathrm{a} \exp[-e^{b-ct}] \quad (9)$$

where Kt is the amount of K released at time t. For the linear model, a is the initial amount of K released and b is the release rate constant over time. For the exponential model, N0 is the maximum amount of K released during the kinetics study and k is the decay rate constant for K release. For the power function, a is the scaling coefficient and b is the exponent

determining the rate of K release over time. For the Elovich model, a is the initial K content, b is the scaling coefficient, and c is the exponential decay rate constant. For the Toth model, a is the capacity-related coefficient, b is a constant that affects the curve shape, and n is the exponent related to the distribution of release sites over time. For the Gompertz model, a is the asymptote representing the maximum release, b controls the position of the inflection point, and c controls the growth rate of K release. These models were applied to describe the K release kinetics under the experimental conditions. The best mathematical model adjusted to each dataset was selected based on the highest coefficient of regression (R2) values and the lowest root mean squared error (RMSE) and Akaike Information Criterion (AIC) values [51].

For the greenhouse experiment, Principal Component Analysis (PCA) was applied to identify patterns in the dataset and evaluate the effects of different K-BBFs on corn growth in two distinct tropical soil types. All statistical analyses were conducted using R (version 4.3.1), and the following packages: tidyverse (version 2.0.0), MASS (version 7.3.60), and multcomp (version 1.24.25) [58–62]. For the FTIR spectra plotting, normalization was conducted using Chemoface (version 1.66) [63].

3. Results and Discussion

3.1. Biochar and Composite Properties

The main properties of the biochars and composites (K-BBFs) produced in this work are shown in Table 3. These physicochemical characteristics are essential to understanding the behavior of each material as a potential potassium fertilizer, especially in relation to its nutrient content, release dynamics, and interaction with soil. Properties such as yield, ash content, total carbon, pH, electrical conductivity (EC), potassium content, functional groups (FTIR), and cation exchange capacity (CEC) were evaluated to compare the influence of feedstock type, pyrolysis temperature, and co-pyrolysis with KCl on the performance of the resulting K-BBFs.

Table 3. The main properties of pure biochars and derived composites.

BBF	Biochar yield	Ash	C	pH		EC	
	(%)					dS m^{-1}	
BBP300	58.6	18.08 ± 0.59	54.9	9.44 ± 0.03	f	16.96 ± 0.03	e
BBP650	32.4	31.08 ± 1.13	55.3	9.97 ± 0.02	c	28.40 ± 0.52	d
CBP300	73.6	56.75 ± 7.69	30.7	7.95 ± 0.15	i	81.03 ± 1.27	b
CBP650	44.4	58.26 ± 0.52	39.2	9.63 ± 0.01	de	69.70 ± 4.74	c
BCH300	46.0	14.40 ± 0.26	66.4	10.11 ± 0.04	c	8.80 ± 0.19	f
BCH650	30.7	20.04 ± 0.52	71.2	9.71 ± 0.05	d	15.08 ± 0.04	e
CCH300	66.2	58.59 ± 0.40	34.8	7.93 ± 0.07	i	75.07 ± 3.12	c

CCH650	45.6	53.80 ± 0.61	39.9	9.56 ± 0.02	ef	72.97 ± 0.59	c
BCM300	69.2	47.56 ± 0.33	27.8	8.52 ± 0.04	g	7.20 ± 0.56	f
BCM650	55.4	61.09 ± 0.73	22.9	10.65 ± 0.02	a	7.40 ± 0.46	f
CCM300	86.4	79.51 ± 1.04	11.2	8.17 ± 0.24	h	87.37 ± 10.56	a
CCM650	73.8	82.96 ± 0.36	12.7	10.41 ± 0.02	b	86.17 ± 1.37	ab

The same letter indicates no significant difference among treatment means by Duncan test at $p < 0.05$. EC: electrical conductivity; BBP: biochar of banana peel; CBP: composite of banana peel; BCH: biochar of coffee husk; CCH: composite of coffee husk; BCM: biochar of chicken manure; CCM: composite of chicken manure.

3.1.1. Yield

Regardless of the feedstock, the pure biochar yield decreased with rising pyrolysis temperature. Biochars derived from CM showed the highest yields, with a 20% decrease as the temperature was elevated to 650 °C. Next were the biochars from BP, which showed a 44% decrease in yield content with increasing pyrolysis temperature. Finally, the biochars from CH showed a 34% reduction as the temperature increased. The highest yield, observed for the chicken manure biochar, can be attributed to its high ash content, with values similar to those reported by Piash et al. (2021) [64], which is likely due to the elevated levels of inorganic compounds that accumulate in the matrix after the volatilization of C, O, N, S, and H compounds, as noted by Domingues et al. [43]. The decrease in all biochar yields with increasing temperature occurs due the thermal degradation of, and greater energy available to break, the strong organic bonds, and the greater volatilization of organic components as the charring conditions intensify [28]. This behavior has also been reported in previous studies using the same biomass types evaluated in this study [43,65]. Higher yields were observed for the composites compared to pure biochars, irrespective of the feedstock and pyrolysis temperature. This is probably due to the deposition of volatile compounds around the biochar caused by the addition of KCl [66]. Potassium chloride acted as a shield, in synergy with the feedstocks, preserving their organic matrix from thermal degradation. Furthermore, K has a positive impact on biochar production, since during the pyrolysis process there is an accumulation of alkali and alkaline earth metals in the biochar that contribute to the catalytic effect, increasing the biochar yield and also the ash content, with K having the greatest impact on the preservation of thermally derived biochar compared to Na, Ca, and Mg [67]. It should also be mentioned that KCl is less susceptible to thermal degradation than the feedstocks' constituents; thus, it is more prone to remaining in the final composite than organic compounds are.

3.1.2. Ash Content

The ash content was significantly influenced by feedstock, pyrolysis temperature, and biochar type, as well as their two-way interactions ($p < 0.05$). Increasing the pyrolysis temperature (650 °C) led to a higher ash content than at a lower temperature (300 °C). Regarding feedstock, chicken manure biochars had the highest ash content, followed by banana peel and coffee husk, which formed distinct statistical groups ($p < 0.05$). The inorganic constituents present in CM biochar ash can act as flame retardants, reducing mass loss during pyrolysis and resulting in higher biochar yield [68]. A higher ash content in the waste derived from animal production systems compared to those of plant origins was also reported by Sarfaraz et al. [69], who found in their work an ash content of 72.6% for chicken litter. The composite biochars exhibited a significantly higher ash content compared to the pure biochars ($p < 0.05$). The interaction between biochar type and pyrolysis temperature showed that composite biochars produced at 650 °C had the highest ash content, while pure biochars at 300 °C had the lowest values. Additionally, the interaction between biochar type and feedstock indicated that chicken manure biochars consistently had higher ash contents, regardless of the biochar type.

3.1.3. Total Carbon Content

For the C content (Table 3) in pure biochars, an increase was observed with the rise in pyrolysis temperature for CH, which reached the highest C values (66% at 300 °C and 71% at 650 °C). In contrast, BP showed no difference in C content with increased pyrolysis temperature (55% at both 300 °C and 650 °C), which is relevant to adding it to soil C with a higher persistence rate. For CM, the relationship was reversed, with C content decreasing as temperature increased (28% at 300 °C and 23% at 650 °C). The increase in C content in CH biochars with increasing pyrolysis temperature may be due to a higher degree of polymerization, leading to a more condensed, aromatic C structure in the biochar matrix [70,71]. The lowest C contents in the CM biochars, and their decrease with increasing temperature, suggest that the organic compounds in this material are more prone to rapid loss with increased pyrolysis temperature before forming biochars with recalcitrant aromatic compounds; additionally, the inorganic matrix may experience relative enrichment over the organic matrix as charring conditions intensify [43]. The thermal degradation of C in carbonate forms is another explanation for the lower C content in animal wastes carbonized at high pyrolysis temperatures. Carbon content increased with the rise in temperature for all composites, which may be attributed to the higher proportion of feedstock used at 650 °C compared to 300 °C.

3.1.4. pH

The pH of the biochars was significantly influenced by the interaction between feedstock, pyrolysis temperature, and biochar type ($p < 0.05$), indicating that these factors act in combination to determine biochar alkalinity and liming value. Among the feedstocks, the chicken manure biochars had the highest pH values, followed by banana peel and coffee husk, which were significantly different from each other ($p < 0.05$). An increase in pH value (Table 3) was observed for pure biochars with increasing pyrolysis temperature for the BP and CM biochars, but this behavior was the opposite for the CH biochar. This increase can be related to the increase in ash content and the presence of minerals, such as carbonates ($CaCO_3$ and $MgCO_3$), as well as alkali elements, such as K, Ca, Mg and Na, mainly in the chicken manure feedstock [72,73]. The pyrolysis process distills the volatile and acidic components producing bio-oil or biogas while maintaining alkaline components, carbonates, and other salts in the ash biochar matrix [69]. The opposite behavior observed for the CH biochar may be due to its specific chemical composition. Enders et al. [74] demonstrated, in a study evaluating 94 types of biochars, that pH can vary widely and depends directly on ash content and pyrolysis temperature, offering an opportunity to adapt each biochar to specific agronomic applications. Nevertheless, the pH values in water of the pure biochars all showed an alkaline nature, since they ranged from 8 to 10.7. The composite biochars exhibited significantly higher pH values than the pure biochars ($p < 0.05$). Similarly, pyrolysis at 650 °C resulted in higher pH values compared to at 300 °C, regardless of feedstock. The interaction between biochar type and feedstock revealed that the composite biochars derived from chicken manure had the highest pH, whereas the pure biochars derived from coffee husk had the lowest pH. Additionally, the three-way interaction (feedstock × temperature × biochar type) confirmed that the composite chicken manure biochars processed at 650 °C exhibited the highest pH values, while the pure coffee husk biochars processed at 300 °C had the lowest pH values.

3.1.5 Electrical Conductivity (EC)

The electrical conductivity (EC), an indirect determination of the soluble salts present in a solution and able to conduct electricity, similar to pH, was significantly influenced by the interaction between feedstock, pyrolysis temperature, and biochar type ($p < 0.05$), indicating that the effects of these factors are interdependent. An increase was observed with the rise in pyrolysis temperature for the pure biochars. The composite biochars exhibited significantly higher EC values than the pure biochars ($p < 0.05$). Among the feedstocks, the chicken manure

biochars consistently had the highest EC values, while the coffee husk biochars showed the lowest EC values across pyrolysis temperatures, results similar to those found by Domingues et al. [43]. The interaction between feedstock and biochar type revealed that the composite chicken manure biochars had the highest EC, whereas the pure coffee husk biochars had the lowest EC. The decrease in EC of the composites produced at 650 °C reflects the lower addition of KCl in the formulation of these composites compared to those formulated at 300 °C. These results highlight the importance of feedstock selection and biochar processing conditions, as higher pyrolysis temperatures and composite formulations generally led to increased EC levels.

3.1.6. Potassium Content

During the pyrolysis process, K in plant tissues and feedstock components is converted into plant-available K, which can then be returned to the soil as fertilizer [75]. The potassium content of the biochars was significantly affected by the interaction between feedstock, pyrolysis temperature, and biochar type ($p < 0.05$), indicating that the response of K levels depended on the combination of these factors (Figure 1). Within each type of feedstock, K levels can also vary among different types of organic wastes (animal and industrial origins, etc.), plant species, cultivation conditions, harvest timing, and even different parts of the plant residue analyzed [9]. As expected, the total K content in the pure biochars was directly dependent on the feedstock and pyrolysis temperature. This finding aligns with the research of Xiu et al. [75], which demonstrated that pyrolysis temperature is the most critical factor influencing K content in corn husk biochar. According to the authors, at pyrolysis temperatures ranging from 300 to 900 °C, the content and transformation process of the different forms of K in the biochar progress through three stages as the charring conditions intensify. Therefore, K tends to concentrate and be converted into highly soluble salts when the feedstock is pyrolyzed, unlike elements that can be volatilized, such as O, N, and S, or transformed into insoluble forms, such as the formed Mg salts [76]. However, the conversion of highly soluble K occurs up to a specific temperature. According to Bilias et al. [9], this threshold is 500 °C, where pyrolysis temperatures below this limit yield biochars with higher relative fractions of soluble K. In contrast, temperatures exceeding 500 °C promote the formation of insoluble K salts, particularly in biochars derived from feedstocks rich in aluminum or silicon compounds that are prone to interact and form K compounds of low solubility [9].

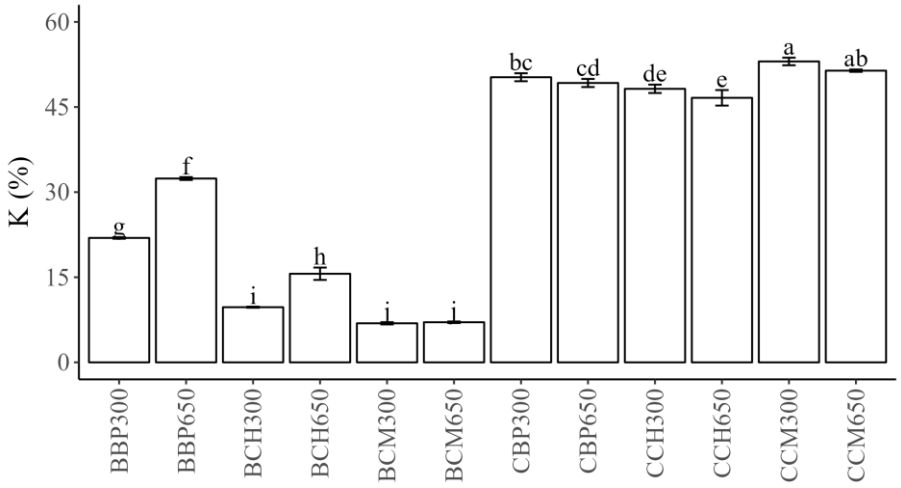

Figure 1. Total potassium (K) content (%) in pure biochars and composites. Means with same letters do not differ according to Duncan' test at p <0.05. BBP: biochar banana peel; CBP: composite banana peel; BCH: biochar coffee husk; CCH: composite coffee husk; BCM: biochar chicken manure; CCM: composite chicken manure; 300 or 650 denotes pyrolysis temperature for biochar or composite.

The relationship between biochar K content and pyrolysis temperature is partially explained by the volatilization of organic compounds and the retention of inorganic ions such as K in the final biochar [28,77]. Among the studied feedstocks, the banana peel biochars exhibited the highest K content at both pyrolysis temperatures, with 22% at 300 °C and 32% at 650 °C, representing a 48% increase in total K content as temperature increased. A similar result was found by Bong et al. [78], who showed that increasing the pyrolysis temperature was the main factor affecting the potassium content of banana peel biochar. This was followed by CH, with K contents of 10% and 16% at 300 °C and 650 °C, respectively, showing a 60% increase. In contrast, CM maintained a relatively constant K content of approximately 7% at both temperatures, indicating no significant enrichment with increasing pyrolysis temperature. The lack of K accumulation in the CM-derived biochars under higher pyrolysis temperatures warrants further investigation. Additionally, potential K losses through volatilization as pyrolysis temperature rises should be explored in future studies. The K content in the BP biochars was significantly higher than that of the other feedstocks studied in this work, as well as biochars derived from other feedstocks reported in the literature [28]. Even at the lowest pyrolysis temperature (300 °C), BP biochar exhibited a high K content (22%), highlighting its strong potential for producing biochar-based K fertilizers. The composite biochars exhibited significantly higher K concentrations than the pure biochars ($p < 0.05$), aligning with the intended formulation goal of achieving a final K content of approximately 50%. The K content

in the composite biochars ranged between 45% and 53%. Potassium retention (Equation (1)) is directly correlated with biochar yield. For the pure biochars, the K retention values were 207 and 169 for BBP300 and BBP650, respectively; 172 and 184 for BCH300 and BCH650; and 159 and 131 for BCM300 and BCM650. These results suggest that K losses or variations in biochar yield occur at different magnitudes depending on the feedstock and pyrolysis conditions.

3.1.7. FTIR Spectroscopy

The FTIR spectral signatures of biochars and their respective composites (Figure 2) revealed significant changes in infrared fingerprints as pyrolysis conditions intensified. Pyrolysis temperature plays a crucial role in shaping the structural and chemical composition of biochars, with higher temperatures promoting the thermal degradation of aliphatic groups and facilitating the formation of more condensed aromatic structures in plant-derived biochars [79]. The biochars derived from BP (Figure 2a) and CH (Figure 2b) exhibited similar spectral signatures, with the slight differences likely attributed to variations in the lignin content of each feedstock [80]. In contrast, the biochars derived from CM (Figure 2c) displayed distinct spectral features, reflecting differences in ash content, mineral composition, and the potential resistance of specific organic functional groups and compounds in chicken manure to thermal degradation under increasing charring conditions. These findings emphasize the strong influence of feedstock composition and pyrolysis conditions on the chemical structure of the resulting biochars. They also highlight the importance of optimizing pyrolysis parameters to tailor biochar properties for specific applications.

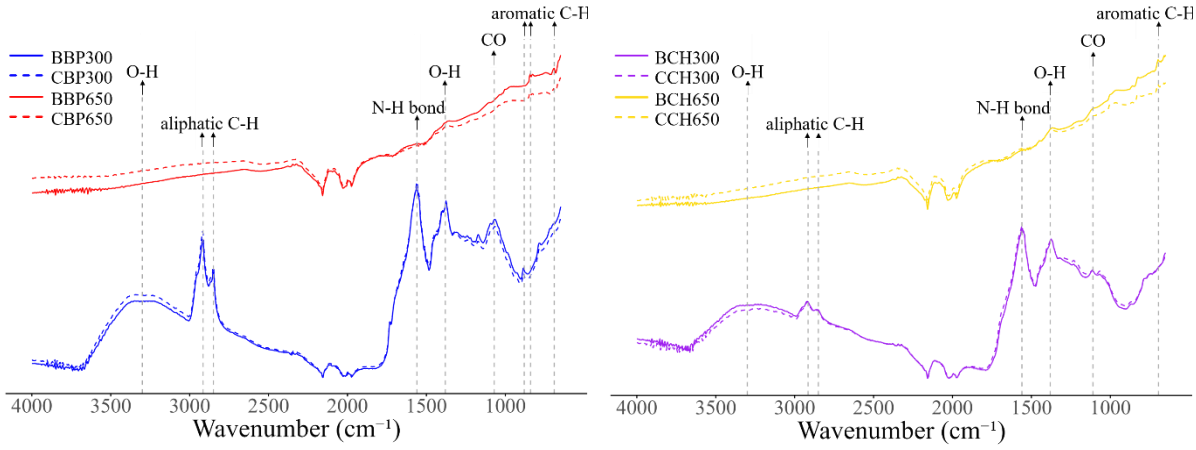

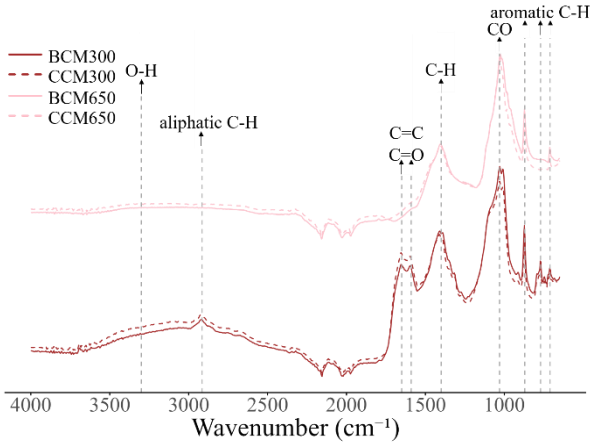

(c)

Figure 2. FTIR spectra of pure and composite biochars pyrolyzed at 300 °C and 650 °C. (a) Banana peel, (b) coffee husk, and (c) chicken manure. BBP: biochar banana peel; CBP: composite of banana peel biochar; BCH: biochar of coffee husk; CCH: composite of coffee husk biochar; BCM: biochar of chicken manure; CCM: composite of chicken manure.

In the biochars derived from BP and CH, aliphatic groups were detected at 300 °C, indicated by peaks in the 2915–2850 cm^{-1} region [43,81]. These peaks were absent in the biochars produced at 650 °C, suggesting the thermal degradation of organic radicals or the aromatic condensation of organic groups as temperature increased [73,75,80]. Similarly, the phenolic O–H bending (1310–1380 cm^{-1}) observed in the plant biochars charred at 300 °C disappeared at 650 °C, further supporting the formation of more condensed aromatic structures at elevated pyrolysis temperatures. In the region around 1560 cm^{-1}, the peaks observed in BP and CH biochars produced at 300 °C could be attributed to C=C stretching in aromatic rings, or possibly to amide (-CONH-) functional groups [54,82,83]. The removal of volatile compounds during carbonization at higher temperatures results in the depletion of functional organic polar groups, leading to a subsequent reduction in a biochar's cation exchange capacity (CEC) [84]. In contrast, the chicken manure biochars exhibited distinct peaks at 1030 cm^{-1} even at higher pyrolysis temperatures, indicating the resistance of their pristine organic matrices to thermal degradation. This resilience is likely due to their high ash content, which may protect organic compounds during pyrolysis [43]. The peaks around 800 cm^{-1} in all the spectra suggest the presence of aromatic rings, which are particularly pronounced in CM biochars. Notably, the addition of KCl did not significantly alter the organic structure or spectral signature of the biochar composites, regardless of feedstock type or pyrolysis temperature.

3.1.8. Cation Exchange Capacity (CEC)

Cation exchange capacity (CEC) is a key factor in evaluating the potential of biochars for agricultural and environmental applications, as it significantly influences the retention of cationic nutrients, including K, in weathered soils [85]. As expected, the CEC values of the BBFs, estimated based on FTIR spectral data and mathematical equations, varied according to feedstock type and pyrolysis temperature (Table 4). The CEC values ranged from 24.4 to 63.1 for the pure biochars and composites formulated at 300 °C, and from 2.9 to 18.2 for those prepared at 650 °C. These values align with those reported in the literature [86]. The decrease in CEC with increasing pyrolysis temperature occurs because lower temperatures generally preserve oxygen-containing functional groups, while higher temperatures lead to the thermal degradation of these organic groups, reducing the final biochar's CEC [55]. The highest CEC values were observed for the banana peel biochars, likely due to the high potassium content of this biomass. During pyrolysis, potassium may intercalate and promote the separation of carbonaceous lamellae through the oxidation of cross-linking carbon atoms [85]. The incorporation of KCl in composite synthesis led to a reduction in CEC. In the composites produced at 300 °C, this reduction was relatively minor: 3.5% for BP, 0.8% for CH, and 7.8% for CM. However, in BBFs produced at 650 °C, the reduction was significantly more pronounced, reaching 44.4% for BP and 31.2% for CH. Interestingly, in the case of CM, the CEC increased with the addition of KCl in the composite produced at 650 °C.

Table 1. Predicted cation exchange capacity (CEC) of pure biochars and derived composites.

Charred matrix	CEC (cmolc kg^{-1})
BBP300	63.1
BBP650	15.4
BCH300	37.9
BCH650	18.2
BCM300	26.5
BCM650	2.9
CBP300	60.9
CBP650	8.6
CCH300	37.6
CCH650	12.5
CCM300	24.4
CCM650	3.2

BBP: biochar from banana peel; CBP: composite from banana peel; BCH: biochar from coffee husk; CCH: composite from coffee husk; BCM: biochar from chicken manure; CCM: composite from chicken manure. Numbers 350 and 650 indicate pyrolysis temperatures used in biochar and composite production.

3.2. Potassium Release Kinetics

Considering that the forms and availability of K in biochar can vary depending on the feedstock and pyrolysis temperature, it is essential to evaluate the release of K over time. This assessment helps determine the optimal conditions for achieving specific agronomic goals, aiding in applications such as recommending K fertilizers for crops. To understand the release dynamics of K from the BBFs, an experiment was conducted to simulate K release in a $CaCl_2$ solution over 28 days (Figure 3). The K release kinetics dataset was fitted to six mathematical models, and the most appropriate model for each biochar and composite, compared to KCl, was selected based on the highest regression coefficients (R2) and the lowest root mean square errors (RMSE) and Akaike Information Criterion (AIC) values [51]. Detailed results for each model are presented in Table A1, Appendix A. Among the evaluated models, the Toth and Gompertz equations provided the best fit (high R2). However, since the Toth equation accounts for the heterogeneous surface of biochar, leading to a nonlinear K release into the solution, it was chosen as the most suitable model for all the treatments to describe the K release from the BBFs over time.

The release of K from K-BBFs (Figure 3) is a complex and non-homogeneous process, exhibiting variable release rates that do not follow a first-order reaction or a simple chemical mechanism [75]. A rapid K release was observed within the first 24 h, followed by a slower release phase, eventually reaching equilibrium after 96 h. All biochars and composites, regardless of feedstock type or pyrolysis temperature, exhibited lower K release rates compared to KCl. After 24 h (Table 5), KCl had released approximately 88% of its total K content, consistent with previous studies [35,36], indicating that K from charred matrices is released more gradually than K from KCl. Therefore, applying high rates of K-rich biochars to soil should be managed carefully to prevent excessive K accumulation in the soil solution and potential K leaching.

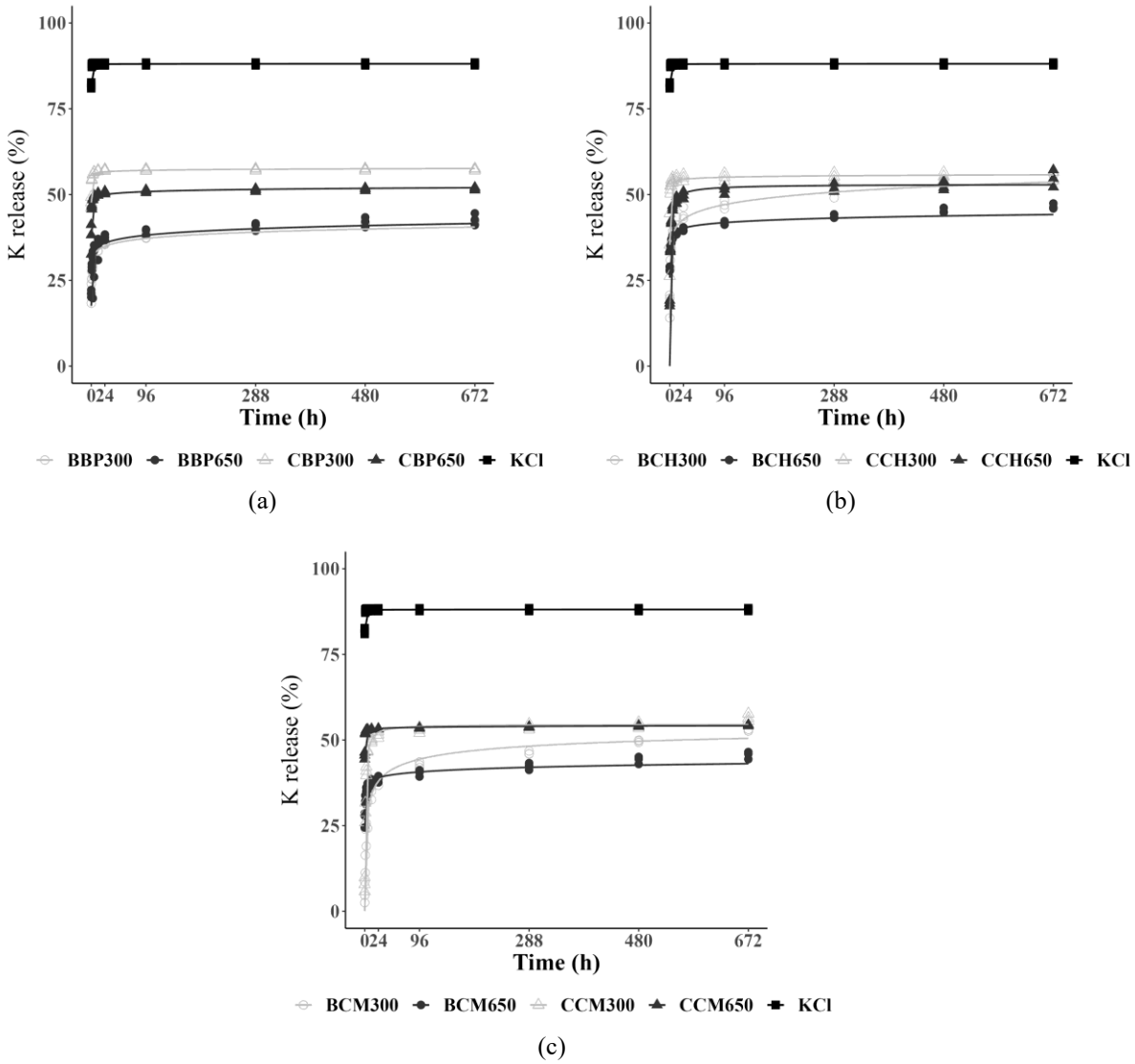

Figure 3. Release kinetics of K (%) in CaCl2 over incubation time for pure and composite biochars compared to KCl: (a) banana peel biochars and composites, (b) coffee husk biochars and composites, (c) chicken manure biochars and composites. BBP: biochar banana peel; CBP: composite banana peel; BCH: biochar coffee husk; CCH: composite coffee husk; BCM: biochar chicken manure; CCM: composite chicken manure.

Table 2. Potassium (% of total K) released in $CaCl_2$ solution over 24 and 672 hours for all treatments.

Treatment	K released in 24 hours (% total K)	K released in 672 hours (% total K)
BBP300	35.7 h	42.0 f
BBP650	37.5 gh	42.8 f
BCH300	44.3 f	55.0 bc
BCH650	39.8 g	46.5 e
BCM300	38.1 gh	52.8 cd
BCM650	38.7g	45.6 e
CBP300	55.8 b	56.3 b
CBP650	50.6 de	51.7 d

CCH300	53.5 bc	55.7 bc
CCH650	50.3 e	56.9 b
CCM300	52.9 cd	56.5 b
CCM650	53.3 bc	54.3 bcd
KCl	88.0 a	88.1 a

The treatment means with the same letter do not differ via the Duncan test at $p < 0.05$. BBP: biochar banana peel; CBP: composite banana peel; BCH: biochar coffee husk; CCH: composite coffee husk; BCM: biochar chicken manure; CCM: composite chicken manure.

Among the pure biochars, BBP300 exhibited the lowest K release within the first 24 h, with 35.7% of its total K content released, whereas BCH300 released 44.3% over the same period. After 28 days, BBP300 remained the biochar with the lowest cumulative K release (42.0%), while BCH300 released the highest amount, reaching 55.0% of its total K. Among the composites, CCH650 had the lowest K release in the first 24 h (50.3% of total applied K), whereas CBP300 released the highest amount (55.8%). By the end of the 28-day period, CBP650 exhibited the lowest cumulative K release (51.7%), while CCH650 and CCM300 had the highest releases, each reaching approximately 57% of the total K being mixed with the washed sand. When comparing the pure biochars and composites, all the composites exhibited a higher K release within the first 24 h than their corresponding pure biochars, a result expected due to the presence of KCl mixed with the feedstocks during co-pyrolysis. However, by the end of the 28 days, CBP650 had the lowest cumulative K release among the composites (52%), which was 36% lower than that of KCl. Notably, CBP650 released K even more slowly than BCH300, which had a total release of 55%. These findings indicate that mixing KCl with a charred matrix is an effective strategy for slowing K release over time, potentially reducing K leaching in soils.

The pyrolysis temperature was a significant factor influencing K release from the pure CH and CM biochars. As the temperature increased from 300 °C to 650 °C, less K was released by the end of the 28-day incubation period. These results align with previous studies, which indicate that pyrolysis temperatures above 500 °C promote a more prevalent inorganic matrix and, surprisingly, result in fewer soluble K salts in biochars [9]. Conversely, BP biochars exhibited a similar K release at both 300 °C and 650 °C, with both amounts being lower than those observed for the CH- and CM-derived biochars. This difference can be attributed to the specific characteristics of the BP-derived biochar, such as its higher cation exchange capacity (CEC) compared to the other BBFs. This property may influence how K is trapped, adsorbed, and released, as well as its overall availability, regardless of the pyrolysis temperature [87]. Therefore, in the BP biochars, the chemical structure and interactions with other components

likely played a crucial role in controlling the rate of K release, leading to distinct behavior compared to the other biochars. Some of the biochars formulated in this study, regardless of pyrolysis temperature, are suitable for use as slow-release K sources while also reducing the proportion of KCl required in the final composite.

The lowest rates of K release in the first 24 h were observed for the BP biochars (Table 5). This can be attributed to their high ash content (Table 3) and highest cation exchange capacity (CEC) (Table 4) among the tested biochars, demonstrating that ash content can slow down K release from biochars [67]. Additionally, studies indicate that K release from organic fertilizers, such as biochar, differs from that of mineral fertilizers, which typically exhibit a release pattern proportional to their application rate. This difference arises from the complex interactions of K with organic and inorganic compounds [88]. Furthermore, the rate of K release depends on the concentration gradient between the biochar and the soil, as well as the equilibrium between the solid and liquid (solution) phases, highlighting the crucial role of time in the nutrient release process [67]. These results suggest that all biochars and composites exhibit a controlled release of K into the solution compared to soluble KCl. Supplying potassium to crops in combination with charred matrices can enhance K retention in the soil for a longer period, supporting plant uptake during critical growth stages when K demand is highest.

The accumulated K content at the end of 672 h (28 days) for all the pure and composite biochars was lower than that reported in other studies on organic K sources [28,37]. In a study evaluating the ability of bentonite co-pyrolyzed with Canna indica to enhance the K release capacity of BBFs, Chen et al. [28] found that co-pyrolysis reduced the total K released from 92.5% to 72.6% after 28 days. Similarly, Cheng et al. [37], who examined K release from composites prepared with distillers' grains, reported that their best composite released 82.35% of its total K in 24 days.

Potassium is highly susceptible to leaching through the soil profile, particularly in sandy soils [89]. Therefore, the development of fertilizers that promote slower K release can improve crop fertilization efficiency, reducing application costs, better meeting plant nutrient demands, and mitigating environmental issues associated with the high solubility and leaching of K from mineral fertilizers. According to ISO 18644 [90], controlled-release fertilizers should not release more than 15% of the nutrient within the first 24 h and no more than 75% over 28 days. In accordance with these guidelines, both pure biochars and composites meet the requirement of not exceeding 75% K release within 28 days, confirming their potential as slow-release fertilizers. However, none of the treatments comply with the first criterion, as they all release

more than 15% of their K within the first 24 h. Similar results were observed by Fachini et al. [35], who evaluated BBFs produced by enriching sewage sludge with KCl. In their study, the powdered BBF also failed to meet the initial release criteria (K release within 24 h), necessitating physical modifications to the K fertilizers, such as the agglomeration of charred powder matrices into pellets or granules, to slow K release during the initial 24 h period.

3.3. Agronomic effectiveness of Biochar-K Composites

Biochar can be used as a soil conditioner to enhance fertility and as a nutrient source for plants [29]. The K-BBFs formulated in this study demonstrated superior performance in controlling K release compared to KCl. Consequently, an experiment was conducted with corn grown in two contrasting soils to evaluate the agronomic efficiency of K-BBFs in supplying K for optimal corn nutrition and growth. To assess the overall effects of different K-BBFs on corn growth in both soil types, Principal Component Analysis (PCA) was performed for each dataset (Figure 4). In Red Oxisol (RO) (Figure 4a), PC1 accounted for 46.09% of the variance, while PC2 explained 18.65%. In Red-Yellow Oxisol (RYO) (Figure 4b), PC1 accounted for 38.64% and PC2 for 20.41%. In both soils, a clear distinction was observed between the pure biochars and composite treatments, indicating significant differences in their effects on soil properties and nutrient availability. The primary factor driving cluster formation was the nutrient content in the soil solution, mainly the availability of K, Ca, and Mg. The addition of KCl during composite production influenced K release into the soil solution, resulting in distinct nutrient availability patterns and clusters. Additionally, PCA revealed that soil type plays a crucial role in K retention and mobility, affecting how treatments interact with soil chemistry. The differences in variance explained by PC1 and PC2 between RO and RYO soils suggest that nutrient dynamics and treatment responses are more structured in RO, whereas RYO exhibits a more dispersed pattern, indicating higher variability or additional influencing factors. These patterns guided further analysis, providing a deeper understanding of the effects of K-BBFs on soil properties and plant traits.

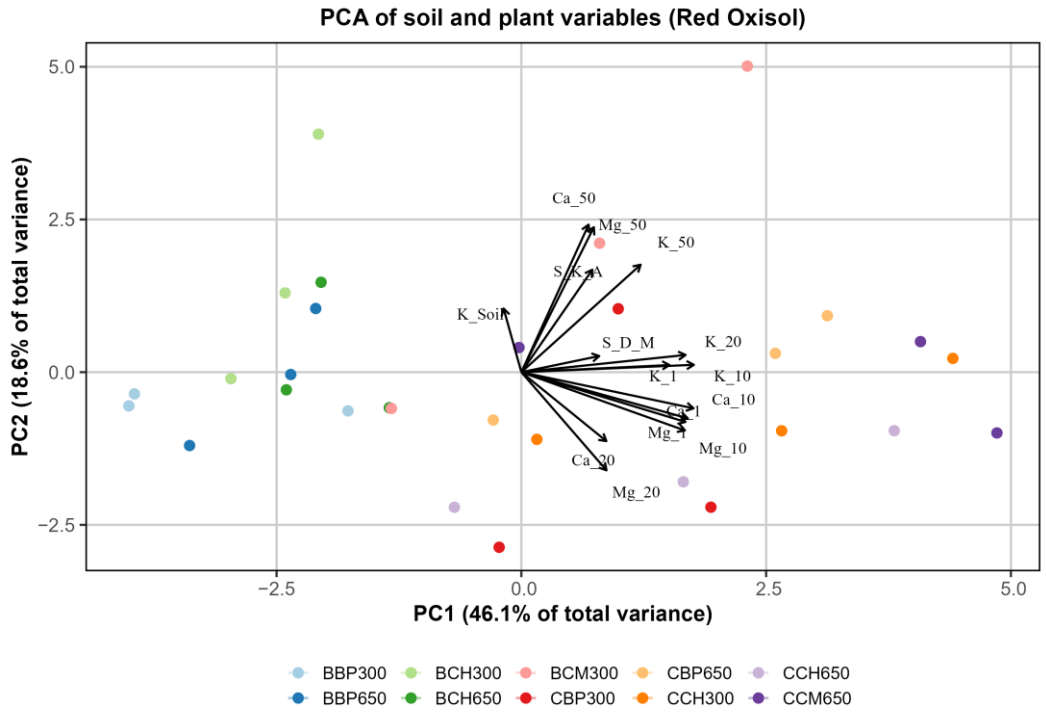

(a)

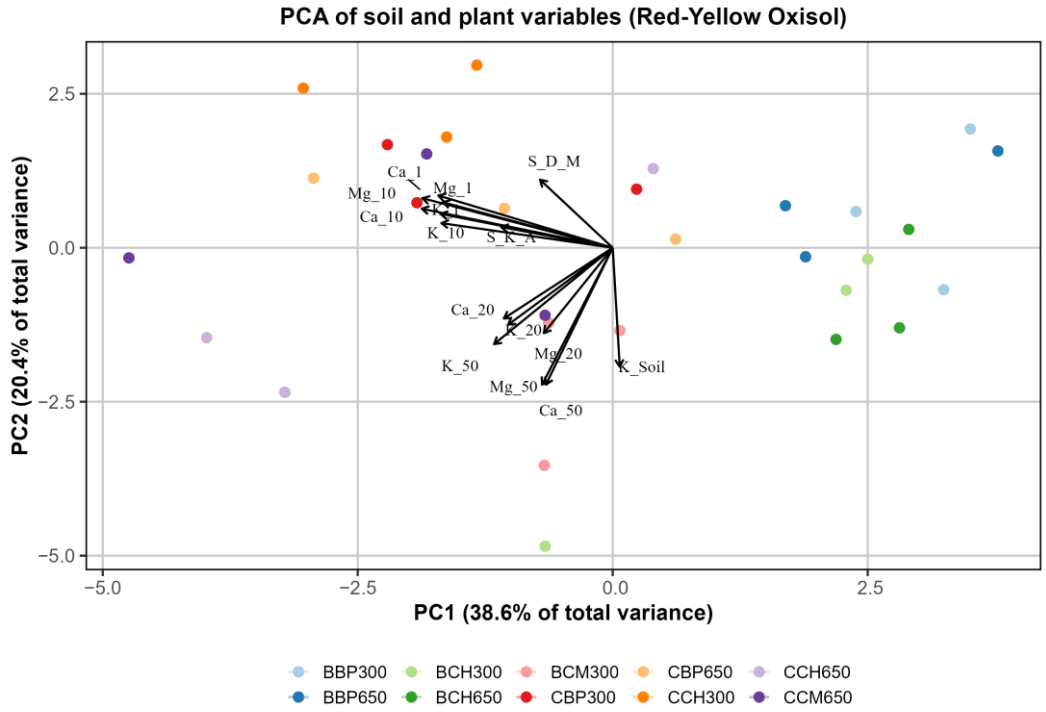

(b)

Figure 4. Principal Component Analysis (PCA) biplot illustrating grouping of treatments in RO (a) and RYO (b) based on soil and plant responses. S_D_M: shoot dry matter; S_K_A: shoot K accumulation; K_Soil: Residual K available in whole soil samples. Ca_1, K_1, Mg_1, Ca_10, K_10, Mg_10, Ca_20, K_20, Mg_20, Ca_50, K_50, Mg_50: Ca, K, and Mg concentrations in soil solution collected at 1, 10, 20, and 50 days after planting.

3.3.1. Dynamics of K Release from K-BBFs in Soil–Plant Systems

To understand the dynamics of K release from K-BBFs in the soil–plant system and how soil texture influences K availability for corn growth, soil solution from the pots was extracted at four different stages of corn growth: 1, 10, 20, and 50 days after planting (Figure 5). Even though the soil solution is not the main nutrient reservoir for plant growth, it reflects, when sampled in sequence, the controlled processes of the mineral and organic phases, ionic balance, solid–liquid soil phase equilibrium, and sorption/desorption reactions; thus, it reflects the processes that control the release rate of K into the soil solution. It also provides insight into the dynamics of K release from the solid phase to the soil solution for the applied fertilizers [91,92].

The release of nutrients from a fertilizer into the soil solution depends on both intrinsic factors, such as its nutrient content, the solubility of the K chemical species, and its physical form [93], as well as extrinsic factors, including soil water content and the soil's ability to retain nutrients in soil colloids. This retention capacity is directly influenced by the mineralogical composition of the soil, particularly its clay content and cation exchange capacity (CEC) [36,94]. The K levels released into the soil solution varied significantly between the two soils (Figure 5), demonstrating that soil texture was the primary factor regulating K availability in this study. The K concentrations in solution were significantly higher in the Red-Yellow Oxisol (RYO) than in the Red Oxisol (RO). In the first extraction for the CCH300 treatment, the K levels in the RYO exceeded 1100 mg L^{-1}, whereas the same treatment in the RO yielded less than 410 mg L^{-1}. This difference can be attributed to variations in clay and organic matter content, as well as CEC, between the two soils. The RO contained 620 g kg^{-1} of clay, whereas the RYO had 470 g kg^{-1}. The treatment with the lowest K levels was BBP300, with 123 mg L^{-1} in the first extraction for the RO and 434 mg L^{-1} for the RYO. This further highlights the significant role of feedstock type in regulating the release of K from biochar into the soil solution, as previously observed in the kinetics experiment. Given the high levels of K in solution, K application through biochar in sandy Oxisol should be performed in split applications. To optimize nutrient availability, biochar or its composite should be applied both at planting and as a topdressing.

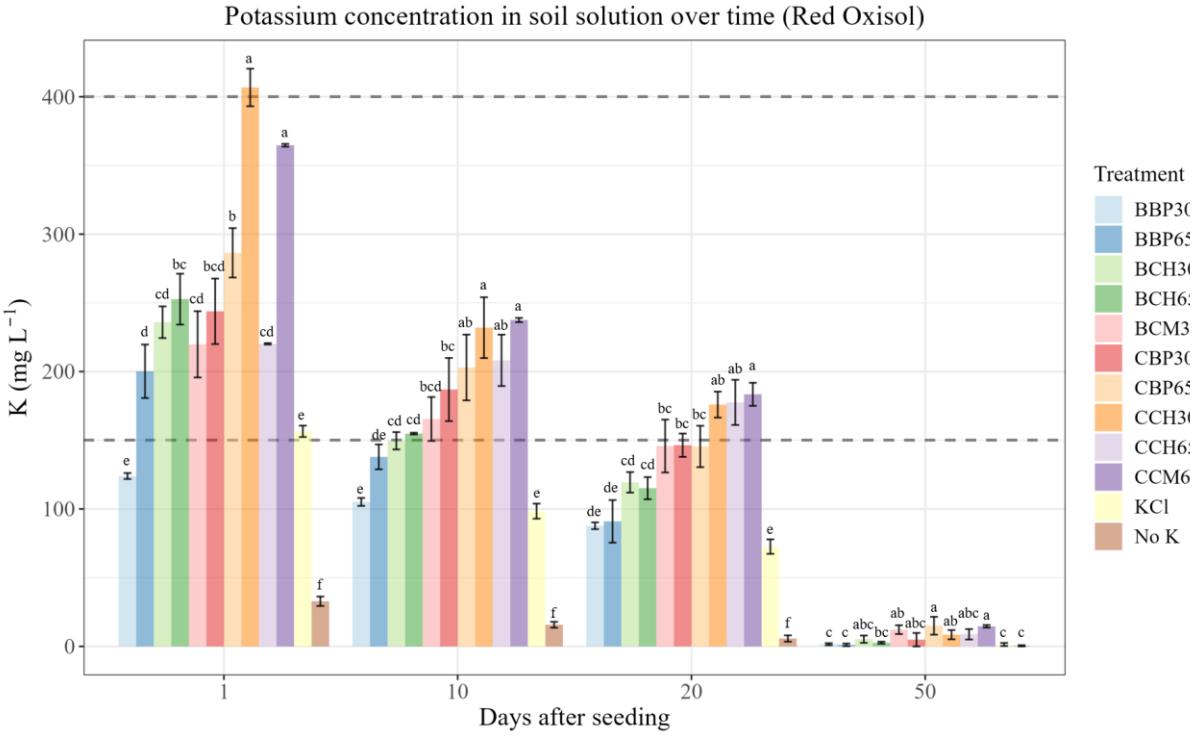

(a)

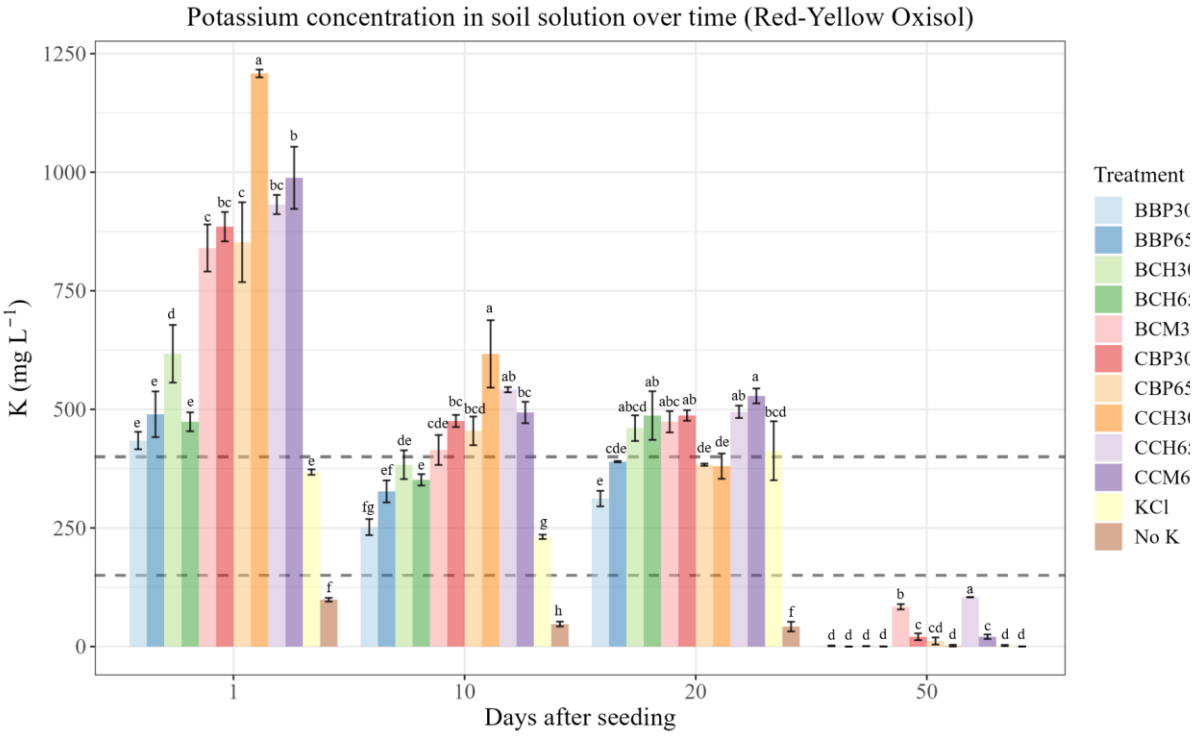

(b)

Figure 5. K contents analyzed in soil solution collected at 1, 10, 20, and 50 days after planting. (a) Red soil. (b) Red-Yellow Soil. BBP: biochar banana peel; CBP: composite banana peel; BCH: biochar coffee husk; CCH: composite coffee husk; BCM: biochar chicken manure; CCM: composite chicken manure. Black dashed line represents ideal (150–400 mg L^{-1}) range of K content in nutritive and hydroponic solutions [80,84]. Different lowercase letters indicate statistically significant differences among treatments for each sampling day, according to Duncan's test ($p < 0.05$).

The pyrolysis temperature also affected K release from the BBFs in both soils. This was clear in the first two extractions for RY, where the pure biochars produced at 650 °C released more K than those produced at 300 °C, especially for the rates of K release verified for the BP and CH biochars and their composites. In the RYO, the trend was similar for the BP biochars but different for the CH biochars. By the third extraction, 20 days after seeding, differences in K release between the pyrolysis temperatures were still observed, though without a clear pattern. For the composites, K release was significantly higher than the pure biochars in the first, second, and third extractions for both soils. This increase was expected due to the addition of KCl in the co-pyrolysis and composite synthesis, as also demonstrated by the kinetic study performed in lysimeters. According to Hoagland and Arnon [95], the ideal K concentration in a nutrient solution for soil-less plant cultivation is 234 mg L^{-1}, but this concentration may fluctuate over time, as the nutrient demand of the plant varies according to its growth stage. This value considers the nutrient balance, pH, and EC of the solution and can serve as a threshold limit for ideal nutrient levels released into the soil solution by different fertilizers. However, the ideal potassium concentration in the nutrient solution can depend on various factors, such as the plant species, the concentration of other nutrients, and the type of system used, with this concentration ranging from 150 to 400 mg L^{-1} [96–100]. For the RYO, all treatments, including the pure biochars, exceeded the upper limit of the suitable range in the first extractions. In contrast, for the RO, only the CCH300 treatment surpassed this value in the first extraction. This indicates that, although the BBFs exhibited a slower release dynamic compared to KCl in the kinetics test, it is evident that in a more complex system, such as the soil–plant system, external factors such as soil texture, CEC, fertilizer CEC, soil OM level, etc., play a crucial role in regulating the K release dynamics from BFFs.

In this study, the application of KCl (positive control) was divided into four doses. As a result, the K concentration in the soil solution of the KCl treatment cannot be directly compared to that of the other treatments. However, it was observed that, in the RYO, the K concentrations in the KCl treatment were much higher than in the RO, approaching the upper limit of 400 mg L^{-1}. This suggests that, even when applied in split doses, K supplied through KCl remains at high concentrations in the soil solution in soils with lower clay contents. This could lead to K leaching through the soil profile in field conditions, resulting in nutrient losses and negatively affecting crop growth and yield. Since K content in the soil solution can fluctuate depending on soil type, this range may include specific cases, such as the RYO. The potassium levels in the solution of the sandy Oxisol are excessively high. Therefore, even when supplied in combination with biochar, K from composites should be applied in split doses to enhance K use

efficiency in soils where sand predominates over clay, particularly in soils with low CEC. In addition to the high solubility of KCl, which necessitates its application in multiple doses, its high chloride content can be harmful to certain crops [5,8,101,102]. Consequently, the higher the K content in a feedstock, the greater the likelihood of producing a biochar that is both K-rich and low in chloride, providing an effective K supply while reducing the need for KCl and excess Cl^- in composite formulations. If not correctly managed, the risk of chloride—a micronutrient—toxicity in soils worldwide may be a serious concern for some crop production, given that KCl is the primary source of K used in agriculture.

It is essential to understand the influence of K in the soil solution on plant growth and the pattern of K uptake by plants. To evaluate the ability of each selected treatment to supply K for corn growth in contrasting soils, a greenhouse pot experiment was conducted over 50 days. Observing the K levels in the soil solution, it is evident that K concentrations decreased over time in all the treatments across both soils, indicating its uptake by corn plants. According to Gamboa [103], the rate of K uptake is relatively slow during the first 30 days after germination but then increases significantly, maintaining a steady growth rate for an additional 20 to 25 days. This explains the sharp decline in K levels in the solution between the third and fourth extractions. In the RYO, K levels fell below 105 mg L^{-1} in the fourth extraction, whereas in the RO, they dropped below 16 mg L^{-1} during the same period. The dynamics of Ca and Mg release were also evaluated on the same days as K (Figures A1 and A2, Appendix A). Similarly to K, Ca and Mg concentrations in the RYO solution were generally higher than in the RO, indicating that soil texture also influences their behavior. Additionally, the strong correlation between Ca and Mg (Figure A3, Appendix A) suggests that these elements exhibit similar dynamics in the soil solution, likely due to their bivalent nature and their combined supply through liming. In contrast, K, being monovalent, follows a different pattern and may be more susceptible to leaching in soils.

3.3.2. Effect of K-BBFs on Corn Growth and Nutrient Uptake

At the end of the experiment, shoot dry matter production was evaluated (Figure 6a, b). All the treatments significantly differed from the negative control in both the RO and RYO, indicating the composites' agronomic efficiency in supplying K to corn plants. In the RO, the treatments showed no differences among themselves and were as effective as KCl in nourishing corn plants. In the RYO, some variations were observed: CBP300 and CBP650 yielded the highest biomass production, comparable to KCl, whereas BCH300 and BCH650 resulted in lower production compared to other treatments, excluding the pots with no K supply. These

differences may be related to the differences in the physicochemical properties of the biochars and their distinct interactions within the fertilizer–soil–plant system. Similar trends have been observed in other studies using biochar-based amendments. For instance, Yang et al. (2024) [104] reported that biochar application improved plant nutrient uptake and biomass production, with significant increases in potassium accumulation depending on the biochar characteristics. Elsaman et al. (2025) [105] also demonstrated that biochar-enriched fertilizers enhanced shoot biomass and K uptake in corn plants, emphasizing the role of K-rich biochars in improving nutrient availability and promoting crop growth under tropical conditions.

Regarding K accumulation in corn plants (Figure 6c, d), differences can be observed among treatments for both soil types. In both soils, all treatments showed significantly higher K accumulation than the control without any K source supply to corn plants, indicating that, in addition to supporting effective biomass production, the K provided by the BBFs was efficiently taken up by the corn plants. The highest K accumulation was seen in the KCl control for both the RO and RYO soils. For the RO, the treatments BCH300, BCM300, and CCM650 were statistically similar to KCl, while in the RYO, none of the treatments achieved K accumulation comparable to KCl. These results align with those of Yang et al. (2024) [104], who also noted that the agronomic performance of biochar-based fertilizers may vary with soil type and biochar source, affecting nutrient retention and plant uptake. Considering that biomass production was similar but the K accumulation in the treatments was slightly lower, it can be inferred that the higher K uptake in the positive (KCl) control treatment represents a form of luxury consumption, in which increased K uptake does not result in higher biomass production [106].

These results demonstrate practical implications in agriculture aimed at optimizing K supply in different types of soil. The biochars and composites produced in this work, mainly those derived from BP, offer a sustainable alternative to mineral fertilizers, such as KCl, promoting a gradual release of the nutrient that aligns with the plant's demand during its growth. However, it is important to know the fertilizer–soil–plant interface well so that applications can be adapted to maximize nutrient use efficiency and crop yield, while avoiding soil K leaching.

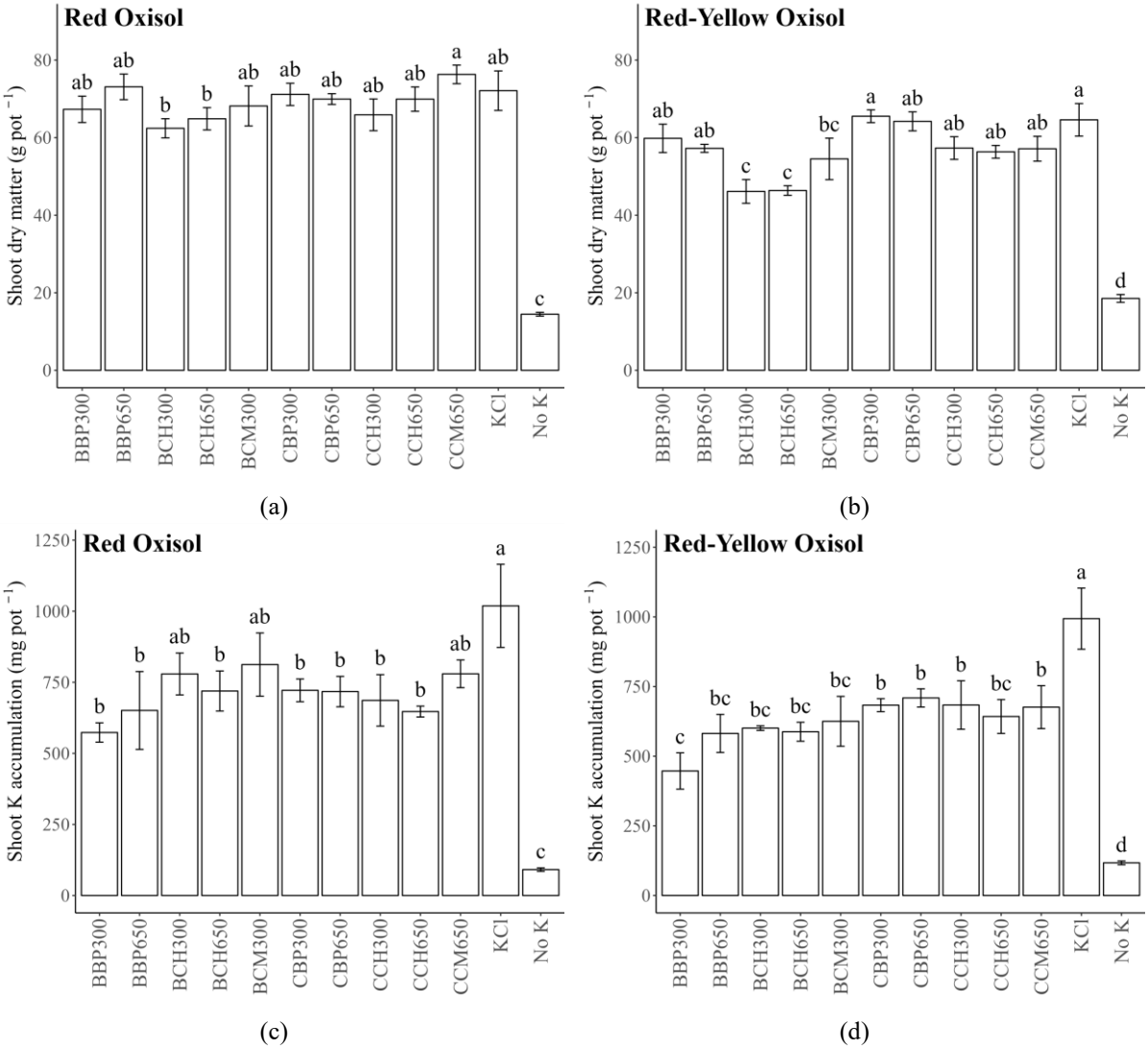

Figure 6. The shoot dry matter production (a, b) and potassium (K) accumulated in corn shoots (c, d) for plants cultivated in the Red and Red-Yellow Oxisols for all the treatments, compared to the positive control (KCl) and negative control (without K addition). The treatment means with the same letter do not differ by Duncan's test at $p < 0.05$. BBP: biochar banana peel; CBP: composite banana peel; BCH: biochar coffee husk; CCH: composite coffee husk; BCM: biochar chicken manure; CCM: composite chicken manure.

3.3.3. Residual Soil Potassium After Corn Harvest

It is possible to observe that the residual K content in the soil after corn cultivation (Figure 7) was lower for the BBFs compared to KCl for all the treatments in both the RO and RYO. This behavior can be explained by the K chemical species present in the K-BBFs. As demonstrated in the release kinetics experiment (Figure 3), the K-BBFs exhibit a much slower release of K than KCl, indicating a likely greater retention of K in the BBFs in less soluble forms and, therefore, K being less readily available to the soil compared to in KCl. This characteristic of the BBFs contributes to their gradual release of K, which can be beneficial in

agricultural systems that require a slower and more continuous availability of K throughout crop growth stages, as observed in corn cultivation. Moreover, since the stability of biochar in the soil environment is variable, being highly dependent on the characteristics of the biochar and the soil–plant system in which it is applied, it is known that the physicochemical and biological properties of biochar can change significantly over time as the material ages [9]. Therefore, studies evaluating biochar aging in complex fertilizer–soil–plant systems are also necessary to understand its fate and the effects of aging on potassium availability for crops grown in succession.

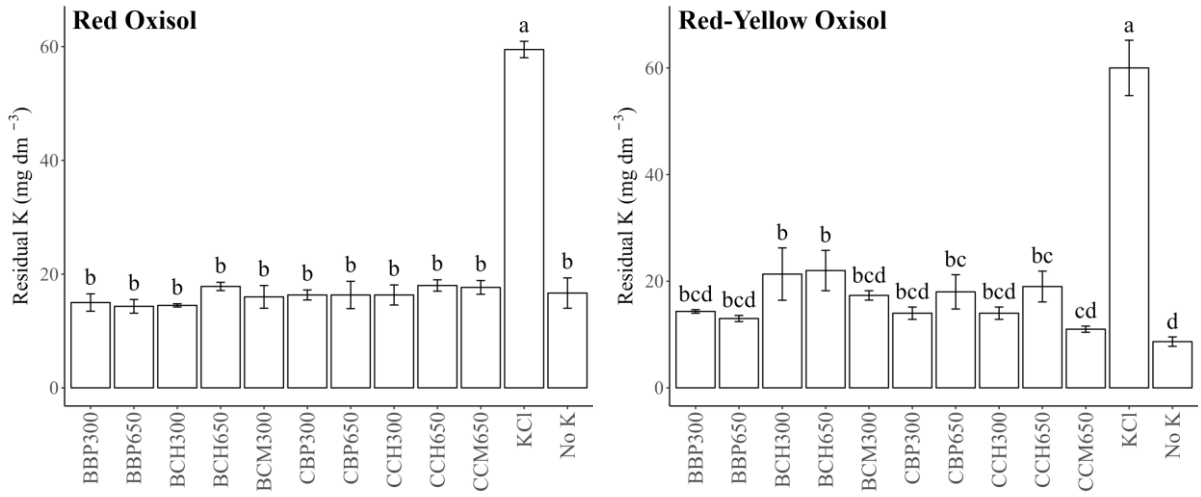

Figure 7. Residual K available in whole soil samples of Red (a) and Red-Yellow (b) Oxisols after 50 days of corn cultivation for all treatments, compared to positive control (KCl) and negative control (without K addition). Treatment means with same letters do not differ by Duncan's test at $p < 0.05$. BBP: biochar banana peel; CBP: composite banana peel; BCH: biochar coffee husk; CCH: composite coffee husk; BCM: biochar chicken manure; CCM: composite chicken manure.

4. Conclusions

The use of potassium-rich biochars offers a viable and sustainable alternative to conventional KCl fertilization, particularly in tropical regions such as Brazil, which has highly weathered and potassium-deficient soils. Among the feedstocks tested, banana peel proved to be the most promising raw material for the production of biochar-based potassium fertilizers (K-BBFs), showing the potential to replace up to 82% of KCl (CBP650) or even replace it completely (BBP300 and BBP650) in corn cultivation. Its high K content, slower release rate, and agronomic effectiveness support its adoption, especially in systems aiming to reduce dependence on KCl. For practical application, farmers cultivating in sandy Oxisols should consider split applications of powdered K-BBFs to reduce nutrient leaching, avoid imbalances

of K, Ca, and Mg in the soil solution, and improve potassium use efficiency. In these soils, the rapid release of K can compromise crop nutrition due to cation competition. Additionally, pelletizing K-BBFs may enhance K retention and help meet international standards for slow-release fertilizers, improving their suitability for field application. While biochars derived from coffee husk and chicken manure also showed promise, further studies are needed to optimize their formulations. Lastly, field trials are essential to evaluate long-term K availability, leaching potential, and crop performance under field conditions. This approach strengthens the foundation for recommending K-BBFs as an effective and regionally adaptable strategy for potassium fertilization in Brazilian agriculture.

Author Contributions: Conceptualization, G.N.T.S.R. and C.A.S.; methodology, G.N.T.S.R. and C.A.S.; formal analysis, G.N.T.S.R.; investigation, G.N.T.S.R. and C.A.S.; resources, C.A.S. and E.G.d.M.; data curation, G.N.T.S.R. and C.A.S.; writing—original draft preparation, G.N.T.S.R.; writing—review and editing, C.A.S. and E.G.d.M.; supervision, C.A.S.; project administration, C.A.S.; funding acquisition, C.A.S. All authors have read and agreed to the published version of the manuscript.

Funding: Many thanks to the Coordination for the Improvement of Higher Education Personnel (CAPES-PROEX/AUXPE 593/2018 and grant # CAPES PRINT: 88887.839592/2023-00), National Council for Scientific and Technological Development (CNPq, grant # 311212/2023-9), and the Foundation for Research of the State of Minas Gerais (FAPEMIG) for the financial support and scholarships provided.

Institutional Review Board Statement: Not applicable.

Informed Consent Statement: Not applicable.

Data Availability Statement: The datasets generated during and/or analyzed during the current study are available from the corresponding author upon reasonable request.

Conflicts of Interest: The authors declare no conflicts of interest.

Appendix A

Appendix A.1

Table A1. K release kinetic coefficients in the $CaCl_2$ solution for BBFs and KCl.

Treatment	Linear			Exponential			Power Function			Elovich			Toth			Gompertz		
	R^2	RMSE	AIC	R^2	RMSE	AIC	R^2	RMSE	AIC	R^2	RMSE	AIC	R^2	RMSE	AIC	R^2	RMSE	AIC
BBP300	0.55	4.40	180.04	0.53	4.51	181.58	0.86	0.08	-59.89	0,53	4,51	181,58	0,88	2,30	143,18	0,90	2,07	136,84
BBP650	0.46	5.30	191.18	0.44	5.39	192.25	0.75	0.12	-37.04	0,44	5,39	192,25	0,79	3,34	165,52	0,81	3,17	162,27
CBP300	0.13	2.66	149.90	0.13	2.66	149.94	0.91	0.02	-154.05	0,13	2,66	149,94	0,95	0,65	67,08	0,96	0,56	58,65
CBP650	0.19	3.86	172.25	0.18	3.87	172.35	0.87	0.04	-107.53	0,18	3,87	172,35	0,91	1,31	109,43	0,89	1,41	113,72
BCH300	0.53	7.57	212.59	0.50	7.78	214.27	0.93	0.09	-53.45	0,50	7,78	214,27	0,94	2,66	151,81	0,87	3,98	175,94
BCH650	0.61	3.27	162.26	0.60	3.33	163.39	0.91	0.04	-99.73	0,60	3,33	163,39	0,90	1,64	122,89	0,83	2,15	139,14
CCH300	0.10	6.02	198.85	0.10	6.03	198.9	0.72	0.08	-59.03	0,10	6,03	198,90	0,84	2,55	149,22	0,84	2,57	149,71
CCH650	0.29	8.97	222.79	0.27	9.04	223.27	0.95	0.07	-68.20	0,27	9,04	223,27	0,69	5,93	199,97	0,95	2,33	143,83
BCM300	0.52	10.05	229.60	0.49	10.46	232.00	0.90	0.23	3.55	0,48	10,46	232,00	0,94	3,56	169,29	0,85	5,58	196,25
BCM650	0.60	3.45	165.45	0.58	3.51	166.53	0.88	0.05	-84.38	0,58	3,51	166,53	0,87	1,94	132,99	0,82	2,32	143,70
CCM300	0.26	12.49	242.64	0.24	12.61	243.21	0.93	0.16	-19.29	0,24	12,61	243,21	0,96	2,85	155,89	0,96	2,92	157,43
CCM650	0.18	2.24	139.50	0.18	2.24	139.54	0.94	0.01	-171.48	0,18	2,24	139,54	0,98	0,34	28,88	0,96	0,50	51,64
KCl	0.06	1.84	127.72	0.06	1.84	127.72	0.81	0.01	-187.18	0,06	1,84	127,72	0,96	0,40	37,48	0,96	0,39	36,94

Appendix A.2.

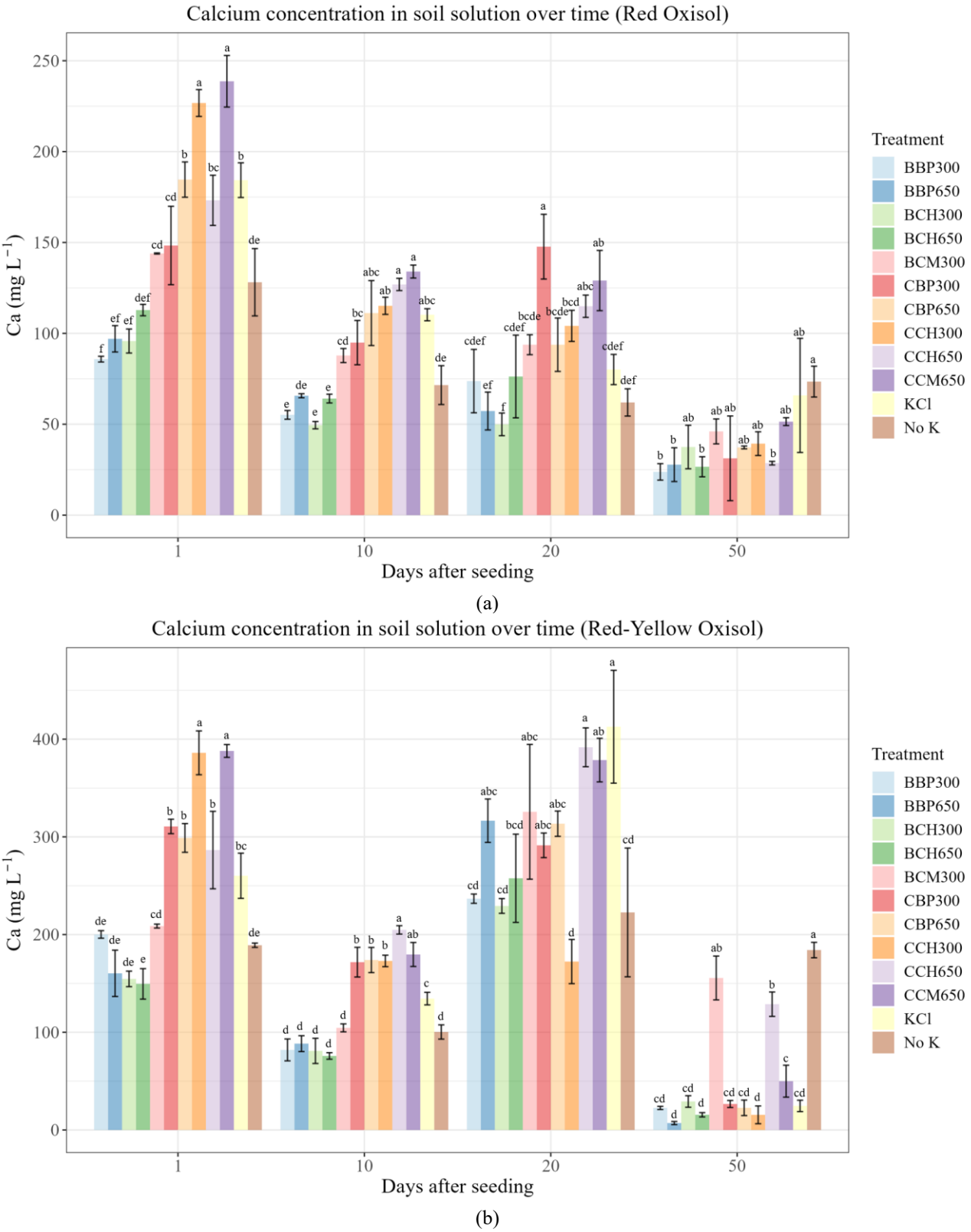

Figure A1. Ca contents analyzed in soil solution collected at 1, 10, 20, and 50 days after planting. (a) Red Oxisol. (b) Red-Yellow Oxisol. BBP: biochar banana peel; CBP: composite banana peel; BCH: biochar coffee husk; CCH: composite coffee husk; BCM: biochar chicken manure; CCM: composite chicken manure. Different lowercase letters indicate statistically

significant differences among treatments for each sampling day, according to Duncan's test ($p < 0.05$).

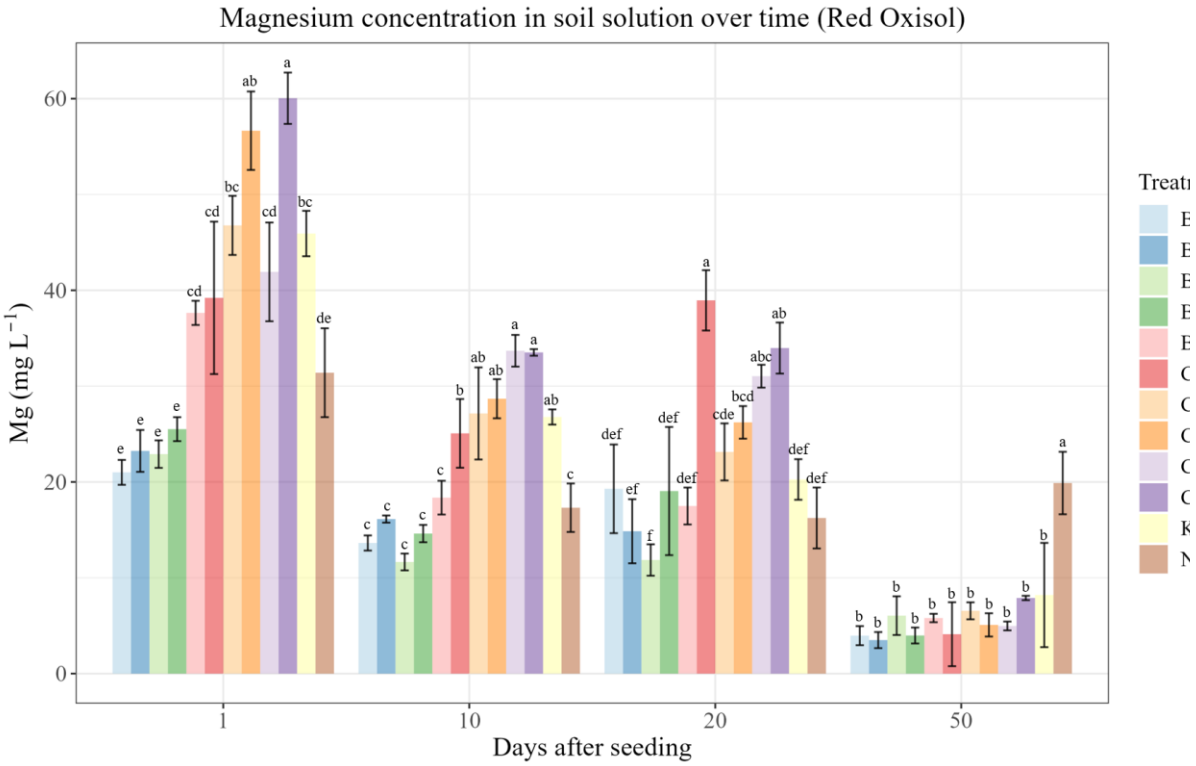

(a)

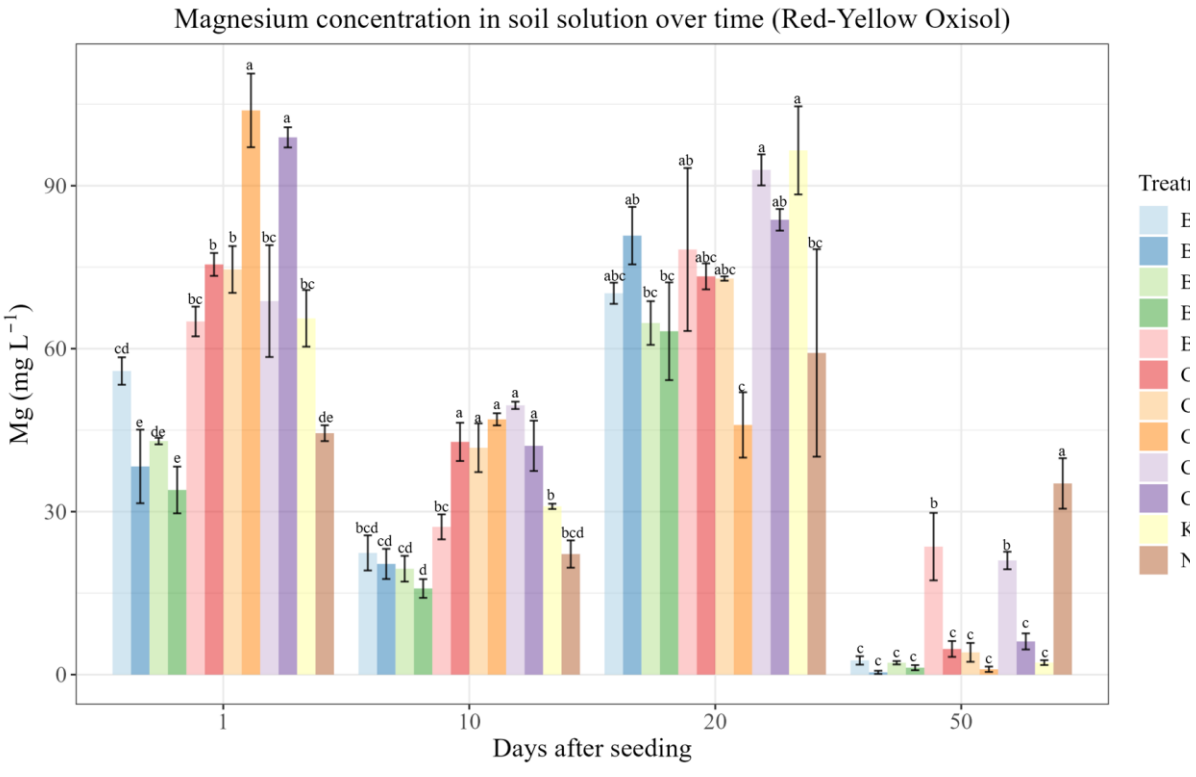

(b)

Figure A2. Mg contents analyzed in soil solution collected at 1, 10, 20, and 50 days after planting. (a) Red Oxisol. (b) Red-Yellow Oxisol. BBP: biochar banana peel; CBP: composite banana peel; BCH: biochar coffee husk; CCH: composite coffee husk; BCM: biochar chicken manure; CCM: composite chicken manure. Different lowercase letters indicate statistically

significant differences among treatments for each sampling day, according to Duncan's test ($p < 0.05$).

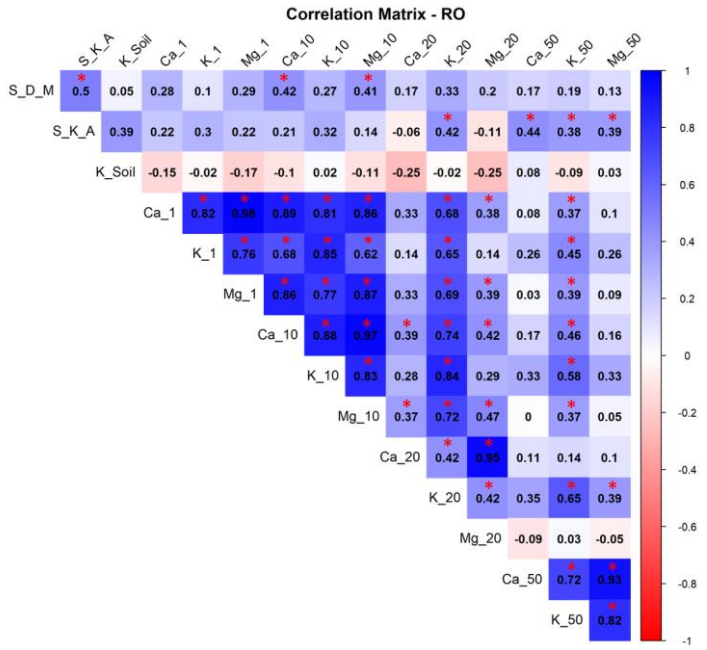

(a)

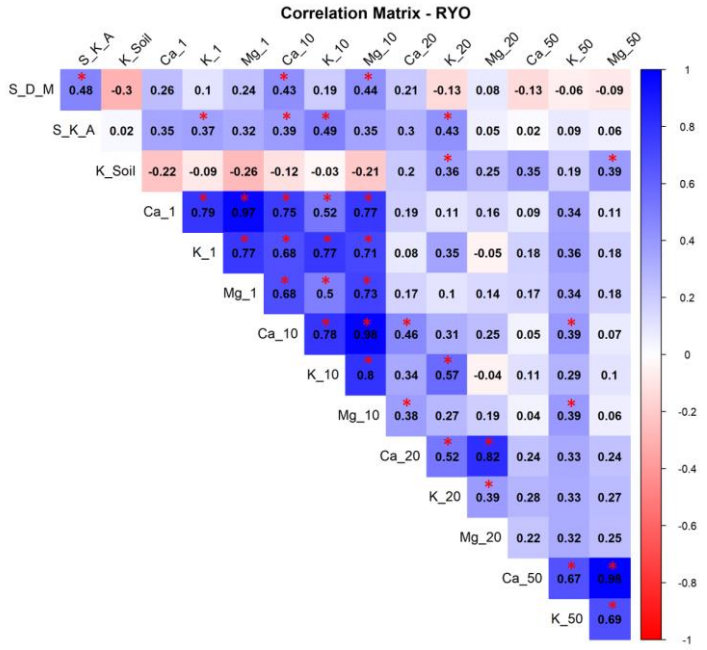

(b)

Figure A3. Pearson correlation matrix of soil chemical properties and corn growth in RO (a) and RYO (b). Red * indicates statistically significant correlations at $p < 0.05$. S_D_M: shoot dry matter; S_K_A: shoot K accumulation; K_Soil: Residual K available in whole soil samples. Ca_1, K_1, Mg_1, Ca_10, K_10, Mg_10, Ca_20, K_20, Mg_20, Ca_50, K_50, Mg_50: Ca, K and Mg concentrations in soil solution collected at 1, 10, 20, and 50 days after planting.

REFERENCES

1. Cui, J.; Tcherkez, G. Potassium Dependency of Enzymes in Plant Primary Metabolism. Plant Physiol. Biochem. 2021, 166, 522–530. https://doi.org/10.1016/j.plaphy.2021.06.017.

2. Johnson, R.; Vishwakarma, K.; Hossen, M.S.; Kumar, V.; Shackira, A.M.; Puthur, J.T.; Abdi, G.; Sarraf, M.; Hasanuzzaman, M. Potassium in Plants: Growth Regulation, Signaling, and Environmental Stress Tolerance. Plant Physiol. Biochem. 2022, 172, 56–69. https://doi.org/10.1016/j.plaphy.2022.01.001.

3. Lopes, A.S.; Guimarães Guilherme, L.R. A Career Perspective on Soil Management in the Cerrado Region of Brazil. Adv. Agron. 2016, 137, 1–72.

4. FAO FAOSTAT. Available online: https://www.fao.org/faostat/en/#data/RFN/visualize (accessed on 30 September 2024).

5. Dadach, M.; Ahmed, M.Z.; Bhatt, A.; Radicetti, E.; Mancinelli, R. Effects of Chloride and Sulfate Salts on Seed Germination and Seedling Growth of Ballota Hirsuta Benth. and Myrtus communis L. Plants 2023, 12, 3906. https://doi.org/10.3390/plants12223906.

6. Liu, L.; Li, X.; Wang, C.; Ni, Y.; Liu, X. The Role of Chloride Channels in Plant Responses to NaCl. Int. J. Mol. Sci. 2024, 25, 19. https://doi.org/10.3390/ijms25010019.

7. Wu, Y.; Lu, J.; Wang, D.; Li, Y.; Feng, Z.; Ye, X. Physiological and Transcriptomic Profiles of Tobacco Seedling Leaves in Response to High Chloride Accumulation. J. Plant Interact. 2024, 19, 2355122. https://doi.org/10.1080/17429145.2024.2355122.

8. Santos, C.; Malta, M.R.; Gonçalves, M.G.M.; Borém, F.M.; Pozza, A.A.A.; Martinez, H.E.P.; de Souza, T.L.; Chagas, W.F.T.; de Melo, M.E.A.; Oliveira, D.P.; et al. Chloride Applied via Fertilizer Affects Plant Nutrition and Coffee Quality. Plants 2023, 12, 885. https://doi.org/10.3390/plants12040885.

9. Bilias, F.; Kalderis, D.; Richardson, C.; Barbayiannis, N.; Gasparatos, D. Biochar Application as a Soil Potassium Management Strategy: A Review. Sci. Total Environ. 2023, 858, 159782. https://doi.org/10.1016/j.scitotenv.2022.159782.

10. Jia, M.; Yu, J.; Li, Z.; Wu, L.; Christie, P. Effects of Biochar on the Migration and Transformation of Metal Species in a Highly Acid Soil Contaminated with Multiple Metals and Leached with Solutions of Different PH. Chemosphere 2021, 278, 130344. https://doi.org/10.1016/j.chemosphere.2021.130344.

11. Enaime, G.; Lübken, M. Agricultural Waste-based Biochar for Agronomic Applications. Appl. Sci. 2021, 11, 8914. https://doi.org/10.3390/app11198914.

12. Shoudho, K.N.; Khan, T.H.; Ara, U.R.; Khan, M.R.; Shawon, Z.B.Z.; Hoque, M.E. Biochar in Global Carbon Cycle: Towards Sustainable Development Goals. Curr. Res. Green Sustain. Chem. 2024, 8, 100409. https://doi.org/10.1016/j.crgsc.2024.100409.

13. Leng, L.; Xiong, Q.; Yang, L.; Li, H.; Zhou, Y.; Zhang, W.; Jiang, S.; Li, H.; Huang, H. An Overview on Engineering the Surface Area and Porosity of Biochar. Sci. Total Environ. 2021, 763, 144204. https://doi.org/10.1016/j.scitotenv.2020.144204.

14. Supraja, K.V.; Kachroo, H.; Viswanathan, G.; Verma, V.K.; Behera, B.; Doddapaneni, T.R.K.C.; Kaushal, P.; Ahammad, S.Z.; Singh, V.; Awasthi, M.K.; et al. Biochar Production and Its Environmental Applications: Recent Developments and Machine Learning Insights. Bioresour. Technol. 2023, 387, 129634. https://doi.org/10.1016/j.biortech.2023.129634.

15. Razzaghi, F.; Obour, P.B.; Arthur, E. Does Biochar Improve Soil Water Retention? A Systematic Review and Meta-Analysis. Geoderma 2020, 361, 114055. https://doi.org/10.1016/j.geoderma.2019.114055.

16. Allohverdi, T.; Mohanty, A.K.; Roy, P.; Misra, M. A Review on Current Status of Biochar Uses in Agriculture. Molecules 2021, 26, 5584. https://doi.org/10.3390/molecules26185584.

17. Pradhan, S.; Abdelaal, A.H.; Mroue, K.; Al-Ansari, T.; Mackey, H.R.; McKay, G. Biochar from Vegetable Wastes: Agro-Environmental Characterization. Biochar 2020, 2, 439–453. https://doi.org/10.1007/s42773-020-00069-9.

18. Weber, K.; Quicker, P. Properties of Biochar. Fuel 2018, 217, 240–261. https://doi.org/10.1016/j.fuel.2017.12.054.

19. Woolf, D.; Lehmann, J.; Ogle, S.; Kishimoto-Mo, A.W.; McConkey, B.; Baldock, J. Greenhouse Gas Inventory Model for Biochar Additions to Soil. Environ. Sci. Technol. 2021, 55, 14795–14805. https://doi.org/10.1021/acs.est.1c02425.

20. Adhikari, S.; Mahmud, M.A.P.; Nguyen, M.D.; Timms, W. Evaluating Fundamental Biochar Properties in Relation to Water Holding Capacity. Chemosphere 2023, 328, 138620. https://doi.org/10.1016/j.chemosphere.2023.138620.

21. Hu, W.; Zhang, Y.; Rong, X.; Zhou, X.; Fei, J.; Peng, J.; Luo, G. Biochar and Organic Fertilizer Applications Enhance Soil Functional Microbial Abundance and Agroecosystem Multifunctionality. Biochar 2024, 6, 3. https://doi.org/10.1007/s42773-023-00296-w.

22. Jiang, Y.; Li, T.; Xu, X.; Sun, J.; Pan, G.; Cheng, K. A Global Assessment of the Long-Term Effects of Biochar Application on Crop Yield. Curr. Res. Environ. Sustain. 2024, 7, 100247. https://doi.org/10.1016/j.crsust.2024.100247.

23. Laird, D. Biochar Amendments Make the Harvesting of Crop Residue for Bioenergy Production Sustainable. Nutr. Cycl. Agroecosystems 2023, 128, 293–307. https://doi.org/10.1007/s10705-023-10281-1.

24. Leite, A.D.A.; Melo, L.C.A.; Hurtarte, L.C.C.; Zuin, L.; Piccolla, C.D.; Werder, D.; Shabtai, I.; Lehmann, J. Magnesium-Enriched Poultry Manure Enhances Phosphorus Bioavailability in Biochars. Chemosphere 2023, 331, 138759. https://doi.org/10.1016/j.chemosphere.2023.138759.

25. Mota, C.P.; Silva, C.A. Biochar–Nitrogen Composites: Synthesis, Properties, and Use as Fertilizer for Maize. AppliedChem 2024, 4, 157–173. https://doi.org/10.3390/appliedchem4020011.

26. Marcińczyk, M.; Oleszczuk, P. Biochar and Engineered Biochar as Slow- and Controlled-Release Fertilizers. J. Clean. Prod. 2022, 339, 130685. https://doi.org/10.1016/j.jclepro.2022.130685.

27. Melo, L.C.A.; Lehmann, J.; Carneiro, J.S.d.S.; Camps-Arbestain, M. Biochar-Based Fertilizer Effects on Crop Productivity: A Meta-Analysis. Plant Soil 2022, 472, 45–58. https://doi.org/10.1007/s11104-021-05276-2.

28. Chen, G.; Wang, Y.; Wang, J.; Wang, J.; Yu, F.; Ma, Q.; Cheng, Z.; Yan, B.; Song, Y.; Cui, X. Production of Potassium-Enriched Biochar from Canna Indica: Transformation and Release of Potassium. Waste Manag. 2023, 164, 119–126. https://doi.org/10.1016/j.wasman.2023.03.044.

29. Hossain, M.Z.; Bahar, M.M.; Sarkar, B.; Donne, S.W.; Ok, Y.S.; Palansooriya, K.N.; Kirkham, M.B.; Chowdhury, S.; Bolan, N. Biochar and Its Importance on Nutrient Dynamics in Soil and Plant; Springer: Singapore, 2020; Volume 2, ISBN 0123456789.

30. Wang, C.; Luo, D.; Zhang, X.; Huang, R.; Cao, Y.; Liu, G.; Zhang, Y.; Wang, H. Biochar-Based Slow-Release of Fertilizers for Sustainable Agriculture: A Mini Review. Environ. Sci. Ecotechnology 2022, 10, 100167. https://doi.org/10.1016/j.ese.2022.100167.

31. Gao, Y.; Fang, Z.; Van Zwieten, L.; Bolan, N.; Dong, D.; Quin, B.F.; Meng, J.; Li, F.; Wu, F.; Wang, H.; et al. A Critical Review of Biochar-Based Nitrogen Fertilizers and Their Effects on Crop Production and the Environment. Biochar 2022, 4, 36. https://doi.org/10.1007/s42773-022-00160-3.

32. Shah, M.H.; Deng, L.; Bennadji, H.; Fisher, E.M. Pyrolysis of Potassium-Doped Wood at the Centimeter and Submillimeter Scales. Energy Fuels 2015, 29, 7350–7357. https://doi.org/10.1021/acs.energyfuels.5b01776.

33. Fachini, J.; Figueiredo, C.C.d.; Frazão, J.J.; Rosa, S.D.; da Silva, J.; Vale, A.T. do Novel K-Enriched Organomineral Fertilizer from Sewage Sludge-Biochar: Chemical, Physical and Mineralogical Characterization. Waste Manag. 2021, 135, 98–108. https://doi.org/10.1016/j.wasman.2021.08.027.

34. Fachini, J.; Figueiredo, C.C.d.; do Vale, A.T.; da Silva, J.; Zandonadi, D.B. Potassium-Enriched Biochar-Based Fertilizers for Improved Uptake in Radish Plants. Nutr. Cycl. Agroecosystems 2023, 128, 415–427. https://doi.org/10.1007/s10705-023-10273-1.

35. Fachini, J.; Figueiredo, C.C.d.; Vale, A.T. do Assessing Potassium Release in Natural Silica Sand from Novel K-Enriched Sewage Sludge Biochar Fertilizers. J. Environ. Manag. 2022, 314, 115080. https://doi.org/10.1016/j.jenvman.2022.115080.

36. Ndoung, O.C.N.; Souza, L.R.d.; Fachini, J.; Leão, T.P.; Sandri, D.; Figueiredo, C.C. de Dynamics of Potassium Released from Sewage Sludge Biochar Fertilizers in Soil. J. Environ. Manag. 2023, 346, 119057. https://doi.org/10.1016/j.jenvman.2023.119057.

37. Cheng, J.; Zhang, J.; Xiao, X.; Yuan, Y.; Liao, X.; Shi, B.; Zhang, S. Potassium Assisted Pyrolysis of Chinese Baijiu Distillers' Grains to Prepare Biochar as Controlled-Release K Fertilizer. Sci. Total Environ. 2023, 884, 163814. https://doi.org/10.1016/j.scitotenv.2023.163814.

38. Jin, J.; Wang, M.; Cao, Y.; Wu, S.; Liang, P.; Li, Y.; Zhang, J.; Zhang, J.; Wong, M.H.; Shan, S.; et al. Cumulative Effects of Bamboo Sawdust Addition on Pyrolysis of Sewage Sludge: Biochar Properties and Environmental Risk from Metals. Bioresour. Technol. 2017, 228, 218–226. https://doi.org/10.1016/j.biortech.2016.12.103.

39. Ahmed, M.J.; Hameed, B.H. Insight into the Co-Pyrolysis of Different Blended Feedstocks to Biochar for the Adsorption of Organic and Inorganic Pollutants: A Review. J. Clean. Prod. 2020, 265, 121762. https://doi.org/10.1016/j.jclepro.2020.121762.

40. Poyilil, S.; Palatel, A.; Chandrasekharan, M. Physico-Chemical Characterization Study of Coffee Husk for Feasibility Assessment in Fluidized Bed Gasification Process. Environ. Sci. Pollut. Res. 2022, 29, 51041–51053. https://doi.org/10.1007/s11356-021-17048-7.

41. Hussein, H.S.; Shaarawy, H.H.; Hussien, N.H.; Hawash, S.I. Preparation of Nano-Fertilizer Blend from Banana Peels. Bull. Natl. Res. Cent. 2019, 43, 26. https://doi.org/10.1186/s42269-019-0058-1.

42. Liu, M.; Li, F.; Liu, H.; Wang, C.H. Synergistic Effect on Co-Gasification of Chicken Manure and Petroleum Coke: An Investigation of Sustainable Waste Management. Chem. Eng. J. 2021, 417, 128008. https://doi.org/10.1016/j.cej.2020.128008.

43. Domingues, R.R.; Trugilho, P.F.; Silva, C.A.; De Melo, I.C.N.A.; Melo, L.C.A.; Magriotis, Z.M.; Sánchez-Monedero, M.A. Properties of Biochar Derived from Wood and High-Nutrient Biomasses with the Aim of Agronomic and Environmental Benefits. PLoS ONE 2017, 12, e0176884. https://doi.org/10.1371/journal.pone.0176884.

44. Sial, T.A.; Khan, M.N.; Lan, Z.; Kumbhar, F.; Ying, Z.; Zhang, J.; Sun, D.; Li, X. Contrasting Effects of Banana Peels Waste and Its Biochar on Greenhouse Gas Emissions and Soil Biochemical Properties. Process Saf. Environ. Prot. 2019, 122, 366–377. https://doi.org/10.1016/j.psep.2018.10.030.

45. SEBRAE Brasil é o 4o Produtor Mundial de Banana. Available online: https://sebrae.com.br/sites/PortalSebrae/artigos/brasil-e-o-4-produtor-mundial-de-banana%2C1f00286bf0837810VgnVCM1000001b00320aRCRD?utm_source=chatgpt.com (accessed on 30 September 2024).

46. Companhia Nacional de Abastecimento Boletim Da Safra de Café. Available online: https://www.conab.gov.br/info-agro/safras/cafe/boletim-da-safra-de-cafe (accessed on 30 September 2024).

47. Corrêa, J.C.; Miele, M. A Cama de Aves e Os Aspectos Agronômicos, Ambientais e Econômicos. In Manejo Ambiental na Avicultura; Embrapa Suínos e Aves: Concórdia, Brazil, 2011.

48. Bigolin, T.; Talamini, E. Impacts of Climate Change Scenarios on the Corn and Soybean Double-Cropping System in Brazil. Climate 2024, 12, 42. https://doi.org/10.3390/cli12030042.

49. Cabral Filho, F.R.; Soares, F.A.L.; Alves, D.K.M.; Teixeira, M.B.; Cunha, F.N.; da Silva, E.C.; Costa, C.T.S.; da Silva, N.F.; Cunha, G.N.; Cavalcante, W.S.d.S. Biomass Accumulation and Technical and Economic Efficiency of Potassium Sources Applied via Fertigation to Corn. Agric. 2022, 12, 497. https://doi.org/10.3390/agriculture12040497.

50. Thenveettil, N.; Reddy, K.N.; Reddy, K.R. Effects of Potassium Nutrition on Corn (Zea mays L.) Physiology and Growth for Modeling. Agric. 2024, 14, 968. https://doi.org/10.3390/agriculture14070968.

51. Morais, E.G.d.; Jindo, K.; Silva, C.A. Biochar-Based Phosphate Fertilizers: Synthesis, Properties, Kinetics of P Release and Recommendation for Crops Grown in Oxisols. Agronomy 2023, 13, 326. https://doi.org/10.3390/agronomy13020326.

52. Lang, T.; Jensen, A.D.; Jensen, P.A. Retention of Organic Elements during Solid Fuel Pyrolysis with Emphasis on the Peculiar Behavior of Nitrogen. Energy Fuels 2005, 19, 1631–1643. https://doi.org/10.1021/ef049739a.

53. Carneiro, J.S.D.S.; Lustosa Filho, J.F.; Nardis, B.O.; Ribeiro-Soares, J.; Zinn, Y.L.; Melo, L.C.A. Carbon Stability of Engineered Biochar-Based Phosphate Fertilizers. ACS Sustain. Chem. Eng. 2018, 6, 14203–14212. https://doi.org/10.1021/acssuschemeng.8b02841.

54. Singh, B.; Camps-Arbestain, M.; Lehmann, J. Biochar: A Guide to Analytical Methods; Csiro Publishing: Collingwood, Victoria, Australia, 2017, ISBN 9781486305094.

55. Lago, B.C.; Silva, C.A.; Melo, L.C.A.; Morais, E.G.d. Predicting Biochar Cation Exchange Capacity Using Fourier Transform Infrared Spectroscopy Combined with Partial Least Square Regression. Sci. Total Environ. 2021, 794, 148762. https://doi.org/10.1016/j.scitotenv.2021.148762.

56. Raij, B.v. Fertilidade Do Solo e Manejo de Nutrientes; International Plant Nutrition Institute: Peachtree Corners, GA, USA, 2011, p. 420.

57. do Carmo, D.L.; Silva, C.A.; de Lima, J.M.; Pinheiro, G.L. Electrical Conductivity and Chemical Composition of Soil Solution: Comparison of Solution Samplers in Tropical Soils. Rev. Bras. Cienc. do Solo 2016, 40, 20140795. https://doi.org/10.1590/18069657rbcs20140795.

58. Wickham, H. Ggplot2: Elegant Graphics for Data Analysis; Springer-Verlag: New York, NY, USA, 2016; Volume 35, ISBN 978-0-387-98140-6.

59. Venables, W.N.; Ripley, B.D. Statistics Complements to Modern Applied Statistics with S; Springer-Verlag: New York, NY, USA, 2002, ISBN 1441930086.

60. Hothorn, T.; Bretz, F.; Westfall, P. Simultaneous Inference in General Parametric Models. Biometrical J. 2008, 50, 346–363. https://doi.org/10.1002/bimj.200810425.

61. Wickham, H.; Averick, M.; Bryan, J.; Chang, W.; McGowan, L.; François, R.; Grolemund, G.; Hayes, A.; Henry, L.; Hester, J.; et al. Welcome to the Tidyverse. J. Open Source Softw. 2019, 4, 1686. https://doi.org/10.21105/joss.01686.

62. Fox, J.; Weisberg, S. An R Companion to Applied Regression; Sage publications: Thousand Oaks, CA, USA, 2018.

63. Nunes, C.A.; Freitas, M.P.; Pinheiro, A.C.M.; Bastos, S.C. Chemoface: A Novel Free User-Friendly Interface for Chemometrics. J. Braz. Chem. Soc. 2012, 23, 2003–2010. https://doi.org/10.1590/S0103-50532012005000073.

64. Piash, M.I.; Iwabuchi, K.; Itoh, T.; Uemura, K. Release of Essential Plant Nutrients from Manure- and Wood-Based Biochars. Geoderma 2021, 397, 115100. https://doi.org/10.1016/j.geoderma.2021.115100.

65. Selvarajoo, A.; Muhammad, D.; Arumugasamy, S.K. An Experimental and Modelling Approach to Produce Biochar from Banana Peels through Pyrolysis as Potential Renewable Energy Resources. Model. Earth Syst. Environ. 2020, 6, 115–128. https://doi.org/10.1007/s40808-019-00663-2.

66. Yin, G.; Zhang, F.; Gao, Y.; He, W.; Zhang, Q.; Yang, S. Increase of Bio-Char Yield by Adding Potassium Salt during Biomass Pyrolysis. J. Energy Inst. 2023, 110, 101342. https://doi.org/10.1016/j.joei.2023.101342.

67. Wu, W.; Yan, B.; Zhong, L.; Zhang, R.; Guo, X.; Cui, X.; Lu, W.; Chen, G. Combustion Ash Addition Promotes the Production of K-Enriched Biochar and K Release Characteristics. J. Clean. Prod. 2021, 311, 127557. https://doi.org/10.1016/j.jclepro.2021.127557.

68. de Oliveira Paiva, I.; de Morais, E.G.; Jindo, K.; Silva, C.A. Biochar N Content, Pools and Aromaticity as Affected by Feedstock and Pyrolysis Temperature. Waste Biomass Valorization 2024, 15, 3599–3619. https://doi.org/10.1007/s12649-023-02415-x.

69. Sarfaraz, Q.; Silva, L.; Drescher, G.; Zafar, M.; Severo, F.; Kokkonen, A.; Molin, G.; Shafi, M.; Shafique, Q.; Solaiman, Z. Characterization and Carbon Mineralization of Biochars Produced from Different Animal Manures and Plant Residues. Sci. Rep. 2020, 10, 2–10. https://doi.org/10.1038/s41598-020-57987-8.

70. Pariyar, P.; Kumari, K.; Jain, M.K.; Jadhao, P.S. Evaluation of Change in Biochar Properties Derived from Different Feedstock and Pyrolysis Temperature for Environmental and Agricultural Application. Sci. Total Environ. 2020, 713, 136433. https://doi.org/10.1016/j.scitotenv.2019.136433.

71. Li, L.; Long, A.; Fossum, B.; Kaiser, M. Effects of Pyrolysis Temperature and Feedstock Type on Biochar Characteristics Pertinent to Soil Carbon and Soil Health: A Meta-Analysis. Soil Use Manag. 2023, 39, 43–52. https://doi.org/10.1111/sum.12848.

72. Yuan, J.H.; Xu, R.K.; Zhang, H. The Forms of Alkalis in the Biochar Produced from Crop Residues at Different Temperatures. Bioresour. Technol. 2011, 102, 3488–3497. https://doi.org/10.1016/j.biortech.2010.11.018.

73. Zhao, S.; Ta, N.; Wang, X. Effect of Temperature on the Structural and Physicochemical Properties of Biochar with Apple Tree Branches as Feedstock Material. Energies 2017, 10, 1293. https://doi.org/10.3390/en10091293.

74. Enders, A.; Hanley, K.; Whitman, T.; Joseph, S.; Lehmann, J. Characterization of Biochars to Evaluate Recalcitrance and Agronomic Performance. Bioresour. Technol. 2012, 114, 644–653. https://doi.org/10.1016/j.biortech.2012.03.022.

75. Xiu, L.; Gu, W.; Sun, Y.; Wu, D.; Wang, Y.; Zhang, H.; Zhang, W.; Chen, W. The Fate and Supply Capacity of Potassium in Biochar Used in Agriculture. Sci. Total Environ. 2023, 902, 165969. https://doi.org/10.1016/j.scitotenv.2023.165969.

76. Karim, A.A.; Kumar, M.; Singh, S.K.; Panda, C.R.; Mishra, B.K. Potassium Enriched Biochar Production by Thermal Plasma Processing of Banana Peduncle for Soil Application. J. Anal. Appl. Pyrolysis 2017, 123, 165–172. https://doi.org/10.1016/j.jaap.2016.12.009.

77. Hien, T.T.T.; Tsubota, T.; Taniguchi, T.; Shinogi, Y. Enhancing Soil Water Holding Capacity and Provision of a Potassium Source via Optimization of the Pyrolysis of Bamboo Biochar. Biochar 2021, 3, 51–61. https://doi.org/10.1007/s42773-020-00071-1.

78. Bong, H.K.; Selvarajoo, A.; Arumugasamy, S.K. Stability of Biochar Derived from Banana Peel through Pyrolysis as Alternative Source of Nutrient in Soil: Feedforward Neural Network Modelling Study. Environ. Monit. Assess. 2022, 194, 70. https://doi.org/10.1007/s10661-021-09691-x.

79. Fakhar, A.; Galgo, S.J.C.; Canatoy, R.C.; Rafique, M.; Sarfraz, R.; Farooque, A.A.; Khan, M.I. Advancing Modified Biochar for Sustainable Agriculture: A Comprehensive Review on Characterization, Analysis, and Soil Performance. Biochar 2025, 7, 8. https://doi.org/10.1007/s42773-024-00397-0.

80. Lehmann, J.; Joseph, S. Biochar for Environmental Management; Routledge: London, UK, 2009, ISBN 9780415704151.

81. Foroutan, R.; Peighambardoust, S.J.; Mohammadi, R.; Peighambardoust, S.H.; Ramavandi, B. Cadmium Ion Removal from Aqueous Media Using Banana Peel Biochar/Fe3O4/ZIF-67. Environ. Res. 2022, 211, 113020. https://doi.org/10.1016/j.envres.2022.113020.

82. Lu, Z.; Zhang, H.; Shahab, A.; Zhang, K.; Zeng, H.; Bacha, A.U.R.; Nabi, I.; Ullah, H. Comparative Study on Characterization and Adsorption Properties of Phosphoric Acid Activated Biochar and Nitrogen-Containing Modified Biochar Employing Eucalyptus as a Precursor. J. Clean. Prod. 2021, 303, 127046. https://doi.org/10.1016/j.jclepro.2021.127046.

83. Chung, N.T.; Thuy, D.T.; Trang, L.H.; Vu, N.T. Evaluating Coffee Husk Biochar as a Sustainable and Novel Adsorbent for Lead and Copper in Wastewater. Biomass Convers. Biorefinery 2025, online ahead of print, 1–17. https://doi.org/10.1007/s13399-025-06674-7.

84. Elnour, A.Y.; Alghyamah, A.A.; Shaikh, H.M.; Poulose, A.M.; Al-Zahrani, S.M.; Anis, A.; Al-Wabel, M.I. Effect of Pyrolysis Temperature on Biochar Microstructural Evolution,

Physicochemical Characteristics, and Its Influence on Biochar/Polypropylene Composites. Appl. Sci. 2019, 9, 7–9. https://doi.org/10.3390/app9061149.

85. Domingues, R.R.; Sánchez-Monedero, M.A.; Spokas, K.A.; Melo, L.C.A.; Trugilho, P.F.; Valenciano, M.N.; Silva, C.A. Enhancing Cation Exchange Capacity Ofweathered Soils Using Biochar: Feedstock, Pyrolysis Conditions and Addition Rate. Agronomy 2020, 10, 824. https://doi.org/10.3390/agronomy10060824.

86. Munera-Echeverri, J.L.; Martinsen, V.; Strand, L.T.; Zivanovic, V.; Cornelissen, G.; Mulder, J. Cation Exchange Capacity of Biochar: An Urgent Method Modification. Sci. Total Environ. 2018, 642, 190–197. https://doi.org/10.1016/j.scitotenv.2018.06.017.

87. Kharel, G.; Sacko, O.; Feng, X.; Morris, J.R.; Phillips, C.L.; Trippe, K.; Kumar, S.; Lee, J.W. Biochar Surface Oxygenation by Ozonization for Super High Cation Exchange Capacity. ACS Sustain. Chem. Eng. 2019, 7, 16410–16418. https://doi.org/10.1021/acssuschemeng.9b03536.

88. Doulgeris, C.; Kypritidou, Z.; Kinigopoulou, V.; Hatzigiannakis, E. Simulation of Potassium Availability in the Application of Biochar in Agricultural Soil. Agronomy 2023, 13, 784. https://doi.org/10.3390/agronomy13030784.

89. Rosolem, C.A.; Steiner, F. Effects of Soil Texture and Rates of K Input on Potassium Balance in Tropical Soil. Eur. J. Soil Sci. 2017, 68, 658–666. https://doi.org/10.1111/ejss.12460.

90. ISO 18644:2016; Fertilizers and Soil Conditioners. Controlled-Release Fertilizer. General Requirements. International Organization for Standardization: Geneva, Switzerland, 2016.

91. McBride, M.B. Environmental Chemistry of Soils; Oxford University Press: Oxford, UK, 1994.

92. Jalali, M. Major Ion Chemistry of Soil Solution of Mountainous Soils, Alvand, Hamedan, Western Iran. Soil Sediment Contam. Int. J. 2011, 20, 493–508. https://doi.org/10.1080/15320383.2011.587040.

93. Najafi-Ghiri, M.; Boostani, H.R.; Hardie, A.G. Investigation of Biochars Application on Potassium Forms and Dynamics in a Calcareous Soil under Different Moisture Conditions. Arch. Agron. Soil Sci. 2022, 68, 325–339. https://doi.org/10.1080/03650340.2020.1834083.

94. Wang, L.; Xue, C.; Nie, X.; Liu, Y.; Chen, F. Effects of Biochar Application on Soil Potassium Dynamics and Crop Uptake. J. Plant Nutr. Soil Sci. 2018, 181, 635–643. https://doi.org/10.1002/jpln.201700528.

95. Hoagland, D.R.; Arnon, D.I. The Water Culture Method for Growing Plants without Soil. Miscellaneous Publications No 354. Circ. Calif. Agric. Exp. Stn. 1941, 347, 461.

96. Cardoso, D.S.C.P.; Sediyama, M.A.N.; Poltronieri, Y.; Fonseca, M.C.M.; Neves, Y.F. Effect of Concentration and N:K Ratio in Nutrient Solution for Hydroponic Production of

Cucumber. Rev. Caatinga 2017, 30, 818–824. https://doi.org/10.1590/1983-21252017v30n401rc.

97. Lin, D.; Huang, D.; Wang, S. Effects of Potassium Levels on Fruit Quality of Muskmelon in Soilless Medium Culture. Sci. Hortic. 2004, 102, 53–60. https://doi.org/10.1016/j.scienta.2003.12.009.

98. Ebrahimi, R.; Souri, M.K.; Ebrahimi, F.; Ahmadizadeh, M. Growth and Yield of Strawberries under Different Potassium Concentrations of Hydroponic System in Three Substrates. World Appl. Sci. J. 2012, 16, 1380–1386.

99. Wilkinson, S.R.; Mays, D.A. Mineral Nutrition. Tall Fescue 2015, 20, 41–73. https://doi.org/10.2134/agronmonogr20.c4.

100. Cometti, N.N.; Furlani, P.R.; Genuncio, G. da C. SOLUÇÕES NUTRITIVAS: COMPOSIÇÃO, FORMULAÇÃO, USOS E ATRIBUTOS. In Nutrição Mineral de Plantas; Fernandes, M.S., Souza, S.R.d., Santos, L.A., Eds.; Sociedade Brasileira de Ciência do Solo: Viçosa, Brazil, 2018; p. 670, ISBN 978-85-86504-23-5.

101. Geilfus, C.M. Review on the Significance of Chlorine for Crop Yield and Quality. Plant Sci. 2018, 270, 114–122. https://doi.org/10.1016/j.plantsci.2018.02.014.

102. Geilfus, C.M. Chloride: From Nutrient to Toxicant. Plant Cell Physiol. 2018, 59, 877–886. https://doi.org/10.1093/pcp/pcy071.

103. Gamboa, A. La Fertilización Del Maiz; Instituto Internacional de la Potasa: Bern, Switzerland, 1980.

104. Yang, Y.; Ahmed, W.; Ye, C.; Yang, L.; Wu, L.; Dai, Z.; Khan, K.A.; Hu, X.; Zhu, X.; Zhao, Z. Exploring the Effect of Different Application Rates of Biochar on the Accumulation of Nutrients and Growth of Flue-Cured Tobacco (Nicotiana tabacum). Front. Plant Sci. 2024, 15, 1225031. https://doi.org/10.3389/fpls.2024.1225031.

105. ELsaman, N.K.; Amin, A.E.E.A.Z.; El-Razek, M.A.; Roshdy, N.M.K. Comparative Effects of Different Types and Doses of Biochar on Soil Quality Indicators and Arugula Growth under Saline Conditions. Sci. Rep. 2025, 15, 10046. https://doi.org/10.1038/s41598-025-92816-w.

106. Wang, R.; Liu, A.; Chen, X.; Wu, Y.; Peng, W. Effect of Potassium Rate on Yield, Potassium Uptake and Canopy Radiation Interception of Direct-Seeded Winter Canola. Chil. J. Agric. Res. 2023, 83, 107–118. https://doi.org/10.4067/S0718-58392023000100107.

Preliminary version of manuscript edited following the rules of ABNT

2.1.2 Potassium recovery from urine via struvite precipitation and biochar-enhanced retention

Gabrielly Nayara Tavares Silva Rodrigues[1], Johannes Lehmann[2], Lucinda Li[2], Carlos Alberto Silva[1]
[1]Escola de Ciências Agrárias de Lavras, Universidade Federal de Lavras, Lavras 37200-900, Brazil; gabriellynts@gmail.com (G.N.T.S.R.); csilva@ufla.br (C.A.S.)
[2]Soil and Crop Sciences, School of Integrative Plant Science, Cornell University, Ithaca, NY, USA; cl273@cornell.edu (J.L.)

Abstract: The sustainable recovery of potassium (K) from human urine represents a key strategy to close nutrient loops and reduce dependence on non-renewable fertilizers. This study investigated K recovery via the precipitation of potassium struvite ($MgKPO_4 \cdot 6H_2O$) from synthetic urine, integrating laboratory experiments with thermodynamic modeling using PHREEQC and Visual MINTEQ, and evaluating biochar as a seeding material to enhance K retention. Optimal recovery conditions were identified at a Mg:K:P molar ratio of 2:1:2 and pH 10, achieving K recovery efficiencies above 78%. PHREEQC simulations successfully predicted K-struvite formation under these conditions, while Visual MINTEQ underestimated saturation and favored competing phosphate phases, underscoring the need for model calibration. Biochar-assisted recovery experiments revealed that wood-derived biochars, particularly those pyrolyzed at 500 °C, enhanced K-struvite precipitation by up to 8% compared to controls, serving as effective nucleation matrices. In contrast, manure-derived biochars released K into solution, compromising recovery. Potassium release kinetics showed that co-pyrolyzed composites (biochar + K-struvite) functioned as slow-release carriers, suggesting potential for agricultural applications. These findings demonstrate the feasibility of coupling K-struvite precipitation with biochar-based matrices to recover and retain K from urine, providing a low-cost, sustainable strategy for nutrient recycling in decentralized sanitation and circular agriculture systems.

Keywords: Potassium recovery; K-struvite; PHREEQC; Visual MINTEQ; urine treatment; biochar; thermodynamic modeling; sustainable sanitation; nutrient recycling.

1. Introduction

The growth of the global human population and the concomitant increasing demand for food have intensified the need for higher agricultural productivity, which has, in turn, negatively impacted the sustainability of agricultural systems (CHEN, Jiao *et al.*, 2018; PRIYA; SARKAR; MAJI, 2024). Achieving higher yields often requires the expansion of productive land, increased land-use pressure, greater reliance on and efficient use of agricultural inputs, and higher labor demand, factors that contribute to the

overexploitation of ecosystem resources (WANG, 2022). Among these inputs, fertilizers are required in the largest quantities, with global consumption exceeding 187 million tons annually to support the production of more than 3 billion tons of food (USMAN *et al.*, 2020).

Mineral fertilizers can create environmental and economic constraints both at their production and application to soil (SANTOLIN *et al.*, 2024). Potassium (K), in particular, is a finite resource that must be mined and whose global supply is concentrated in a few countries, making it geopolitically and economically vulnerable (MURRELL *et al.*, 2020). This issue is especially critical in Brazil, which imports more than 97% of the K used in agriculture, exposing the national food production system to external risks and supply instability (FAO, 2023). Increasing the sustainable supply of K is therefore essential to ensuring resilient and circular nutrient systems in agriculture. Alternative sources such as urine-derived fertilizers have attracted attention for their potential to reduce dependency on mined K and improve nutrient recycling, in alignment with the United Nations' Sustainable Development Goals (SDGs) (WEI *et al.*, 2025).

Although human urine accounts for less than 1% of domestic wastewater by volume, it contributes approximately 80% of the nitrogen (N), 56% of the phosphorus (P), and 63% of the potassium (K) found in household effluents (RANDALL; NAIDOO, 2018; SALIU; OLADOJA; SAUVÉ, 2023). The concentrations of these nutrients in human urine vary according to dietary habits, water intake, physical activity, age, and other environmental factors (PATHY; RAY; PARAMASIVAN, 2021). Human urine contains potassium concentrations ranging from 0.16 to 4 g L^{-1}, making it a relevant and underutilized source for K recovery and sustainable fertilizer production (Pathy et al., 2021; Randall & Naidoo, 2018). Given the growing interest in nutrient recycling and the dependency on imported K fertilizers in many regions, urine offers a promising alternative to close the potassium loop in agriculture.

Studies evaluating different techniques for nutrient recovery, particularly N and P, from urine, are well documented in the literature, with struvite precipitation being one of the most extensively investigated methods (GUNNARSSON; LALANDER; MCCONVILLE, 2023; MARTIN *et al.*, 2022). Ammonium (N-)Struvite (magnesium ammonium phosphate, $MgNH_4PO_4 \cdot 6H_2O$) preferentially precipitates in the presence of ammonium and has been widely studied by the scientific community. However, its potassium analog, K-struvite (magnesium potassium phosphate, $MgKPO_4 \cdot 6H_2O$), can also be precipitated and represents the most viable pathway for K recovery from urine,

while simultaneously contributing to the sustainable production of a valuable fertilizer for plant growth (KABDAŞLI; SICILIANO; *et al.*, 2022).

N-struvite precipitation is primarily facilitated by two factors: its low solubility (pKsp of 13.26) compared to K-struvite precipitation (pKsp 12.2), and the fact that at the optimal pH for N-struvite precipitation, the formation of other solids such as $Mg(OH)_2$ and $Mg_3(PO_4)_2$, which reduce purity, is minimized (KABDAŞLI; KUŞÇUOĞLU; *et al.*, 2022; XU *et al.*, 2015; YANG *et al.*, 2019). Although N-struvite formation is thermodynamically favored in solution, prioritizing the precipitation of K-struvite over N-struvite can be strategically justified from agronomic, environmental and operational perspectives. This is because K concentrations in fresh urine are typically higher than those of ammonium, with reported average values of 33.9 mmol L^{-1} for K^+ and 29.1 mmol L^{-1} for NH_4^+-N (LIU *et al.*, 2024). Also, ammonium can be recovered through alternative methods within the solution. NH_4^+ can be removed from the solution beforehand by recovering ammonia (NH_3) gas through processes such as stripping, vacuum thermal stripping, membrane-based systems and electrochemical technologies, which enable NH_4^+ removal with lower chemical input and energy demand, enhancing K-struvite precipitation efficiency (CHEN, Tse Lun *et al.*, 2021; HE *et al.*, 2024; KOGLER *et al.*, 2024; WU, Haotian; VANEECKHAUTE, 2022). Additionally, unlike N, K does not volatilize at all and does not leach easily when bound in K-struvite. Therefore, K-struvite synthesis should be prioritized, particularly when intended for application to tropical or sandy soils, or when producing balanced slow-release fertilizers that simultaneously supply both P and K.

The presence of other competitive ions in urine, such as Ca^{2+} and Na^+, can also compete with K during struvite crystal formation (KABDAŞLI; SICILIANO; *et al.*, 2022). This competition can be mitigated by removing or balancing these competing ions prior to the K-struvite precipitation process. High calcium (Ca) concentrations can inhibit K-struvite precipitation due to the strong interaction between Ca^{2+} and PO_4^{3-}, resulting in the formation of poorly soluble calcium phosphate ($Ca_3(PO_4)_2$), which becomes increasingly insoluble under alkaline conditions (KABDAŞLI; SICILIANO; *et al.*, 2022).

Another critical factor affecting K-struvite precipitation is pH. Alkaline conditions favor K recovery, with optimal pH values for K-struvite formation typically ranging between 9 and 11 (HUANG *et al.*, 2019). Furthermore, the molar ratio of Mg:K:P plays a significant role in promoting K-struvite precipitation, as the addition of excess Mg^{2+} and PO_4^{3-} to the solution can enhance recovery efficiency (LIU *et al.*, 2024).

Studies investigating the addition of K-struvite seeds or pre-formed crystals have reported a positive impact on potassium recovery (GAO *et al.*, 2018). Shan et al. (SHAN *et al.*, 2022) demonstrated that the introduction of small pre-formed K-struvite crystals into the solution reduced the activation energy required for nucleation, thereby accelerating the crystallization process. Additionally, the authors observed the formation of larger and more uniform crystals. This phenomenon is attributed to heterogeneous nucleation, where the presence of seed material lowers the energy barrier for K-struvite formation. Consequently, heterogeneous nucleation is widely employed in industrial struvite crystallization processes (GUAN *et al.*, 2023). However, alternative, low-cost seed materials have been insufficiently explored for enhancing K recovery from wastewater.

In particular, the potential of biochar as a heterogeneous nucleation site for K-struvite formation remains largely unexplored, and this study aims to evaluate its performance in both synthetic and modeled urine systems. While previous studies have investigated the influence of pH and Mg:K:P molar ratios on K-struvite precipitation, it remains unclear whether these parameters exert similar effects in the presence of solid seed materials, such as biochar, especially considering the diversity in surface chemistry, porosity, and charge characteristics across biochar types. To date, no study has systematically assessed biochar-assisted K-struvite formation using both experimental and modeling approaches. Furthermore, most thermodynamic models assume instantaneous chemical equilibrium, neglecting the effects of reaction kinetics. However, the formation of K-struvite crystals depends on dynamic processes such as nucleation, ion availability, and crystal growth rate, which are influenced by operational factors like mixing and resting times (MUHMOOD *et al.*, 2018; NATIVIDAD-MARIN; WILLIAM BURNS; SCHNEIDER, 2023). These kinetic aspects remain insufficiently understood and may significantly affect recovery efficiency under practical conditions. Understanding these kinetic effects is critical to designing efficient recovery systems, especially because model predictions alone may overestimate recovery under real-world conditions.

Therefore, this study aims to investigate and address the following scientific questions: i) How do pH and Mg:K:P molar ratio affect the recovery of dissolved potassium as K-struvite from synthetic urine?; ii) Can biochar be used as an effective seeding material to enhance K recovery from urine as K-struvite?; iii) How does the presence and type of biochar influence the effect of pH and Mg:K:P molar ratio on K-

struvite precipitation efficiency? iv) What is the optimal combination of mixing and resting times to maximize K recovery as K-struvite under controlled conditions?

2. Materials and Methods

2.1. Preparation of Synthetic Urine

Synthetic urine was prepared in the laboratory based on the formulation proposed by Kabdaşlı et al. (2022) (Table 1). The preparation followed three main criteria:

i) Urea was excluded due to its competition with K during struvite precipitation;

ii) Three Mg:K:P molar ratios were evaluated: the base ratio present in the synthetic urine formulation (Kabdaşlı et al., 2022) hereafter referred to as initial molar ratio, the stoichiometric ratio of pure K-struvite (1:1:1), and a modified ratio with excess magnesium and phosphate (2:1:2). Magnesium and phosphate concentrations were increased by adding magnesium chloride ($MgCl_2$) and sodium phosphate ($NaHPO_4$). Potassium content remained unchanged from the original synthetic urine formulation described by Kabdaşlı et al. (2022);

iii) Three pH conditions were evaluated: the observed pH of the synthetic urine without any adjustment (6.7) and two alkaline levels adjusted to pH 9 and pH 10. Adjustments were made using a 1 mol L^{-1} NaOH solution, and pH was measured with an Orion Star™ A211 benchtop pH meter (Thermo Fisher Scientific, Beverly, MA, USA).

The combination of molar ratios and pH conditions resulted in nine experimental treatments used for K-struvite precipitation. These are summarized in Table 2, which details the Mg:K:P molar ratio, pH condition, and corresponding pH value for each treatment.

Table 1 Composition of synthetic urine based on Kabdaşlı et al. (2022).

Name	Composition	Concentration (g L^{-1})
Calcium Chloride	$CaCl_2 \cdot 2H_2O$	0.65
Magnesium chloride	$MgCl_2$	0.30
Sodium Chloride	NaCl	4.60
Sodium Sulfate	Na_2SO_4	2.30
Sodium Citrate	$Na_3C_6H_8O_7 \cdot 2H_2O$	0.65
Sodium oxalate	$Na_2C_2O_4$	0.02

Monopotassium Phosphate	KH_2PO_4	1.41
Potassium Chloride	KCl	1.60
Creatinine	$C_4H_7N_3O$	1.10

Table 2 Experimental conditions for K-struvite precipitation, including Mg:K:P molar ratios, pH treatments, and final pH values.

Code	Mg:K:P Molar Ratio	pH Condition	pH Value
U_iR_pHO	Initial molar ratio	Observed	6.7*
U_iR_pH9	Initial molar ratio	Adjusted to 9	9.0
U_iR_pH10	Initial molar ratio	Adjusted to 10	10.0
U_1R_pHO	1:1:1 (K-struvite stoichiometry)	Observed	6.7*
U_1R_pH9	1:1:1 (K-struvite stoichiometry)	Adjusted to 9	9.0
U_1R_pH10	1:1:1 (K-struvite stoichiometry)	Adjusted to 10	10.0
U_2R_pHO	2:1:2 (Mg and P in excess)	Observed	6.7*
U_2R_pH9	2:1:2 (Mg and P in excess)	Adjusted to 9	9.0
U_2R_pH10	2:1:2 (Mg and P in excess)	Adjusted to 10	10.0

*Unadjusted pH refers to the native pH of the synthetic urine solution (6.7) prior to NaOH addition.

2.2. Precipitation Experiments

All combinations listed in Table 2 were evaluated under the following precipitation protocol: the K-struvite precipitation experiments were conducted in 50 mL Falcon tubes, each containing 40 mL of the evaluated solutions (Table 2). The tubes were sealed and placed on a shaker for a mixing time of 30 minutes, followed by a resting period for nucleation of again 30 minutes. After the resting period, the solution was filtered through 0.45 μm membranes and analyzed for residual K concentration using atomic absorption spectrophotometry (Model 210/211VGP with 220GF graphite furnace and 220AS autosampler, Buck Scientific, East Norwalk, CT, USA).

2.3. Thermodynamic Modeling using PHREEQC and Visual MINTEQ

To understand the precipitation mechanisms of and predict K-struvite ($MgKPO_4 \cdot 6H_2O$) precipitation from the synthetic urine used in this study, simulations were performed using PHREEQC (v3.8.6) and Visual MINTEQ (v4.0). Both software packages are widely applied to predict solid phase formation based on chemical

equilibrium and the composition of the solution. The simulations aimed to evaluate K-struvite precipitation by calculating the saturation index (SI) and the distribution of chemical species within the synthetic urine matrix (Table 1). The SI was calculated as the logarithmic ratio between the ionic activity product and the solubility constant (Ksp), following standard geochemical modeling principles. As discussed by Khalidy & Santos (2021), the SI is a key parameter used to assess the precipitation or dissolution potential of mineral phases, allowing the identification of undersaturated ($SI < 0$), saturated ($SI = 0$), or supersaturated ($SI > 0$) conditions with respect to a given mineral.

To enhance the robustness of the simulations, both programs were used in parallel, enabling comparison across different thermodynamic databases and modeling outcomes. The *minteq.v4* database was selected due to its proven reliability in predicting struvite and related phosphate minerals (Natividad Marín et al., 2023), and its widespread adoption in similar studies. Since the K-struvite phase is not included in standard thermodynamic databases, its solubility product (pKsp = 12.2 at 25 °C, Xu et al., 2015), was manually incorporated into the models. The Na-struvite phase was also included, based on its reported solubility product (pKsp = 11.6 at 25 °C). This customization was essential to accurately represent the precipitation potential of these mineral phases.

Beyond estimating saturation conditions, the modeling approach also aimed to provide mechanistic insights into the precipitation behavior of K-struvite under varying pH and ionic conditions, and to identify possible competing mineral phases. These simulations contributed to the interpretation of experimental findings and helped elucidate the chemical drivers of K recovery efficiency.

The high variability in saturation index predictions across databases, as previously reported in the literature, reinforces the importance of both clearly specifying the database used and validating the model against experimental evidence. Simulations were performed using synthetic urine compositions with Mg:K:P molar ratios of the initial formulation, 1:1:1, and 2:1:2, at 25 °C, with pH adjusted from the native value to 9 and 10, assuming a total volume of 1 L. This volume was adopted only for modeling standardization and does not correspond to the volume used in lab experiments. Calculations were based on thermodynamic equilibrium, evaluating the SI ($SI \geq 0$) of all solid phases present in the database, without enforcing precipitation.

2.4. Chemical factors affecting K-struvite synthesis

Given that the simulations performed using PHREEQC and Visual MINTEQ do not account for kinetic effects, an experiment was conducted to evaluate the influence of mixing and resting time on K-struvite precipitation from synthetic urine. For this purpose, synthetic urine with a Mg:K:P molar ratio of 2:1:2 and pH adjusted to 10 was used. The experiment was carried out in 50 mL Falcon tubes, each containing 40 mL of the prepared solution. Four mixing times (Tm) (0.5, 1, 6, and 24 hours) and four resting times (Tr) (0.5, 1, 6, and 24 hours) were evaluated. Each tube was first agitated for the designated mixing time, followed by a static resting period corresponding to the specified resting time. After the resting phase, the solutions were filtered using 0.45 µm membranes, and the filtrates were collected for analysis. The residual potassium content in the filtered solutions was then determined by atomic absorption spectrophotometry.

2.5. Biochar Synthesis

Two feedstocks with distinct characteristics were selected for biochar production: dairy manure and maple wood. The maple wood was collected in the city of Ithaca, New York (USA), ground using a hammer mill, and sieved to a 2 mm particle size prior to biochar production. Dairy manure was obtained from the Cornell University Ruminant Center. It was freshly collected from the barn floor, outside the cows' sand bedding, to avoid contamination with bedding material. The manure was then oven-dried at 105 °C until it reached a constant weight, sieved to 2 mm, and stored for later pyrolysis. For pyrolysis, the dried feedstocks were placed in a charcolator (ISWARDI *et al.*, 2025), a muffle furnace (Fisher Isotemp Model 126, Thermo Fisher Scientific, Waltham, MA) equipped with a drum and a rotating paddle operating at a constant speed to ensure homogenization of the material. To prevent oxygen ingress during pyrolysis, the drum was sealed, and nitrogen gas (N_2) was continuously injected throughout the process at a flow rate of 1 L min^{-1}. The heating program included two stages: an initial ramp of 5 °C min^{-1} until reaching 240 °C, followed by a second ramp of 2.5 °C min^{-1} until the target pyrolysis temperature (300, 500, or 700 °C) was reached. The target temperature was maintained for 60 minutes. After this residence time, the furnace was turned off, and tap water was circulated through an external cooling coil attached to the drum to accelerate the cooling process. Once cooled, the biochar was collected, weighed to determine yield, and stored in airtight containers to prevent moisture uptake.

2.6. Composite Biochar Synthesis

To evaluate whether pre-treatment of feedstocks with Mg and P could enhance the effectiveness of biochar as a seed material for K-struvite precipitation, portions of the dairy manure and maple wood were pre-treated with magnesium chloride ($MgCl_2$) and sodium phosphate ($NaHPO_4$) prior to pyrolysis to produce MgP-enriched biochars. Briefly, $MgCl_2$ and $NaHPO_4$ were mixed with the feedstocks to match the Mg:K:P molar ratio used in the target synthetic urine solution (2:1:2), soaked in deionized water (1:10 solid-to-liquid ratio), and stirred with a magnetic stir bar for 30 minutes. The mixture was then oven-dried at 70 °C (until constant weight) and subsequently pyrolyzed at 500 °C, following the procedure previously described.

2.7. Struvite-biochar interaction

To assess the potential of biochar as a matrix for K-struvite precipitation, 2 g of each biochar were added to 50 mL Falcon tubes containing 40 mL of synthetic urine. In this case, synthetic urine was evaluated using both, the initial molar ratio and a 2:1:2 ratio, with pH adjusted to 10 for both conditions. Both mixing time and resting time were initially set to 30 minutes. After the time for full struvite nucleation, the solution was filtered through 0.45 mm membranes and the remaining K concentration was measured by atomic absorption spectrophotometry.

In addition to the fixed-time experiment, the influence of mixing and resting time was also evaluated by applying four different durations for each parameter (0.5, 1, 6, and 24 hours). For this purpose, synthetic urine with a Mg:K:P molar ratio of 2:1:2 and pH adjusted to 10 was used, and the selected biochar was derived from maple wood pyrolyzed at 500 °C. Tubes were first agitated for the specified Tm, followed by the corresponding resting time. As in previous experiments, samples were filtered and analyzed to determine the residual K concentration in solution.

2.8. Kinetics of Potassium Release

To evaluate the release of K from the formed compounds, a sequential extraction experiment was conducted using a 0.01 mol L^{-1} calcium chloride ($CaCl_2$) solution. This extractant was selected as a mild agent commonly used to simulate potassium availability in environmental systems. Five conditions were evaluated in separate experiments, each

performed in triplicate: (i) pure biochar (BC); (ii) a composite prepared by mixing K-struvite with biomass prior to pyrolysis (BC_S); (iii) a physical mixture of K-struvite and biochar (BC+S); (iv) pure K-struvite (S); and (v) pyrolyzed struvite (Sp).

To obtain pure K-struvite, a synthetic urine solution was prepared with a Mg:K:P molar ratio of 2:1:2 and pH adjusted to 10. After precipitation, the solution was filtered using 0.45 µm membranes, and the solid retained on the membrane was collected and oven-dried at 70 °C until reaching constant weight.

Maple wood was used as the feedstock for biochar production. Three types of materials were prepared and pyrolyzed: (i) pure biochar produced solely from maple wood (BC), (ii) composite biochar produced by mixing maple wood with K-struvite precipitated from U_2R_pH10 prior to pyrolysis (BC_S), and (iii) pure K-struvite (Sp). These materials were placed into previously weighed lidded crucibles and inserted into the same muffle furnace (Fisher Isotemp Model 126, Thermo Fisher Scientific, Waltham, MA) described previously, this time without the rotating paddle. To prevent oxygen ingress during pyrolysis, the drum was sealed, and nitrogen gas (N_2) was continuously injected throughout the process at a rate of 1 L min^{-1}. The furnace heating rate followed two ramps: first at 5 °C min^{-1} until reaching 240 °C, followed by 2.5 °C min^{-1} until reaching the target temperature of 300 °C, which was maintained for 60 minutes. After the residence time, the furnace was turned off, and tap water was circulated through an external coil to accelerate the cooling process. Once cooled, the crucibles were weighed to determine yield, and the biochars were stored in airtight containers to prevent moisture uptake.

For the extraction experiments, 2 grams of each material were placed on pre-weighed 0.45 µm membrane filters, mounted on glass funnels positioned over 50 mL Falcon tubes. At each extraction time interval (0.5, 1, 6, 12 and 24 hours), a fresh aliquot of 40 mL of $CaCl_2$ solution was passed through each sample, and the resulting extract was collected in the Falcon tube beneath the funnel. The potassium content in each extract was determined by atomic absorption spectrophotometry. Based on these results, the cumulative amount of K released at each time point was calculated and converted into the K release rate (%) according to Equation 2:

$$K\ release\ (\%) = \left(\frac{K_t}{K_{t0}}\right) * 100 \qquad \text{(Eq.2)}$$

Where K_t is the cumulative K content at each evaluated time (mg kg^{-1}), and K_{t0} is the initial total K content (mg kg^{-1}) placed in each sample.

To describe the release kinetics of potassium, the experimental data were fitted to five commonly used kinetic models: linear (Equation 3), power function (Equation 4), Elovich (Equation 5), parabolic (Equation 6), and exponential models (Equation 7). The selection of the best-fitting model was based on the coefficient of determination (R^2), the root mean square error (RMSE), and the Akaike information criterion (AIC), with preference given to models showing the highest R^2 and the lowest RMSE and AIC values.

$$K_t = a + bt \quad (3)$$

$$K_t = at^b \quad (4)$$

$$K_t = a + b\exp(-ct) \quad (5)$$

$$K_t = a + bt^{1/2} \quad (6)$$

$$K_t = N_0\exp(-kt) \quad (7)$$

Where Kt is the amount of K released at time t. For the linear model (Equation 3): a is the initial amount of K released, and b is the constant release rate over time. For the power function model (Equation 4): a is the scaling coefficient, and b is the exponent that determines the rate of K release over time. For the Elovich model (Equation 5): a is the initial K content, b is the scaling coefficient, and c is the exponential decay rate constant. For the parabolic diffusion model (Equation 6): a is the intercept representing the initial release, and b is the diffusion-related coefficient associated with $t^{1/2}$, indicating a diffusion-controlled release mechanism. For the exponential model (Equation 7): N_0 is the maximum amount of K released during the experiment, and k is the decay rate constant. These models were applied to describe the K release kinetics under the experimental conditions.

2.9. Statistical Analysis

All experimental data were subjected to statistical analysis using R software (R Core Team, 2024). For each experiment, an analysis of variance (ANOVA) was performed. When significant differences were detected ($p < 0.05$), treatment means were compared using Tukey's post hoc test ($p < 0.05$). Results are presented as treatment means with standard deviations and statistical groupings. Analyses were conducted using the R packages *tidyverse*, *MASS*, and *multcomp* (FOX; WEISBERG, 2018; HOTHORN;

BRETZ; WESTFALL, 2008; VENABLES; RIPLEY, 2002; WICKHAM, 2016; WICKHAM *et al.*, 2019).

3. Results and Discussion

3.1. Influence of molar ratio and pH on K recovery through K-struvite precipitation

The first experiment was conducted by increasing the original molar ratio of Mg:K:P to 1:1:1 and 2:1:2 to assess the influence of excess Mg and P on K-struvite precipitation. For this experiment, the pH was kept constant at 10 (Fig. 2a). The second experiment was performed by varying the pH of the synthetic urine while maintaining the Mg:K:P molar ratio at 2:1:2, aiming to evaluate the effect of solution pH on K-struvite precipitation (Fig. 2b).

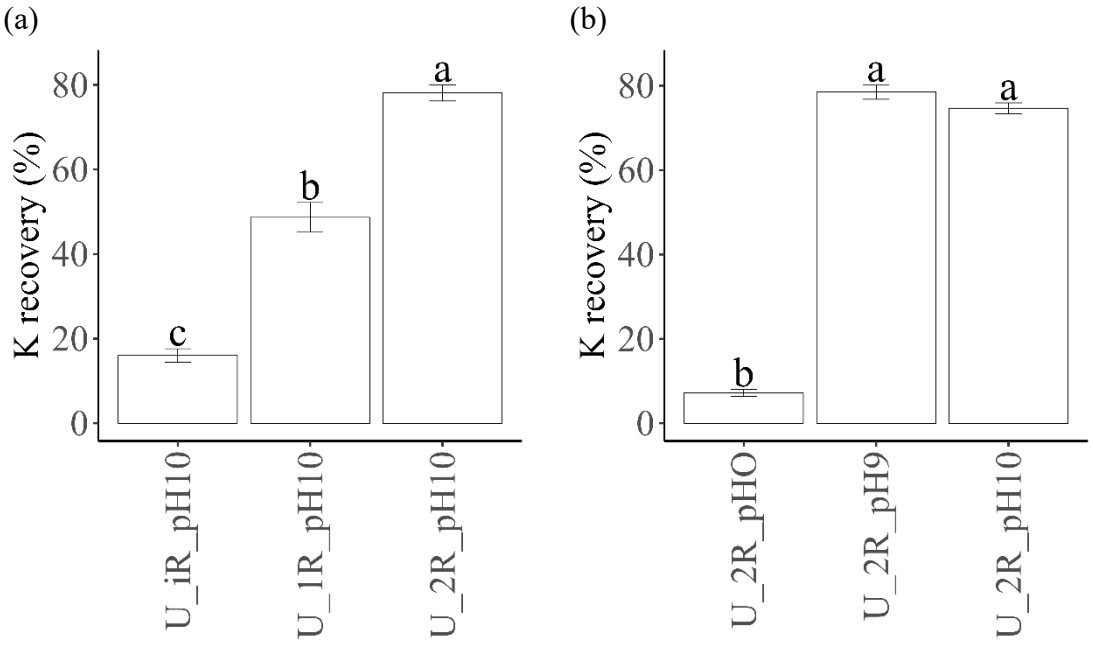

Figure 8. Effect of Mg and P overdoses (a) and pH adjustment (b) on K-struvite recovery from synthetic urine. U = synthetic urine; iR = initial molar ratio; 1R = 1:1:1 molar ratio; 2R = 2:1:2 molar ratio; pHO, pH9, and pH10 correspond to the evaluated initial and adjusted pH values. Error bars represent standard deviation; different letters indicate statistically significant differences among treatments according to Tukey's test ($p < 0.05$).

The results clearly indicate that the addition of Mg and P was essential to significantly enhance K recovery from synthetic urine. When the Mg:K:P molar ratio was increased from the initial condition (U_iR_pH10) to 1:1:1 (U_1R_PH10), K recovery

rose from 16% to over 48% (Fig 2 a). Recovery was even higher when the molar ratio was adjusted to 2:1:2 (U_2R_PH10), reaching values above 78%. These results are consistent with those reported by Gao et al. (2018) and Kabdaşlı et al.(2022), who also observed increased K recovery with excess Mg and P in solution. These improvements are due to the creation of supersaturated conditions with excess Mg and P, which promote K-struvite precipitation and compensate for competing phosphate solids (KABDAŞLI; SICILIANO; *et al.*, 2022). Although higher Mg and P levels enhance recovery, they may slightly reduce precipitate purity and increase costs, necessitating careful optimization for practical applications.

Regarding pH, it is clear that alkaline conditions, specifically increasing pH to values above 9, significantly enhance K recovery. When the solution pH was increased from approximately 6.7 to around 9, K recovery rose from 7% to 78%. However, further increasing the pH to approximately 10 did not result in a significant improvement in K recovery compared to pH 9. This finding is consistent with several studies evaluating K-struvite precipitation under conditions involving real urine, synthetic urine and other types of wastewater (HU *et al.*, 2020; XU *et al.*, 2024; YANG *et al.*, 2019). The limited improvement at higher pH values could be related to the formation of competing phosphate minerals, such as hydroxyapatite, which may decrease the purity and limit additional gains in K recovery (WEI *et al.*, 2025). In addition, pH strongly affects the chemical equilibrium of the system: at higher pH values, species such as $Mg(OH)_2$ and other magnesium phosphates may co-precipitate, reducing the availability of Mg^{2+} for K-struvite formation (WEI *et al.*, 2025). Although pH 10 is often cited as optimal for K-struvite crystallization, further increases may favor the precipitation of other phases and introduce more sodium into the system when NaOH is used for pH adjustment, which can also reduce the purity of the final product (HUANG *et al.*, 2019).

3.2. Modeling Using PHREEQC and Visual MINTEQ

Using PHREEQC, K-struvite precipitation was predicted at all ratios, with increasing SI values from 2.01 (original) to 3.26 (1:1:1) and 3.67 (2:1:2), indicating greater precipitation potential with Mg and P enrichment. In contrast, Visual MINTEQ did not predict K-struvite precipitation in any scenario, with SI values consistently below zero and no solid phase formed. PHREEQC predicted hydroxyapatite potential formation across all conditions, and consistently high saturation indices for magnesium phosphate ($Mg_3(PO_4)_2$), with SI values increasing from 2.99 to 7.51 across the tested molar ratios.

Additionally, magnesium hydrogen phosphate ($MgHPO_4$) became supersaturated at the 1:1:1 and 2:1:2 ratios (SI = 0.89 and 1.31, respectively), indicating that both phosphate minerals may act as competing phases under enriched conditions. In contrast, Visual MINTEQ did not predict precipitation of these phases, as all corresponding SI values remained negative. These differences were also reflected in the calculated ionic strength, which was slightly higher in PHREEQC (0.207 – 0.407 mol/kgw) compared to MINTEQ (0.194 – 0.2637 mol/kgw), potentially affecting chemical compound speciation and saturation outcomes.

In PHREEQC, Na-struvite ($MgNaPO_4 \cdot 6H_2O$) showed increasing SI values and potential for precipitation as the molar ratio increased, although no solid phase was formed since precipitation was not forced. In contrast, Visual MINTEQ predicted the formation of hydroxyapatite and $MgNaPO_4$, for all scenarios. These alternative phases also impacted predicted ion removal. Visual MINTEQ showed substantial phosphate removal, up to 96.97% at the 1:1:1 ratio and 85.05% at 2:1:2, while K^+ remained entirely in solution. Mg^{2+} and Ca^{2+} were also removed via formation of competing mineral phases. These findings suggest that although K-struvite did not precipitate in the models, PHREEQC indicated favorable conditions for its formation through positive SI values, while Visual MINTEQ did not recognize K-struvite as a viable solid phase and instead favored alternative phosphate mineral pathways.

When evaluating the influence of pH on precipitation behavior, the simulations clearly showed that alkaline conditions are essential for K-struvite formation. A noticeable difference between the two software tools also becomes evident. In Visual MINTEQ, K-struvite was not predicted to precipitate at any pH level, with SI values decreasing from -0.975 at pH 6.68 to -2.258 at pH 10. In contrast, PHREEQC showed a progressive increase in the SI for K-struvite as the pH increased from 6.68 to 9 and 10, with values of 0.33, 2.77, and 3.67, respectively, which demonstrated that increasing the original solution pH to around 9 or 10 is essential for enhancing K recovery. These results are in agreement with previous studies showing optimal precipitation of K-struvite under alkaline conditions (HU *et al.*, 2020; XU *et al.*, 2024; YANG *et al.*, 2019).

A widely discussed limiting factor for K-struvite precipitation in the literature is the concentration of Na^+ ions, which can also precipitate as Na-struvite ($MgNaPO_4 \cdot 7H_2O$). However, some studies have shown that the optimal pH for Na-struvite formation is around 12, slightly above the ideal range for K-struvite precipitation (HUANG *et al.*, 2019; XU *et al.*, 2024). This further supports the selection of a pH

between 9 and 10 as the optimal range for promoting full K-struvite formation. In the simulations, the influence of pH on Na-struvite behavior was evident. In PHREEQC, no precipitation was forced, but the saturation index for Na-struvite increased with rising pH, indicating greater thermodynamic potential for its formation under alkaline conditions. Similarly, Visual MINTEQ predicted Na-struvite precipitation only at pH 9 and 10, but not at pH 6.68, where the saturation index remained below zero. These results confirm that alkaline conditions not only favor K-struvite precipitation but also enhance the likelihood of competing Na-struvite formation, which may decrease the overall phosphate recovery.

Cross-validation between simulations and experimental data reinforces the robustness of the adopted methodology and contributes to advancing selective nutrient recovery strategies in complex effluent systems, such as synthetic urine. The increasing trend in K-struvite saturation index predicted by PHREEQC aligns with the laboratory findings, which demonstrated that an excess of Mg and P and the increase in pH is essential to promote struvite precipitation. These results support the observation by Natividad-Marín et al. (2023) that thermodynamic models are useful tools for identifying favorable precipitation conditions. However, such models often overlook key factors like reaction kinetics, induction time, and crystal growth dynamics, which strongly influence precipitation outcomes under real experimental conditions Furthermore, the differences in solution composition and ionic strength between synthetic effluents and natural systems, such as soils, for which Visual MINTEQ was originally developed, along with its assumption of instantaneous equilibrium, may limit the predictive accuracy when applied to engineered nutrient recovery processes (GUSTAFSSON, 2014).

Given that PHREEQC and Visual MINTEQ simulations do not account for the influence of time on K-struvite precipitation, an experiment was carried out to evaluate the effect of different mixing and resting times on K-struvite formation from synthetic urine (Fig. 3). It is known that in homogeneous solutions such as synthetic urine, nucleation requires higher levels of supersaturation of Mg^{2+} and PO_4^{3-} and energy input (SHAN *et al.*, 2022) . In a study on (N-)Struvite precipitation from produced water generated during oil and gas extraction, Hu et al. (2020) estimated that precipitation efficiency increases rapidly within the first 10 minutes, reaching equilibrium within the following 20 minutes, consistent with earlier studies that reported an optimal struvite crystallization time between 20 and 30 minutes (MUHMOOD *et al.*, 2018).

For K-struvite, regardless of the mixing and resting times evaluated, potassium recovery from synthetic urine with a Mg:K:P molar ratio of 2:1:2 at pH 10 exceeded 75% across all treatments. However, the best K removal was achieved with 1 hour of mixing followed by 30 minutes of resting, enabling plentiful nucleation (81.7%). The inverse setup (30 minutes mixing + 1 hour resting), as well as the condition using 1 hour for both stages, also showed statistically similar performance (81.6%). The lowest removal efficiency was observed with 24 hours of mixing followed by 1 hour of resting (75.7%). These results indicate that K-struvite precipitation does not occur instantly but requires a minimum period of mixing and rest, emphasizing the role of kinetic factors in the synthesis of K-struvite, as also reported by Natividad-Marin et al. (2023). The authors showed that the precipitation time of struvite is a complex phenomenon influenced by various kinetic parameters, from the initial induction time required for nucleus formation to the rate at which ions are removed from the solution and crystals grow and aggregate.

The effect of resting time on K-struvite precipitation was strongly influenced by the mixing duration. For shorter mixing times (0.5 h and 1 h), resting time had a more pronounced effect, with statistically significant differences among treatments. In these cases, the best performance was achieved with 1 hour of resting, while excessive resting (24 h) led to a reduction in recovery, possibly due to redissolution or recrystallization in less favorable forms. When mixing time was extended to 6 or 24 hours, differences between resting times became less pronounced, suggesting that sufficient agitation promotes more stable and complete crystal formation, reducing the system's sensitivity to subsequent resting periods.

This behavior is not predicted by thermodynamic models, which assume instantaneous equilibrium among chemical species under specific conditions (such as pH, molar ratio, and ionic strength). Although simulations using PHREEQC and Visual MINTEQ indicate supersaturation of K-struvite under certain scenarios, actual precipitation depends on additional factors that influence crystal nucleation and growth. Furthermore, in thermodynamic modeling, the choice of software and its configuration can significantly affect the results of struvite precipitation simulations, even when using the same initial input data. This underscores the importance of understanding the modeling architecture of each tool and, ideally, validating simulation results with experimental data to ensure reliable predictions (NATIVIDAD-MARIN; WILLIAM BURNS; SCHNEIDER, 2023).

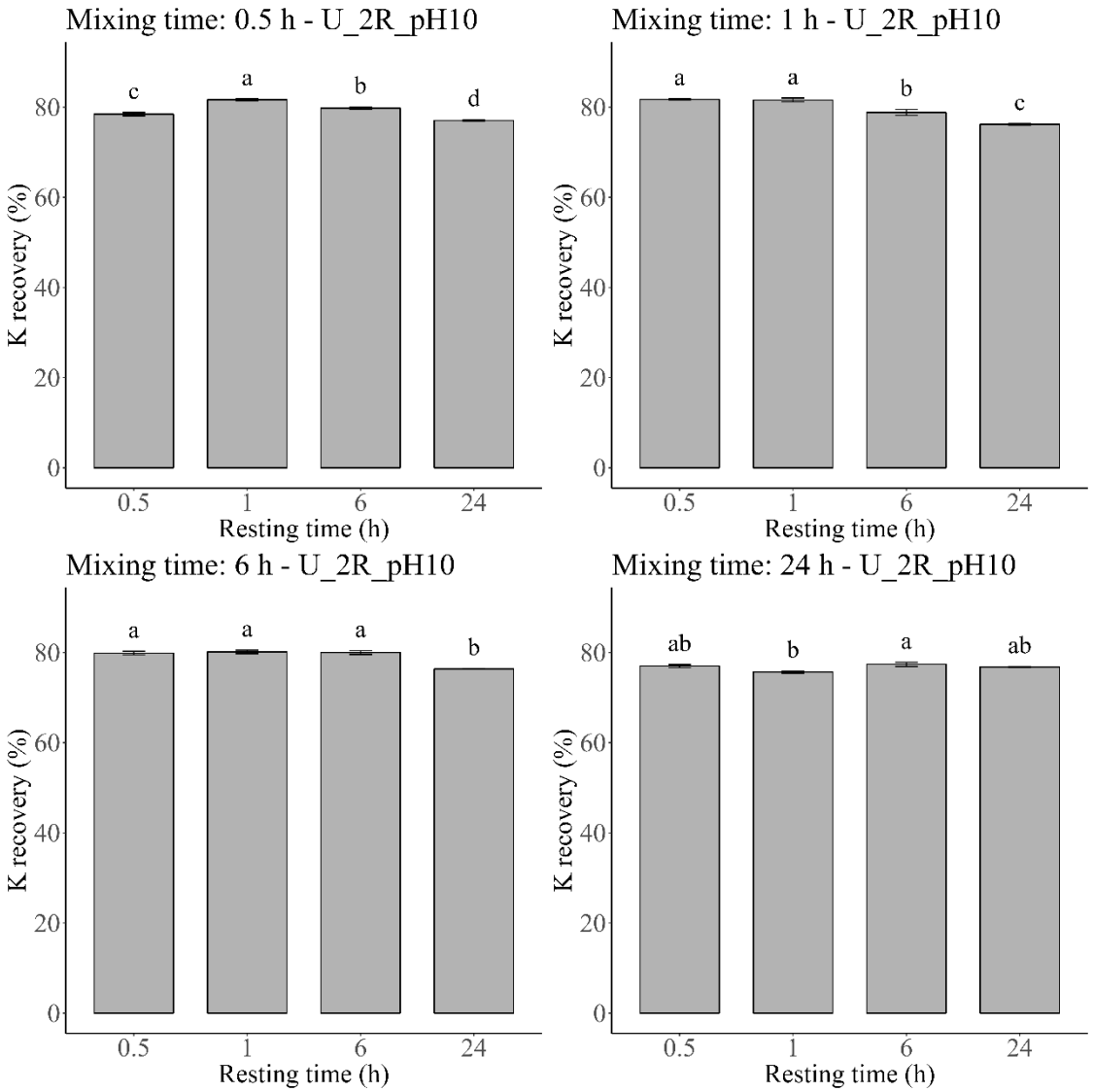

Figure 9. Effect of different mixing and resting times on K-struvite formation from synthetic urine. Bars represent potassium recovery (%) under varying combinations of mixing and resting durations. Error bars represent standard deviation; different letters indicate statistically significant differences among treatments according to Tukey's test ($p < 0.05$).

Table 3. Simulations performed using PHREEQC and Visual MINTEQ under different Mg:K:P molar ratios (original, 1:1:1, and 2:1:2) at pH 10 to optimize K-struvite synthesis.

Parameter	Mg:K:P Original Ratio | pH 10		Mg:K:P 1:1:1 | pH 10		Mg:K:P 2:1:2 | pH 10	
	PHREEQC	Visual MINTEQ	PHREEQC	Visual MINTEQ	PHREEQC	Visual MINTEQ
Precipitated phase(s)	None (no forced precipitation)	Hydroxyapatite, Na-struvite,	None (no forced precipitation)	Hydroxyapatite, Na-struvite,	None (no forced precipitation)	Hydroxyapatite, Na-struvite,
Hydroxyapatite SI	19.79	0	19.28	0	18.94	0
K-struvite SI	2.01	-0.152	3.26	-0.193	3.67	-2.258
Magnesium Phosphate SI	2.99	-3.305	6.44	-1.663	7.51	-1.777
Magnesium H phosphate SI	-0.38	-2.517	0.89	-2.552	1.31	-2.607
Na-struvite SI	2.16	0	3.51	0	4.03	0
Hydroxyapatite (mmol/L)	—	0.88	—	0.88	—	0.88
K-struvite (mmol/L)	—	0	—	0	—	0
Magnesium Phosphate (mmol/L)	—	0	—	0	—	0
Magnesium H phosphate (mmol/L)	—	0	—	0	—	0
Na-struvite (mmol/L)	—	3.06	—	29.03	—	60.87
Ca^{2+} removal (%)	—	99.98	—	99.95	—	99.94
K^{+} removal (%)	—	0	—	0	—	0
Mg^{2+} removal (%)	—	97.267	—	91.54	—	95.78
Na^{+1} removal (%)	—	1.674	—	12.85	—	21.024
PO_4^{3-} removal (%)	—	55.169	—	99.71	—	99.86
Ionic strength (mol/kgw)	0.207	0.194	0.299	0.221	0.407	0.2637

Table 4. Simulations performed with both PHREEQC and Visual MINTEQ across different pHs (original, 9 and 10) at fixed Mg:K:P molar ratio 2:1:2.

Parameter	Mg:K:P 2:1:2 | pH 6.68		Mg:K:P | 2:1:2 | pH 9		Mg:K:P 2:1:2 | pH 10	
	PHREEQC	Visual MINTEQ	PHREEQC	Visual MINTEQ	PHREEQC	Visual MINTEQ
Precipitated phase(s)	None (no forced precipitation)	Hydroxyapatite, Magnesium H phosphate	None (no forced precipitation)	Hydroxyapatite, Na-struvite,	None (no forced precipitation)	Hydroxyapatite, Na-struvite,
Hydroxyapatite SI	10.85	0	18.72	0	18.94	0
K-struvite SI	0.33	-0.975	2.77	-0.219	3.67	-2.258
Magnesium Phosphate SI	0.86	-2.375	5.75	-1.589	7.51	-1.777
Magnesium H phosphate SI	1.28	0	1.41	-1.569	1.31	-2.607
Na-struvite SI	0.57	-0.727	3.09	0	4.03	0
Hydroxyapatite (mmol/L)	—	0.87	—	0.88	—	0.88
K-struvite (mmol/L)	—	0	—	0	—	0
Magnesium Phosphate (mmol/L)	—	0	—	60.25	—	0
Magnesium H phosphate (mmol/L)	—	50.59	—	0	—	0
Na-struvite (mmol/L)	—	0	—	0	—	60.87
Ca^{2+} removal (%)	—	98.39	—	99.90	—	99.94
K^{+} removal (%)	—	0	—	0	—	0
Mg^{2+} removal (%)	—	79.61	—	94.812	—	95.78
Na^{+1} removal (%)	—	0		22.36		21.024
PO_4^{3-} removal (%)	—	83.63	—	98.88	—	99.86
Ionic strength (mol/kgw)	0.381	0.2775	0.402	0.2561	0.407	0.2637

3.3. Struvite-biochar mixture for maximum K retention

The addition of biochars as seed material did not significantly enhance K recovery from synthetic urine (Fig. 4). In fact, addition of dairy manure biochar produced at 500°C appeared to have a negative effect, as it resulted in a 9% lower recovery rate compared to the solution alone. This may be explained by the ability of the biochar to release K into the solution, producing the opposite effect of what was intended. A similar result was reported by Wu et al. (2023), who, in a study evaluating different K adsorbents, demonstrated that certain pristine biochars can release K into the solution rather than adsorbing it. These findings also suggest that manure-derived biochars may interfere with K-struvite formation due to the presence of competing ions or soluble organic matter that disrupts supersaturation or nucleation.

The slightly improved performance of adding MgP to the biochar observed in this study may be attributed to mechanisms described by Leite et al. (LEITE *et al.*, 2023), who demonstrated that pre-enriching animal manures with magnesium hydroxide prior to pyrolysis increased the formation of Mg–P phases (such as $Mg_3(PO_4)_2 \cdot 8H_2O$ and $MgNH_4PO_4$) and reduced the crystallinity and abundance of calcium phosphate minerals like hydroxyapatite. This shift in mineral composition enhanced P availability by reducing the formation of less soluble Ca–P species and potentially altering the biochar surface structure. In the context of K-struvite recovery, these Mg-induced modifications may facilitate nucleation or reduce competitive adsorption of phosphate, indirectly contributing to improved K recovery.

Interestingly, the wood-based MgP composite (W_500_MgP) showed no significant improvement over the non-treated wood biochar, which could suggest that the mechanisms enhancing P solubility in manure-based systems may not fully apply to low-ash woody feedstocks, where Ca content and mineral phases are less dominant. This observation reinforces the conclusion that the effectiveness of Mg enrichment is highly dependent on the biochar feedstock and its inherent Ca/Mg ratio.

For the U_2R solution (Fig. 4b), the trend was similar; however, both pure biochar and adding MgP resulted in approximately 82% K recovery, nearly 8% higher than the solution alone without biochar. This suggests that this type of biochar has the potential to improve K recovery from synthetic urine by acting as a seed and promoting K-struvite nucleation. These findings are consistent with previous studies showing that seed addition can enhance nutrient recovery from solution (HU *et al.*, 2020; SHAN *et al.*, 2022). The fact that this enhancement persisted even under highly supersaturated conditions (U_2) reinforces that the physical and chemical properties of the biochar surface play a critical role in promoting or inhibiting struvite formation. In this case, the addition of Mg and P prior to biochar production did not have a

significant effect on K recovery. Still, the slightly better performance of adding MgP to wood biochar suggests that surface modification can provide some additional benefit, although the intrinsic compatibility of wood biochar with struvite precipitation appears to be the dominant factor.

Altogether, these results emphasize that beyond the chemical composition, surface interactions between biochar and the solution environment influence nucleation, growth, or even redissolution of struvite phases, and should be considered when designing biochar-assisted nutrient recovery systems.

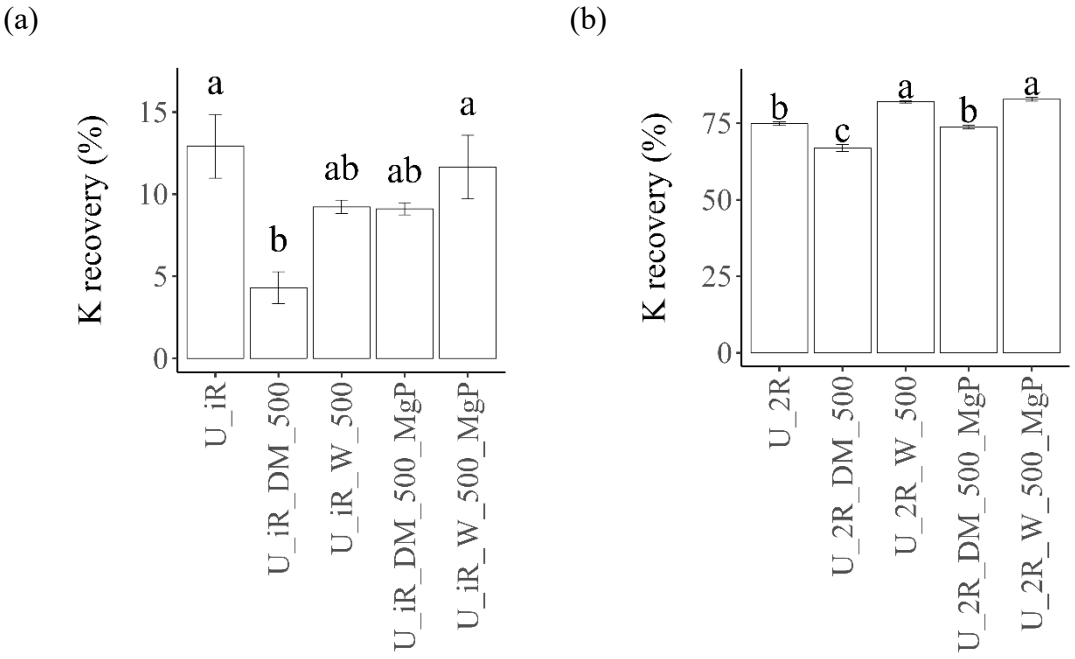

Figure 10. Influence of biochars on potassium recovery from synthetic urine under two different molar ratios: (a) original molar ratio (U_iR) and (b) optimized molar ratio (U_2R, 2:1:2). Treatments included biochars produced from dairy manure (DM) and wood (W) at 500 °C, both in pure form and pretreated with magnesium and phosphate (MgP). Error bars represent standard deviation; different letters indicate statistically significant differences among treatments according to Tukey's test ($p < 0.05$).

This study also evaluated whether the pyrolysis temperature (300, 500, and 700 °C) used in biochar production could influence its effectiveness as a seed material for K-struvite precipitation from synthetic urine. In experiments with the initial molar ratio solution, the addition of biochars did not enhance K recovery, consistent with previous observations (Fig 4a). However, pyrolysis temperature appeared to influence the residual K concentration in the solution. Increasing the pyrolysis temperature from 300 to 500 °C led to a decrease in K

recovery for both dairy manure and wood-derived biochars, suggesting that higher temperatures may promote the release of soluble K into the solution (XIU *et al.*, 2023).

Interestingly, further increasing the temperature from 500 to 700 °C had the opposite effect: biochars produced at 700 °C resulted in higher K recovery than those produced at 500 °C, indicating reduced K release at an even higher temperature. These findings are consistent with those of Bilias et al. (2023), who reported that pyrolysis temperatures above 500 °C promote the formation of a more inorganic matrix and, unexpectedly, result in lower concentrations of soluble K salts in biochars. Moreover, the trend observed here is further supported by Xiu et al. (2023), who showed that although total K increases with pyrolysis temperature, its distribution among chemical forms shifts significantly. At moderate temperatures (around 500 °C), a portion of the K becomes immobilized in less available phases, while at 700 °C, the relative abundance of exchangeable K increases again, improving its potential availability. This shift in speciation may help explain the partial recovery observed at higher temperatures in our experiments. Despite this relative improvement at 700 °C, none of the manure or wood-derived biochars outperformed the control without biochar, suggesting limited compatibility with K-struvite formation under the original molar condition.

For the solution with Mg and P in excess, as in the previous experiments (Fig 4b), the addition of biochars led to greater K recovery compared to the solution with Initial molar ratio, demonstrating that, regardless of seed material, the adjustment of the Mg:K:P molar ratio is crucial for effective K recovery from synthetic urine. Nevertheless, pyrolysis temperature again had a noticeable effect. In contrast to the solution with Initial molar ratio results, biochars produced at 700 °C exhibited the lowest recovery rates with the solution with Mg and P in excess. Additionally, consistent with earlier findings, wood-derived biochars outperformed those produced from dairy manure. This suggests that differences in surface chemistry and intrinsic K content between biochars derived from manure and wood play a critical role in K-struvite recovery.

Manure-based biochars likely contain higher concentrations of K in soluble or exchangeable forms, which may be released into solution during the reaction and interfere with the target precipitation pathway. This interpretation is supported by Wu et al. (2021), who demonstrated that biochars with higher ash content, typical of manure-based feedstocks, tend to retain greater total K, but a portion of this K is gradually released into solution, particularly when present in exchangeable or weakly bound forms. In contrast, wood-derived biochars typically contain less inherent K, reducing such interference and functioning more reliably as passive nucleation surfaces. The best-performing biochar was made from wood at 300°C, which

achieved a K recovery approximately 7% higher than the control solution without biochar. This result reinforces the potential of low-temperature wood biochars to act as effective nucleation matrices for K-struvite, possibly due to preserved negative functional groups and a chemically inert structure that limits ion release into solution.

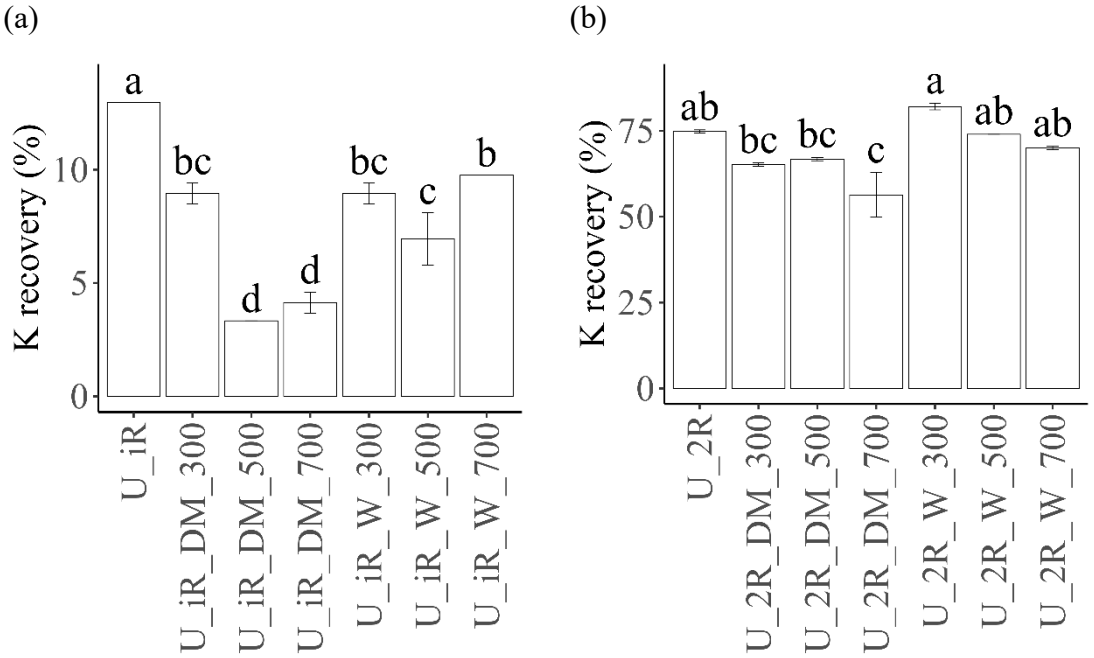

Figure 11. Influence of pyrolysis temperature (300, 500, and 700 °C) on potassium recovery from synthetic urine using biochars derived from dairy manure (DM) and wood (W) as seed materials. (a) Results for the original molar ratio solution (U_iR); (b) results for the optimized 2:1:2 molar ratio solution (U_2R). Error bars represent standard deviation; different letters indicate statistically significant differences among treatments according to Tukey's test ($p < 0.05$).

An additional experiment was conducted to evaluate the influence of mixing and resting times on potassium recovery from synthetic urine with the addition of biochar. In this experiment, wood-derived biochar pyrolyzed at 500 °C was used, and the U_2R solution, adjusted to pH 10, was applied. The highest potassium removal efficiency (81.4%) was achieved with 30 minutes of mixing followed by 1 hour of resting. Comparable results were observed for the reverse sequence, 1 hour of mixing followed by 30 minutes of resting, and for the condition with 1 hour allocated to both stages, each yielding approximately 80.5% recovery. The lowest removal efficiency (70%) was recorded for the condition involving 24 hours of mixing followed by 30 minutes of resting, suggesting that extended mixing times do not

enhance K-struvite precipitation and may, in fact, increase the release of potassium from the biochar into the solution.

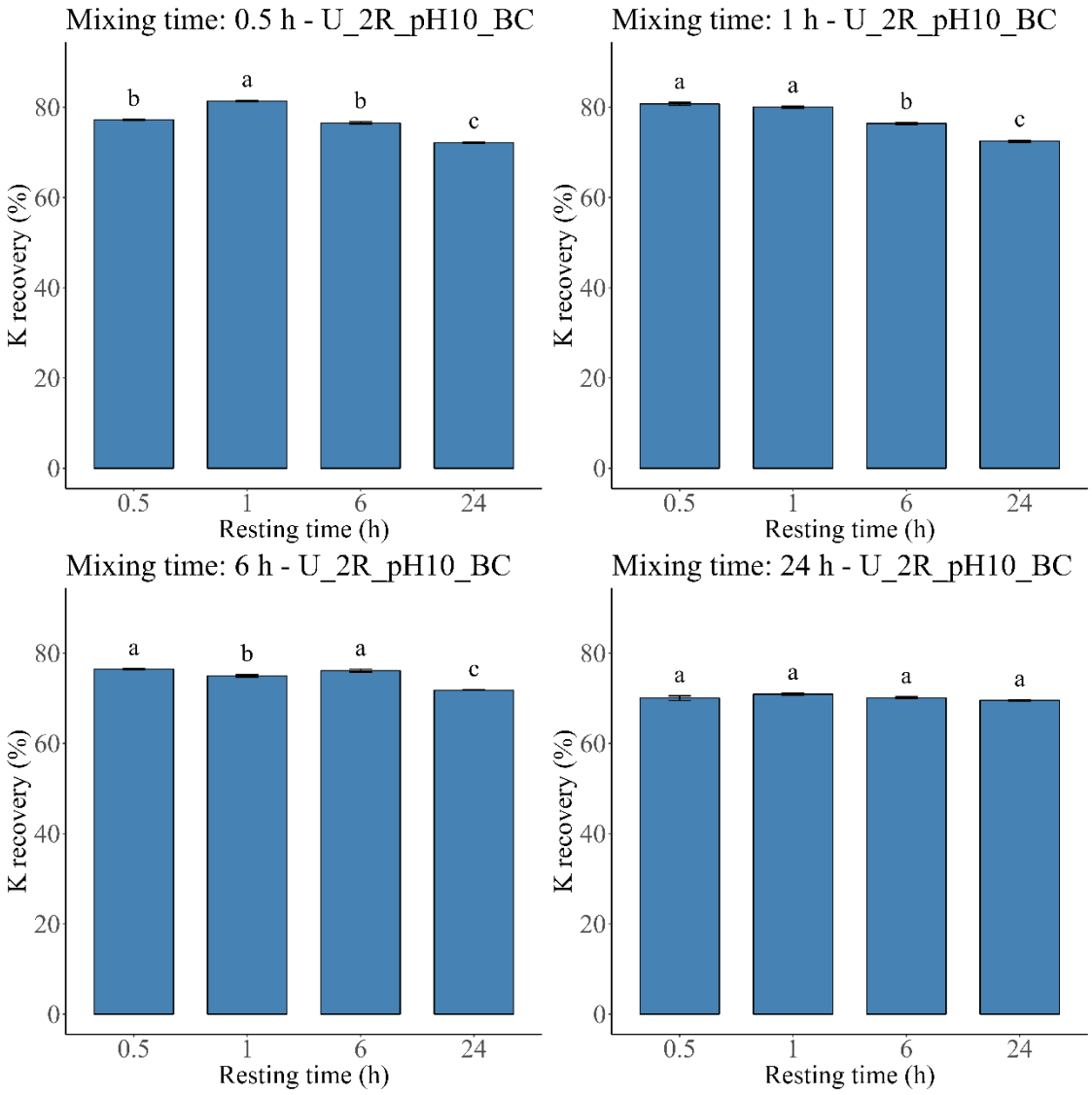

Figure 12. Effect of different mixing and resting times on K-struvite formation from synthetic urine using wood-derived biochar (500 °C) as a seed material. Bars represent potassium recovery (%) under varying combinations of mixing and resting durations. Error bars represent standard deviation; different letters indicate statistically significant differences among treatments according to Tukey's test ($p < 0.05$).

These results are consistent with those observed in the absence of biochar, indicating that the kinetic behavior of K-struvite formation remains largely governed by mixing and resting time, regardless of the presence of solid support. In both cases, moderate mixing (0.5 to 1 hour) followed by brief resting (0.5 to 1 hour) yielded the best performance, while excessive resting (24 hours) consistently reduced potassium recovery. When mixing time was extended to 24 hours, the influence of resting time became negligible, suggesting that sufficient agitation

stabilizes the system, likely by allowing complete nucleation and growth of K-struvite crystals prior to any resting phase.

3.4. Kinetics of Potassium Release

To understand the release dynamics of K from formed compounds, an experiment was conducted to simulate K release in a $CaCl_2$ solution over 24 hours (Fig. 7). The K release kinetics dataset was fitted to five mathematical models, and the most appropriate model for each sample, was selected based on the highest regression coefficients (R^2) and the lowest root mean square errors (RMSE) and Akaike Information Criterion (AIC) values (Table A3). Among the evaluated models, the Power function equation provided the best fit (high R^2).

The potassium release kinetics revealed distinct behaviors among the evaluated materials. Pure K-struvite (S) and its pyrolyzed form (Sp) exhibited rapid and high K release, surpassing 75% within the first few hours, confirming their potential as readily available K sources under mild extraction conditions. However, the slightly lower release observed for Sp suggests that pyrolysis may reduce K accessibility, possibly due to increased crystallinity or surface occlusion. The physical mixture of biochar and K-struvite (BC+S) also showed a high release rate, slightly below that of S, indicating minor interference, potentially due to transient adsorption or physical diffusion constraints imposed by the biochar matrix. In contrast, the composite biochar (BC_S), formed by co-pyrolyzing biomass with K-struvite, resulted in significantly lower and slower K release. This suggests that thermal treatment altered the structure or composition of the mineral phase, likely encapsulating K within the carbon matrix and converting it into less soluble forms, thereby functioning as a slow-release material. As expected, the pure biochar released minimal K, confirming its inert role in nutrient availability. These findings highlight the importance of processing conditions in determining the solubility and potential agronomic functionality of K-containing biochar-based materials.

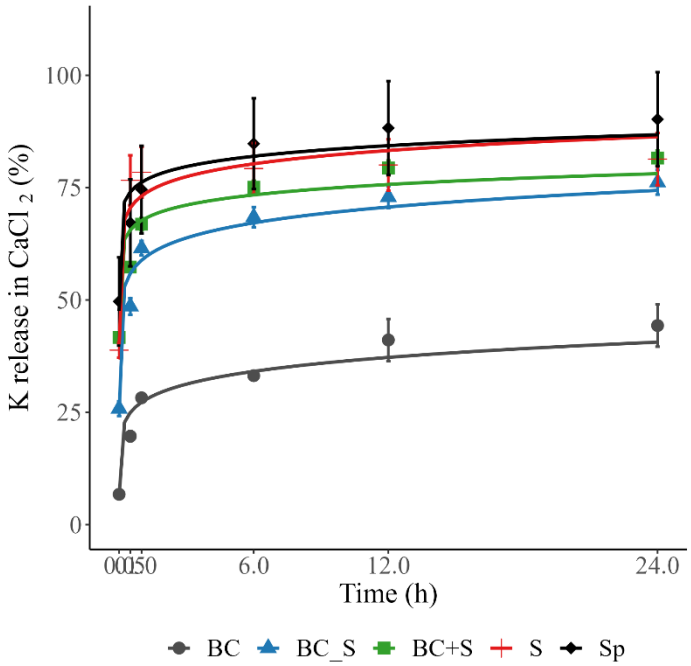

Figure 13. Potassium release kinetics from different biochar-based materials and K-struvite forms in 0.01 mol L^{-1} $CaCl_2$ solution over 24 hours. Treatments include: BC = pure biochar; BC_S = composite biochar formed by co-pyrolyzing biochar with K-struvite; BC+S = physical mixture of biochar and K-struvite; S = pure K-struvite; and Sp = pyrolyzed K-struvite. Error bars represent standard deviation (n = 3). Lines represent fitted power-law model curves for K release over time.

4. Conclusions

This study offers evidence that potassium recovery from human waste streams is not only technically feasible but can be enhanced through intelligent material integration and informed process design. The use of thermodynamic modeling, when combined with targeted experimental validation, strengthens the case for predictive tools in nutrient recovery system planning, provided their limitations are clearly understood. The promising performance of biochar as a seed material, particularly when derived from lignocellulosic feedstocks, highlights the potential of integrating waste-derived materials into decentralized sanitation solutions. However, the variability in performance across feedstocks signals a need for careful material selection and process standardization. Beyond technical validation, these findings point to the strategic role of potassium recovery in supporting nutrient security and reducing dependency on imported fertilizers, especially in contexts such as Brazil, where over 97% of K is externally sourced. Unlocking this potential will require supportive policies for circular sanitation, investment in small-scale treatment infrastructure, and clear quality standards for recovered products. Future research should focus on real urine matrices, assess contaminant risks, and explore long-term product stability under field conditions. Importantly, system scalability and

user acceptability will determine whether this approach transitions from lab feasibility to field deployment.

REFERENCES

BILIAS, Fotis; KALDERIS, Dimitrios; RICHARDSON, Clive; BARBAYIANNIS, Nikolaos; GASPARATOS, Dionisios. Biochar application as a soil potassium management strategy: A review. **Science of the Total Environment**, vol. 858, no. August 2022, p. 159782, 2023. DOI 10.1016/j.scitotenv.2022.159782. Available at: https://doi.org/10.1016/j.scitotenv.2022.159782.

CHEN, Jiao; LÜ, Shaoyu; ZHANG, Zhe; ZHAO, Xuxia; LI, Xinming; NING, Piao; LIU, Mingzhu. Environmentally friendly fertilizers: A review of materials used and their effects on the environment. **Science of the Total Environment**, vol. 613–614, p. 829–839, 2018. DOI 10.1016/j.scitotenv.2017.09.186. Available at: https://doi.org/10.1016/j.scitotenv.2017.09.186.

CHEN, Tse Lun; CHEN, Li Heng; LIN, Yupo J.; YU, Chang Ping; MA, Hwong wen; CHIANG, Pen Chi. Advanced ammonia nitrogen removal and recovery technology using electrokinetic and stripping process towards a sustainable nitrogen cycle: A review. **Journal of Cleaner Production**, vol. 309, no. April, p. 127369, 2021. DOI 10.1016/j.jclepro.2021.127369. Available at: https://doi.org/10.1016/j.jclepro.2021.127369.

FAO. FAOSTAT. 2023. Available at: https://www.fao.org/faostat/en/#data/RFN/visualize.

FOX, John; WEISBERG, Sanford. **An R companion to applied regression**. [*S. l.*]: Sage publications, 2018.

GAO, Yukun; LIANG, Benliang; CHEN, Huaxiang; YIN, Penggang. An experimental study on the recovery of potassium (K) and phosphorous (P) from synthetic urine by crystallization of magnesium potassium phosphate. **Chemical Engineering Journal**, vol. 337, no. December 2017, p. 19–29, 2018. DOI 10.1016/j.cej.2017.12.077. Available at: https://doi.org/10.1016/j.cej.2017.12.077.

GUAN, Qian; LI, Yingpeng; ZHONG, Yun; LIU, Wei; ZHANG, Jiajie; YU, Xin; OU, Ranwen; ZENG, Guisheng. A review of struvite crystallization for nutrient source recovery from wastewater. **Journal of Environmental Management**, vol. 344, no. June, p. 118383, 2023. DOI 10.1016/j.jenvman.2023.118383. Available at: https://doi.org/10.1016/j.jenvman.2023.118383.

GUNNARSSON, Matilda; LALANDER, Cecilia; MCCONVILLE, Jennifer R. Estimating environmental and societal impacts from scaling up urine concentration technologies. **Journal of Cleaner Production**, vol. 382, no. November 2022, p. 135194, 2023. DOI 10.1016/j.jclepro.2022.135194. Available at: https://doi.org/10.1016/j.jclepro.2022.135194.

GUSTAFSSON, Jon Petter. Visual MINTEQ 3.1. , p. 1–73, 2014. Available at: https://vminteq.lwr.kth.se/.

HE, Jiazhou; ZHOU, Jieqin; YANG, Kui; LUO, Liang; WANG, Pan; WANG, Zhiwei; MA, Jinxing. Pulsed electric field drives chemical-free membrane stripping for high ammonia recovery from urine. **Water Research**, vol. 251, no. January, p. 121129, 2024. DOI 10.1016/j.watres.2024.121129. Available at: https://doi.org/10.1016/j.watres.2024.121129.

HOTHORN, Torsten; BRETZ, Frank; WESTFALL, Peter. Simultaneous inference in general parametric models. **Biometrical Journal**, vol. 50, no. 3, p. 346–363, 2008. https://doi.org/10.1002/bimj.200810425.

HU, Lei; YU, Jiuling; LUO, Hongmei; WANG, Huiyao; XU, Pei; ZHANG, Yanyan. Simultaneous recovery of ammonium, potassium and magnesium from produced water by struvite precipitation. **Chemical Engineering Journal**, vol. 382, no. July 2019, p. 123001, 2020. DOI 10.1016/j.cej.2019.123001. Available at: https://doi.org/10.1016/j.cej.2019.123001.

HUANG, Haiming; ZHANG, Dingding; WANG, Wenjun; LI, Bing; ZHAO, Ning; LI, Jing; DAI, Jiankun. Alleviating Na+ effect on phosphate and potassium recovery from synthetic urine by K-struvite crystallization using different magnesium sources. **Science of the Total Environment**, vol. 655, p. 211–219, 2019. DOI 10.1016/j.scitotenv.2018.11.259. Available at: https://doi.org/10.1016/j.scitotenv.2018.11.259.

ISWARDI, Aditya H.; HUBBLE, Andrew H.; LEHMANN, Johannes; GOLDFARB, Jillian L. Can batch lab-scale studies of slow pyrolysis describe biochar yields and properties upon upscaling to a continuous auger kiln? **Journal of Cleaner Production**, vol. 496, no. July 2024, p. 145150, 2025. DOI 10.1016/j.jclepro.2025.145150. Available at: https://doi.org/10.1016/j.jclepro.2025.145150.

KABDAŞLI, Işık; KUŞÇUOĞLU, Sezen; TÜNAY, Olcay; SICILIANO, Alessio. Assessment of K-Struvite Precipitation as a Means of Nutrient Recovery from Source Separated Human Urine. **Sustainability (Switzerland)**, vol. 14, no. 3, 2022. https://doi.org/10.3390/su14031082.

KABDAŞLI, Işık; SICILIANO, Alessio; LIMONTI, Carlo; TÜNAY, Olcay. Is K-Struvite Precipitation a Plausible Nutrient Recovery Method from Potassium-Containing Wastes?—A Review. **Sustainability (Switzerland)**, vol. 14, no. 18, 2022. https://doi.org/10.3390/su141811680.

KHALIDY, Reza; SANTOS, Rafael M. Assessment of geochemical modeling applications and research hot spots—a year in review. **Environmental Geochemistry and Health**, vol. 43, no. 9, p. 3351–3374, 2021. DOI 10.1007/s10653-021-00862-w. Available at: https://doi.org/10.1007/s10653-021-00862-w.

KOGLER, Anna; SHARMA, Neha; TIBURCIO, Diana; GONG, Meili; MILLER, Dean M.; WILLIAMS, Kindle S.; CHEN, Xi; TARPEH, William A. Long-Term Robustness and Failure Mechanisms of Electrochemical Stripping for Wastewater Ammonia Recovery. **ACS Environmental Au**, vol. 4, no. 2, p. 89–105, 2024. https://doi.org/10.1021/acsenvironau.3c00058.

LEITE, Aline do Amaral; MELO, Leônidas Carrijo Azevedo; HURTARTE, Luis Carlos Colocho; ZUIN, Lucia; PICCOLLA, Cristiano Dela; WERDER, Don; SHABTAI, Itamar; LEHMANN, Johannes. Magnesium-enriched poultry manure enhances phosphorus bioavailability in biochars. **Chemosphere**, vol. 331, no. April, 2023. https://doi.org/10.1016/j.chemosphere.2023.138759.

LIU, Qiting; SUN, Wenhui; ZENG, Qianhao; ZHANG, Haodong; WU, Chengyang; LICHTFOUSE, Eric; LIU, Hongbo. Integrated processes for simultaneous nitrogen, phosphorus, and potassium recovery from urine: A review. **Journal of Water Process**

Engineering, vol. 59, no. December 2023, p. 104975, 2024. DOI 10.1016/j.jwpe.2024.104975. Available at: https://doi.org/10.1016/j.jwpe.2024.104975.

MARTIN, Tristan M.P.; ESCULIER, Fabien; LEVAVASSEUR, Florent; HOUOT, Sabine. Human urine-based fertilizers: A review. **Critical Reviews in Environmental Science and Technology**, vol. 52, no. 6, p. 890–936, 2022. DOI 10.1080/10643389.2020.1838214. Available at: https://doi.org/10.1080/10643389.2020.1838214.

MUHMOOD, Atif; WU, Shubiao; LU, Jiaxin; AJMAL, Zeeshan; LUO, Hongzhen; DONG, Renjie. Nutrient recovery from anaerobically digested chicken slurry via struvite: Performance optimization and interactions with heavy metals and pathogens. **Science of the Total Environment**, vol. 635, p. 1–9, 2018. DOI 10.1016/j.scitotenv.2018.04.129. Available at: https://doi.org/10.1016/j.scitotenv.2018.04.129.

MURRELL, T. Scott; MIKKELSEN, Robert L.; SULEWSKI, Gavin; NORTON, Robert; THOMPSON, Michael L. **Improving potassium recommendations for agricultural crops**. [*S. l.*: *s. n.*], 2020. https://doi.org/10.1007/9783030591977.

NATIVIDAD-MARIN, Leynard; WILLIAM BURNS, Max; SCHNEIDER, Phil. A comparison of struvite precipitation thermodynamics and kinetics modelling techniques. **Water Science and Technology**, vol. 87, no. 6, p. 1393–1422, 2023. https://doi.org/10.2166/wst.2023.061.

PATHY, Abhijeet; RAY, Jyotiprakash; PARAMASIVAN, Balasubramanian. Challenges and opportunities of nutrient recovery from human urine using biochar for fertilizer applications. **Journal of Cleaner Production**, vol. 304, p. 127019, 2021. DOI 10.1016/j.jclepro.2021.127019. Available at: https://doi.org/10.1016/j.jclepro.2021.127019.

PRIYA, E.; SARKAR, Sudipta; MAJI, Pradip K. A review on slow-release fertilizer: Nutrient release mechanism and agricultural sustainability. **Journal of Environmental Chemical Engineering**, vol. 12, no. 4, p. 113211, 2024. DOI 10.1016/j.jece.2024.113211. Available at: https://doi.org/10.1016/j.jece.2024.113211.

RANDALL, D. G.; NAIDOO, V. Urine: The liquid gold of wastewater. **Journal of Environmental Chemical Engineering**, vol. 6, no. 2, p. 2627–2635, 2018. https://doi.org/10.1016/j.jece.2018.04.012.

SALIU, Toyin Dunsin; OLADOJA, Nurudeen Abiola; SAUVÉ, Sébastien. Eco-friendly and sustainability assessment of technologies for nutrient recovery from human urine—a review. **Frontiers in Sustainability**, vol. 4, no. January, p. 1–20, 2023. https://doi.org/10.3389/frsus.2023.1338380.

SANTOLIN, Julia; VLAEMINCK, Siegfried E.; APPIAH-TWUM, Hanson; VAN WINCKEL, Tim; SPILLER, Marc. Consequential LCA of NPK fertilizers from microbial, animal, plant, and mineral origin highlights resource constraints and environmental impacts. **Journal of Cleaner Production**, vol. 457, no. April, p. 142312, 2024. DOI 10.1016/j.jclepro.2024.142312. Available at: https://doi.org/10.1016/j.jclepro.2024.142312.

SHAN, Jinhua; LIU, Hongbo; LONG, Shiping; ZHANG, Haodong; LICHTFOUSE, Eric. Electrochemical crystallization for recovery of phosphorus and potassium from urine as K-

struvite with a sacrificial magnesium anode. **Environmental Chemistry Letters**, vol. 20, no. 1, p. 27–33, 2022. DOI 10.1007/s10311-021-01333-5. Available at: https://doi.org/10.1007/s10311-021-01333-5.

USMAN, Muhammad; FAROOQ, Muhammad; WAKEEL, Abdul; NAWAZ, Ahmad; CHEEMA, Sardar Alam; REHMAN, Hafeez ur; ASHRAF, Imran; SANAULLAH, Muhammad. Nanotechnology in agriculture: Current status, challenges and future opportunities. **Science of the Total Environment**, vol. 721, p. 137778, 2020. DOI 10.1016/j.scitotenv.2020.137778. Available at: https://doi.org/10.1016/j.scitotenv.2020.137778.

VENABLES, William N.; RIPLEY, Brian D. **Statistics Complements to Modern Applied Statistics with S**. [*S. l.*: *s. n.*], 2002. Available at: http://www.amazon.com/dp/1441930086.

WANG, Xiukang. Managing Land Carrying Capacity: Key to Achieving Sustainable Production Systems for Food Security. **Land**, vol. 11, no. 4, 2022. https://doi.org/10.3390/land11040484.

WEI, Lin; TANG, Yiming; ZHANG, Tingting; JI, Junjie; ZHANG, Qiang; DONG, Yugang; LUO, Lei; DING, Xiaoke; KONG, Jianyu. Factors influencing K-struvite purity via phosphorus coprecipitation in synthetic urine: Verification, quantification, and modelling. **Environmental Research**, vol. 264, no. P1, p. 120346, 2025. DOI 10.1016/j.envres.2024.120346. Available at: https://doi.org/10.1016/j.envres.2024.120346.

WICKHAM, Hadley. **ggplot2: Elegant Graphics for Data Analysis. Springer-Verlag New York**. [*S. l.*: *s. n.*], 2016. vol. 35, . Available at: http://link.springer.com/10.1007/978-0-387-98141-3.

WICKHAM, Hadley; AVERICK, Mara; BRYAN, Jennifer; CHANG, Winston; MCGOWAN, Lucy; FRANÇOIS, Romain; GROLEMUND, Garrett; HAYES, Alex; HENRY, Lionel; HESTER, Jim; KUHN, Max; PEDERSEN, Thomas; MILLER, Evan; BACHE, Stephan; MÜLLER, Kirill; OOMS, Jeroen; ROBINSON, David; SEIDEL, Dana; SPINU, Vitalie; … YUTANI, Hiroaki. Welcome to the Tidyverse. **Journal of Open Source Software**, vol. 4, no. 43, p. 1686, 2019. https://doi.org/10.21105/joss.01686.

WU, Haotian; FOSTER, Xavier; KAZEMIAN, Hossein; VANEECKHAUTE, Céline. N, P, K recovery from hydrolysed urine by Na-chabazite adsorption integrated with ammonia stripping and (K-)struvite precipitation. **Science of the Total Environment**, vol. 857, no. October 2022, 2023. https://doi.org/10.1016/j.scitotenv.2022.159277.

WU, Haotian; VANEECKHAUTE, Céline. Nutrient recovery from wastewater: A review on the integrated Physicochemical technologies of ammonia stripping, adsorption and struvite precipitation. **Chemical Engineering Journal**, vol. 433, no. July 2021, 2022. https://doi.org/10.1016/j.cej.2021.133664.

WU, Wenzhu; YAN, Beibei; ZHONG, Lei; ZHANG, Rui; GUO, Xiang; CUI, Xiaoqiang; LU, Wenlong; CHEN, Guanyi. Combustion ash addition promotes the production of K-enriched biochar and K release characteristics. **Journal of Cleaner Production**, vol. 311, no. May, p. 127557, 2021. DOI 10.1016/j.jclepro.2021.127557. Available at: https://doi.org/10.1016/j.jclepro.2021.127557.

XIU, Liqun; GU, Wenqi; SUN, Yuanyuan; WU, Di; WANG, Yuning; ZHANG, Honggui; ZHANG, Weiming; CHEN, Wenfu. The fate and supply capacity of potassium in biochar used in agriculture. **Science of the Total Environment**, vol. 902, no. March, 2023. https://doi.org/10.1016/j.scitotenv.2023.165969.

XU, Kangning; LI, Hui; LIN, Fangyu; WANG, Chengwen; ZHENG, Min. Optimization of potassium (K) recovery via electrochemical precipitation of K-struvite upon magnesium addition in urine. **Journal of Environmental Chemical Engineering**, vol. 12, no. 5, p. 114159, 2024. DOI 10.1016/j.jece.2024.114159. Available at: https://doi.org/10.1016/j.jece.2024.114159.

XU, Kangning; LI, Jiyun; ZHENG, Min; ZHANG, Chi; XIE, Tao; WANG, Chengwen. The precipitation of magnesium potassium phosphate hexahydrate for P and K recovery from synthetic urine. **Water Research**, vol. 80, p. 71–79, 2015. DOI 10.1016/j.watres.2015.05.026. Available at: http://dx.doi.org/10.1016/j.watres.2015.05.026.

YANG, Yuanquan; LIU, Jun; WANG, Baomin; LIU, Runqing; ZHANG, Tingting. A thermodynamic modeling approach for solubility product from struvite-k. **Computational Materials Science**, vol. 157, no. November 2018, p. 51–59, 2019. DOI 10.1016/j.commatsci.2018.10.037. Available at: https://doi.org/10.1016/j.commatsci.2018.10.037.

Supplementary information

Table A 2. Ionic composition of synthetic solutions with different Mg:K:P molar ratios (fixed pH 10) (mmol L^{-1})

Íon	U_iR_pH 10	U_1R_pH 10 (mmol/L)	U_2R_pH 10
K^+	31.83	31.83	31.83
Mg^{2+}	3.15	31.71	63.55
Ca^{2+}	4.42	4.42	4.42
Na^+	183.02	225.84	289.52
Cl^-	115.44	172.56	236.24
SO_4^{2-}	16.19	16.19	16.19
$Citrate^{3-}$	2.21	2.21	2.21
$Oxalate^{2-}$	0.15	0.15	0.15
PO_4^{2-}	10.36	31.77	63.61

Table A 3. Ionic composition of synthetic urine solutions with different pH values (mmol·L^{-1}) at a Mg:K:P molar ratio of 2:1:2

Íon	U_2R pH_pHO	U_2R_pH9 (mmol/L)	U_2R_pH 10
K^+	31.83	31.83	31.83
Mg^{2+}	63.55	63.55	63.55
Ca^{2+}	4.42	4.42	4.42
Na^+	224.53	269.52	289.52
Cl^-	236.24	236.24	236.24
SO_4^{2-}	16.19	16.19	16.19
$Citrate^{3-}$	2.21	2.21	2.21
$Oxalate^{2-}$	0.15	0.15	0.15
PO_4^{2-}	63.61	63.61	63.61

Table A 4. K release kinetic coefficients in the $CaCl_2$ solution for the formed compounds.

BC	Model	R2	RMSE	AIC
	Linear	0.65	7.71	130.63
	Power	0.96	0.13	-17.09
	Elovich	0.58	8.46	133.96
	Parabolic	0.84	5.23	116.67
	Exponential	0.58	8.46	133.96
BC_S	Model	R2	RMSE	AIC
	Linear	0.51	12.20	147.13
	Power	0.96	0.07	-37.86
	Elovich	0.46	12.71	148.61
	Parabolic	0.73	9.01	136.22
	Exponential	0.46	12.71	148.61
BC+S	Model	R2	RMSE	AIC
	Linear	0.57	9.19	136.94
	Power	0.92	0.07	-40.95
	Elovich	0.53	9.58	138.42
	Parabolic	0.79	6.34	123.55
	Exponential	0.53	9.58	138.42
S	Model	R2	RMSE	AIC
	Linear	0.42	12.48	147.95
	Power	0.71	0.13	-16.22
	Elovich	0.39	12.75	148.71
	Parabolic	0.59	10.43	141.49
	Exponential	0.39	12.75	148.71
Sp	Model	R2	RMSE	AIC
	Linear	0.19	14.09	152.32
	Power	0.92	0.08	-34.73
	Elovich	0.18	14.18	152.54
	Parabolic	0.36	12.57	148.21
	Exponential	0.18	14.18	152.54

3 FINAL REMARKS

This thesis was driven by the need to rethink the use and application of conventional potassium fertilizers in tropical agricultural systems. Throughout the development of this research, several challenges were encountered, the main one being how to reconcile the production of biochar with Brazil's high demand for potassium inputs. The first challenge overcome was identifying organic residues that were not only rich in K, but also technically viable for pyrolysis and economically relevant, meaning they are produced in large quantities and in geographically concentrated areas. Another limitation faced was the relatively low environmental appeal associated with potassium recovery, in contrast to nutrients such as nitrogen and phosphorus, which are more often prioritized in waste management studies. Nonetheless, potassium is a non-renewable resource and, in the case of Brazil, largely imported, significantly increasing production costs for farmers.

Additionally, while the recovery of K from liquid residues is still underexplored compared to other nutrients or contaminants, it holds strong economic potential, especially when directed toward agricultural applications that foster a circular economy. This work was able to demonstrate effective ways to recover potassium from both solid and liquid waste streams, resulting in products with real potential for agricultural use. The results provide practical insight into the development of potassium-rich biochar-based fertilizers and their application in soils with contrasting physical and chemical characteristics. Furthermore, this thesis showed that liquid waste sources, such as human urine, contain high concentrations of potassium that can be sustainably recovered through chemical precipitation, with biochar acting as a crystallization seed. It also demonstrated the usefulness of modeling tools, such as PHREEQC, for supporting the development of nutrient recovery techniques in complex liquid systems.

Future research should advance these technologies, particularly under field conditions and in real effluent systems, to validate their efficiency at the scale of national agricultural production and decentralized sanitation. The findings presented here are not an end point, but rather an invitation to expand the dialogue between agricultural sustainability, waste management and environmental chemistry.